HOST UNIVERSITY: Lund University

DEPARTMENT: Division of Fire Safety Engineering

Academic Year 2015-2016

ELEVATED FIRES

Kseniia Polukhina

Promoter(s): Nils Johansson

Master thesis submitted in the Erasmus Mundus Study Programme

International Master of Science in Fire Safety Engineering

DISCLAIMER

This thesis is submitted in partial fulfilment of the requirements for the degree of *The International Master of Science in Fire Safety Engineering (IMFSE)*. This thesis has never been submitted for any degree or examination to any other University/programme. The author(s) declare(s) that this thesis is original work except where stated. This declaration constitutes an assertion that full and accurate references and citations have been included for all material, directly included and indirectly contributing to the thesis. The author(s) gives (give) permission to make this master thesis available for consultation and to copy parts of this master thesis for personal use. In the case of any other use, the limitations of the copyright have to be respected, in particular with regard to the obligation to state expressly the source when quoting results from this master thesis. The thesis supervisor must be informed when data or results are used.

29.04.2016

Kseniia Polukhina

Read and approved.

Summary/Abstract

The primary objective of the present study is to evaluate the effect of the fire source elevation on the main fire parameters, by implementing laboratory experiments. In modern Fire Safety Engineering practice, it is often assumed that fire always commences at the floor level. However, it is not always the case. For instance, many residential fires were initiated by the ignition of ovens and stoves leading to the fire base to be raised above the floor by at least a meter. A series of tests with fire source located at different heights were conducted in the 1/3 scale of the ISO standard fire room. Heat Release Rate, Mass Loss Rate, temperatures inside the enclosure and radiative heat flux at the floor were measured. Results showed that when fires are elevated so that the flame is completely inside the smoke layer, they yield higher heat release rate, mass loss rate and heat flux than fires near the floor. At the same time, if the fire source is elevated to a level, where no considerable interaction with the smoke layer takes place, it will result in a less hazardous fire, as conditions critical to life safety develops slower than for the floor fire.

The secondary objective is to establish whether the existing modelling software and analytical models are sufficient for simulating elevated fires. This is studied by comparison of the experimental results with simulation performed in FDS and hand calculations. Three simulations reproducing the experimental tests were performed using the FDS tool supplemented with an environmental feedback model. Simultaneously, hand calculations of HRR, MLR, HGL temperature and height were conducted by applying fire dynamics principles. FDS outputs and theoretical results were compared with the experimental ones. From the comparison it was learnt that current hand calculations and FDS models cannot sufficiently predict the impact of the source elevation on the development of fire parameters. The study provides speculations on factors that can be responsible for changes caused by the fire elevation. It also reasons why analytical and numerical models cannot account for these changes. However, no practical solution is provided in this work.

В задачи настоящего исследования входит, во-первых, оценить по основным параметрам, применяемым для анализа пожаров, фактор высоты, на которой находится источник возгорания, путем осуществления лабораторных экспериментов. В современной практике инженерной противопожарной безопасности принято считать, что возгорание начинается на уровне пола. Однако это не всегда верно. Так, частой причиной пожаров, возникших в жилых помещениях, становятся электропечи, размещённые по меньшей мере в метре от поверхности пола. Нами был проведён ряд экспериментов с источниками возгорания, размещёнными на разных высотах относительно уровня пола. Исследования проводились в лабораторных условиях на базе модели комнаты ISO 1/3. Были проанализированы скорость высвобождения тепла, коэффициент потери массы, температуры внутри закрытого пространства и радиационного теплового потока на уровне пола. Результаты исследования показали, что пожары, возникшие на уровне формирования дымового слоя, характеризуются более высокой скоростью выделения тепла, более высокой скоростью потери массы и теплового потока, чем пожары, возникшие вблизи пола. В то же время, размещение источника возгорания на высоте, где не происходит значительного взаимодействия с дымовым слоем, вызывает менее опасный огонь, так как проявление критических для жизни параметров противопожарной безопасности замедляется.

Во-вторых, для нас было важным установить, насколько эффективны существующее программное обеспечение и аналитические модели для прогнозирования развития ситуации. Что демонстрируется посредством сопоставления результатов расчетов, выполненных с применением FDS модели, и данных, расчитанных вручную. В процессе исследования нами был проведён ряд экспериментов, моделирующих ситуацию пожара, в рамках которого были применены FDS методики, дополненные моделью ответной реакции окружающей среды. Одновременно были проведены расчёты вручную таких показателей, как СВТ, КПМ, температуры и высоты дымового слоя, путем применения принципов динамики пожаров. FDS результаты и результаты теоретических расчётов были сопоставлены с экспериментальными данными, после чего было установлено, что как расчеты с применением FDS моделирования, так и расчеты, полученные вручную, не могут в достаточной степени прогнозировать влияние фактора высоты размещения источника возгорания на динамику параметров пожара. Исследование содержит ряд предположений о факторах, влияющих на динамику пожара в зависимости от высоты расположения источников возгорания, а также изложение причин, по которым аналитические модели и FDS технологии не являются достаточно эффективными для решения поставленных задач. Тем не менее, никакого практического решения проблемы не данное исследование не предполагает.

Table of contents

List of tables and figures 6
1 Introduction & Objectives 9
1.1 Introduction 9
1.2 Objectives 10
1.3 Limitations 11
2 Methodology 12
2.1 Experiments 12
2.2 Modelling 12
2.3 Analytical methods 13
2.3.1 Two-zone model concept 13
3 Experiments 14
3.1 Experimental Setup 14
3.1.1 Room dimensions 14
3.1.2 Enclosure materials 14
3.1.3 Measurements 14
3.1.4 Fire source 16
3.1.5 Performance 16
3.2 Experimental Results and Analysis 17
3.2.1 MLR 17
3.2.2 HRR 19
3.2.3 Combustion Efficiency 20
3.2.4 Hot Gas Layer Temperature and Interface height 22
3.2.5 Radiative Heat flux 25
4 Modelling 26
4.1 Grid Size 26
4.2 Setup 27
4.3 FDS Results 28
4.3.1 Mass Loss Rate 29
4.3.2 HRR 30
4.3.3 HGL Temperature and Height 32

4.3.4 Heat Flux 34
5 Analytical Methods 36
5.1.1 MLR 36
5.1.2 HRR 37
5.1.3 HGL Temperature and Interface Position 39
6 Discussions 47
RQ1. How will the heat release rate be affected by the elevation of the fire source? 47
RQ2. How will hot gas layer properties (such as temperature and hot gas layer height) be affected by the elevation of the fire source? 49
RQ3. How will radiative heat flux to the floor be affected by the elevation of the fire source? 50
RQ4. Does elevation of the fire source influences the speed of the growth of the fire parameters (HRR, HGL Temperature and height, heat flux etc.) 51
RQ5. Is it possible to account for the elevation of the fires source in existing fire modelling softwares? 53
RQ6. Is it possible to account for the elevation of the fires source using existing hand-calculations methods for fire safety engineering? 59
7 Uncertainties and Validity of the Study 64
7.1 Uncertainties and Sources of Error 64
7.2 Validity 66
8 Conclusions 68
9 Acknowledgement 69
10 References 70
Appendices 72
Appendix A. HRR Calculations 72
Appendix B. Hot Gas Layer Temperature and Height, Reduction Method 76
Appendix C. Method 1 77
Appendix D. Method 2 81
Appendix E. FDS inputs for scenario 1. 86

List of tables and figures

Figure 1. A schematic of the stratified case [14] 13
Figure 2.Schematic set-up of the experiment. 15
Figure 3.Position of the thermocouples on the thermocouple tree. 15
Figure 4. Photos made during the experiment; from left to right: Scenario 1, Scenario 2, Scenario 3..... 17
Figure 5. Variation of MLR over time for 3 different elevation scenariosand free burning..... 18
Figure 6. Variation of HRR over time for three elevated scenarios and free burning 19
Figure 7. Variation of combustion efficiency over time for three elevation scenarios. 21
Figure 8. Variation of the hot gas layer height over time for three elevated scenarios and free burning . 22
Figure 9. Variation of the hot gas layer temperature over time for three elevation scenarios. 23
Figure 10. Photo made during the experiments depicting the flame – smoke layer interaction..... 24
Figure 11. Variation of the received radiative heat flux at the floor over time for three elevation scenarios..... 25
Figure 12. Total MLR calculated in FDS..... 29
Figure 13. Comparison of the MLR calculated in FDS and measured experimentally..... 30
Figure 14. HRR calculated during the FDS simulation..... 31
Figure 15.Comparison of the HRR calculated in FDS and measured experimentally..... 31
Figure 16. HGL Temperature calculated by FDS..... 32
Figure 17. HGL Height calculated by FDS 33
Figure 18. Comparison of the HGL Temperatures calculated in FDS and measured experimentally. 33
Figure 19. Comparison of the HGL Height calculated in FDS and measured experimentally. 34
Figure 20. Radiative Heat Flux at floor calculated by FDS..... 34
Figure 21. Comparison of the Heat flux calculated in FDS and measured experimentally..... 35
Figure 22. Variation of analytically found HRR over time for three elevation scenarios..... 38
Figure 23.Comparison of the HRR calculated analytically and measured experimentally. 38
Figure 24. Hot gas layer temperature estimated using Method 1 for every elevation scenario..... 39
Figure 25. Comparison of the HGL Temperatures calculated from Method 1 and measured experimentally. 40
Figure 26. Comparison of the HGL Temperatures calculated from Method 1 using HRR of free burning Heptane with measured experimentally..... 41
Figure 27. Hot gas layer temperature estimated using Method 2 for every elevation scenario..... 42
Figure 28. Comparison of the HGL Temperatures calculated from Method 2 and measured experimentally. 42
Figure 29. Comparison of the HGL Temperatures calculated from Method 2 using HRR of free burning Heptane with measured experimentally..... 43
Figure 30. Hot gas layer height estimated using Method 2 for every elevation scenario. 44
Figure 31. Comparison of the HGL Height calculated from Method 2 and measured experimentally. 44
Figure 32. Comparison of the HGL heights calculated from Method 2 using HRR of free burning Heptane with experimentally measured ones. 45
Figure 33. Relations between HRR and fire elevation. 47
Figure 34. Relations between MLR and fire elevation..... 48
Figure 35. Relations between HGL Temperature and fire elevation..... 49
Figure 36. Relations between HGL Height and fire elevation..... 50

Figure 37. Relations between Heat fluxes received at floor and fire elevation. 51
Figure 38. Relations between fire growth and fire elevation. 52
Figure 39. Relations between MLR calculated in FDS and fire elevation 54
Figure 40. Relations between HRR calculated in FDS and fire elevation. 54
Figure 41. Relations between HGL Temperature calculated in FDS and fire elevation. 56
Figure 42. Relations between HGL heights calculated in FDS and fire elevation. 57
Figure 43. Relations between Heat Flux to the floor calculated in FDS and fire elevation 58
Figure 44. Relations between analytically found HRR and fire elevation. 60
Figure 45. Relations between HGL temperatures calculated using Method 1 and fire elevation. 60
Figure 46. Relations between HGL temperatures calculated using Method 2 and fire elevation. 61
Figure 47. Relations between HGL heights calculated using Method 2 and fire elevation. 62
Figure 48. Schematic depiction of two zone model concept. 76
Figure 49. Variation of the effective conduction coefficient over time 78
Figure 50. Schematic depiction of the stratified case 81
Figure 51. Variation of the effective conduction coefficient over time 82

Table 1.Presentation of how different methods are associated with the different research questions (RQs) 12
Table 2. Property of the material the enclosure is made of 14
Table 3. MLR and MLRPUA used for the simulations 27
Table 4. Values and fraction of MLRPUA used for ramp function. 27
Table 5. Extreme values of differences in values of HRR and MLR between Scenario 1 and Scenarios 2 and 3. 48
Table 6. Extreme values of differences in values of HGL Temperatures between Scenario 1 and Scenarios 2 and 3. 49
Table 7. Extreme values of differences in values of HGL height between Scenario 1 and Scenarios 2 and 3. 50
Table 8. Extreme values of differences in values of received heat flux between Scenario 1 and Scenarios 2 and 3. 51
Table 9.Comparison of the effect of elevation on HRR found experimentally and predicted by FDS. 55
Table 10. Comparison of the effect of elevation on HGL temperature found experimentally and predicted by FDS. 56
Table 11. Comparison of the effect of elevation on HGL height found experimentally and predicted by FDS. 57
Table 12. Comparison of the effect of elevation on heat flux found experimentally and predicted by FDS. 58
Table 13. Comparison of the effect of elevation on HRR found experimentally and predicted analytically. 60
Table 14.Comparison of the effect of elevation on HGL temperature found experimentally and predicted analytically by Methods 1 and 2. 61

Table 15. Comparison of the effect of elevation on HGL height found experimentally and predicted analytically by Methods 2 62
Table 16.The variation of values due to averaging, scenario 1 65
Table 17.The variation of values due to averaging, scenario 3 66
Table 18. Properties of the boundaries' material 78
Table 19. Results of the Method 1 calculation for scenario 1 79
Table 20. Results of the Method 1 calculation for scenario 2 79
Table 21. Results of the Method 1 calculation for scenario 3. 80
Table 22. Results of the Method 1 calculation using HRR of free burn test for all elevation scenarios. 80
Table 23. Results of the Method 2 calculation for scenario 1. 84
Table 24. Results of the Method 2 calculation for scenario 2. 84
Table 25. Results of the Method 2 calculation for scenario 3. 85
Table 26. Results of the Method 2 calculation using HRR of free burn test for all elevation scenarios. 85

1 Introduction & Objectives

1.1 Introduction

In modern Fire Safety Engineering practice, the horizontal position of the fire in the room is presumed to be a critical factor. Several fire parameters' equations were adjusted for the fires that are located in the corner or along the wall. [1] The impact of these configurations have been accepted by fire safety engineering society for many years and have been broadly applied to fire design and fire investigation methods. Surprisingly, not much attention is paid to a vertical position of the fire. This parameter is simply almost never mentioned in most important fire engineering books of our time, such as SFPE. [2] Most of the experimental studies on fire behavior, such as fire plume correlations [2] have been carried out with the fire source placed near the floor level or in the way that avoids any interactions between the smoke layer and the actual fire. It might be thought that the fire elevation has no significance on the development of the fire or that such fire scenario occurs hardly ever. The latter is hardly to be the reason, as in real life situation the fire can occur at some height above the floor. For instance, in many cases of residential fires the place of origin started by the stove or similar cooking equipment. According to NFPA [3] between 2009 and 2013 in USA 45% of all residential fires were caused by cooking equipment. The number of fires initiated by forgotten stove, in Sweden between years 1996 and 2009, made up 9.8% of all residential fires. [4] For industrial fires the problem is also not uncommon, as fires are often initiated in faulty equipment or wires positioned on the walls or due to the leakage in pipes transporting flammable liquids and gases. Between the years 2006 and 2010 13% of USA industrial fires were caused by piping transporting flammable or combustible liquids and gases and 7% of industrial fires were initiated by electrical wires and cable insulation. [5] There is no precise statistic on how many of these fires were elevated, but this possibility cannot be excluded.

Several previous studies have been conducted with respect to the effect of the fire elevation, on its development and parameters. However, the existing studies are generally focused only on a specific phenomenon (e.g. ghosting fires [6]) or a particular compartment type. For instance, by use of the analytical model, Zukoski in his work on smoke filling in a compartment with the floor leakage [7], estimated that if the fire was elevated, the smoke filled up the room slower, compared to the case with a fire near the floor. Mounaud [8] carried out a set of tests in compartments with vertical openings in order to investigate the species generation and transport from compartment fires with source being elevated at three different heights. He thoroughly examined the effect of ceiling impingement on heat transfer and plume characteristics, thus, he did not answer how this changed the combustion efficiency. Backovsky [9] studied how the fire elevation affected behavior of under ventilated fires if the air inlet was located high, by examination of the temperature profiles. Zhang et al [10] were concerned about ship fires, so they have studied the effect of elevation on pool fire behavior in a closed compartment that represented a ship cabin. They have found out that if the fire was elevated high enough to reach the ceiling, the mass loss rate was much greater than for the fire in the open air. Moreover, they have discovered that the combusting efficiency got smaller with the elevation and it got even smaller if the flames impinged the ceiling. Zhang et al concluded that during the early stage, the fires that impinged the ceiling were more dangerous as they yield greater heat release rate. Zhang et al [11] were also interested in elevated fires in ship compartments, underground structures and nuclear power plants with only horizontal vents. Therefore, Zhang et al performed another experimental study on elevated fires, but this time in a ceiling vented compartment. The results revealed that for the fires that were elevated higher the overall oxygen concentration was higher, the fuel loss rate and light extinction coefficient were smaller, the gas temperature was lower and the smoke descending was slower. Basing on these results Zhang and colleagues concluded that the elevated fires in ceiling vented compartments were less hazardous than

fires at the floor level. [11] Jie Wang et al [12] made a physical model, that as nearly as possible, represented aircraft cargo compartment in order to study how fire elevation can affect activation of smoke detectors. Thus, he was mainly concerned with the earliest stage of the fire development, which made this work differ from the studies performed by others. [12] The results of the cargo compartment study showed that the ceiling temperature rise and concentration of O_2/CO/CO_2 inside the compartment depended on the elevation of the fuel.

Most of the existing papers are concentrated on the fully-developed stage, thus, they cannot be applied for the early stage when evacuation normally takes place. Only several experimental studies used compartments with vertical openings, which is the most common case in residential and industrial buildings. Only a few scientists looked at how MLR, HRR and combustion efficiency is affected by the elevation of the fire. Though, these parameters are of great importance for the fire development and for the conditions during the pre-flashover stage when life safety is an issue. As the safety of the occupants often is the primary objective of the fire safety engineering, it is of a great importance to determine whether the elevated fires cause more danger to the life of occupants than the fires at the floor. Therefore, in this work a number of tests are performed in a single enclosure with a vertical opening in one of its walls. The attention is mainly drawn to the fire parameters such as MLR and HRR and conditions critical for the life safety - temperature in the enclosure and heat flux received at the floor.

1.2 Objectives

The first objective of this thesis is to study the influence of the fire source elevation on development of conditions hazardous for life safety in a compartment. The second objective is to investigate if the elevation can be accounted for in simple hand-calculation methods used in fire safety engineering or with numerical tools.

The main research questions (RQ) to be answered in this work are:

1) *How will the heat release rate be affected by the elevation of the fire source?*

The Heat Release Rate is the principle fire parameter used in fire safety engineering to characterize fire behavior. HRR is present in the key calculations of the fire dynamics, such as plume correlations, duration of combustion, temperature inside the enclosure etc.

2) *What is the effect of the fire elevation on hot gas layer properties (such as temperature and hot gas layer height)?*

Properties of the hot gas layer are vital for the safety of the occupants of a burning building. The rate at which the smoke layer descends and its temperature determine the time available for the safe escape from the building. When the smoke reaches the level of the occupants' height, the threat of suffocation by smoke is critical.

3) *How will radiative heat flux to the floor be affected by the elevation of the fire source?*

Heat flux received at the floor level is another important factor for life safety objectives. The heat flux of 2.5kW is considered to be untenable for people, therefore, it is of great importance to know if the elevation of the fire source can lead to higher values of this parameter. [13]

4) *Does elevation of the fire source influence the speed of the growth of the fire parameters (HRR, HGL Temperature and height, heat flux etc.)?*

As it was said, when designing the safe evacuation, the time available until the untenable conditions are reached, is the central factor. For this reason it is important to study whether the fire elevation can accelerate the development of the hazardous conditions.

5) *Is it possible to account for the elevation of the fire source in existing fire modelling software?*

In the modern fire safety engineering practice, FSE design is often performed with the assistance of the modelling softwares based on Computational Fluid Dynamics (CFD) methods. However, the ability of the common simulation tools to account for the effects of fire elevation was never previously studied.

6) *Is it possible to account for the elevation of the fire source using existing hand-calculations methods for fire safety engineering?*

Even if the fire simulation tools get more and more powerful, theoretical calculations methods still continue to be the dominating FSE approach. As it was discussed in the Introduction, most of the experimental studies, that gave rise to the common estimating methods, were carried out with the fire source near or at the floor level. Thus, it is essential to know whether these methods are suitable even for the raised fire source.

The way how these questions will be answered and discussed in detail in the chapter "Methodology".

1.3 Limitations

Most of the limitations of this study are caused by the availability and condition of the fire lab equipment. The gas analyser was not working properly and could not calculate the volume concentration of the carbon monoxide in the exhaust air, because of that, the estimation of HRR was uncertain. Several significant fire parameters could not be studied since there were no suitable equipment. Those parameters are: concentration of $CO/CO_2/O_2$ at different elevations inside the enclosure and light extinction coefficient to determine the smoke density.

The largest fire testing room available was the 1/3 scale of the standard ISO fire enclosure. As this room was not of actual size, achieved results would have to be scaled in order to apply for the real size situation and this might lead to certain errors. Findings might not be applicable for the rooms with dissimilar geometry to the one of the test enclosure. Moreover, available enclosure had only one opening, which is not representable for actual compartments. Furthermore, as only one single enclosure was used, the results cannot characterize fires in multiple room compartments.

Another factor limiting the application of the findings is the duration of the implemented tests. For the tests, a relatively small amount of fuel was used that restricted fire developing from overpassing its growth stage. For this reason, obtained results will not be relevant for the fires in the steady state or in decay stage. Additionally, the phenomena of flashover was not covered by this study.

2 Methodology

In previous chapter, the objectives of this work and the main research questions (RQ) were stated. In order to answer the first four questions the fire parameters of the elevated fires can be compared to the corresponding parameters of fires at floor level. Therefore, the fire parameters mentioned in the RQ 1-4 will be found for elevated enclosure fires and for fires at floor level experimentally and by use of the CFD models. The fire parameters discussed in the RQ 1-3 will also be found analytically. To answer RQ6 analytical and experimental results will be compared. By comparing experimental results with results from simulation, it is possible to conclude whether the chosen modelling software is able to represent the effect of the elevation, thus answering RQ5.

The three research methods that are used in this work are:

- Experiments
- CFD Modelling
- Application of analytical methods

How the different research methods are applied in order to answer the six research questions are presented in Table 1.

Table 1.Presentation of how different methods are associated with the different research questions (RQs).

Method	RQ 1	RQ 2	RQ 3	RQ 4	RQ 5	RQ 6
Experiments	x	x	x	x	x	x
Modeling					x	
Analytical methods						x

2.1 Experiments

The first component of the practical part of this work is a performance of the experiments in the fire laboratory. A 1/3 scale of the ISO fire room model is used for the tests. Three scenarios are tested:

1. Fire at floor of the enclosure;
2. Fire elevated to 1/3 of the height of the enclosure;
3. Fire elevated to 2/3 of the height of the enclosure.

When all necessary data is collected, the analysis of the obtained results can be performed to answer the first four questions of the study. A full description of the experimental setup and the results are presented in chapter 3.

2.2 Modelling

Once the experimental part is completed, the experimental set-up is modelled in FDS and all scenarios tested in the laboratory are simulated. The results achieved by computer simulation are compared to experimental ones in order to validate the capacity of FDS to represent elevated fires. A full description of the setup in the numerical model and the results is presented in the chapter 4.

2.3 Analytical methods

As the final stage of the work, fire parameters of interest will be analytically estimated using methods discovered during the literature study. This will be followed by comparison of theoretical results with ones obtained in the experimental tests.

2.3.1 Two-zone model concept

A two-zone model was chosen for the analysis as the leading theoretical concept. This concept is widely applied in the FSE practice and it assumes that in pre-flashover compartment fires two distinct layers form: an upper layer consisting of hot gases and lower layer consisting of cooler air. It is assumed that each layer has a uniform temperature, addressed in this paper as: hot gas layer (HGL) temperature – T_g, and lower layer cool temperature – T_a. The interface between these two zones is located at the height – H_D. In literature such an enclosure model is also known as a stratified case.

On the figure below a schematic stratified case and typical for this case pressure profile is depicted (Figure 1).

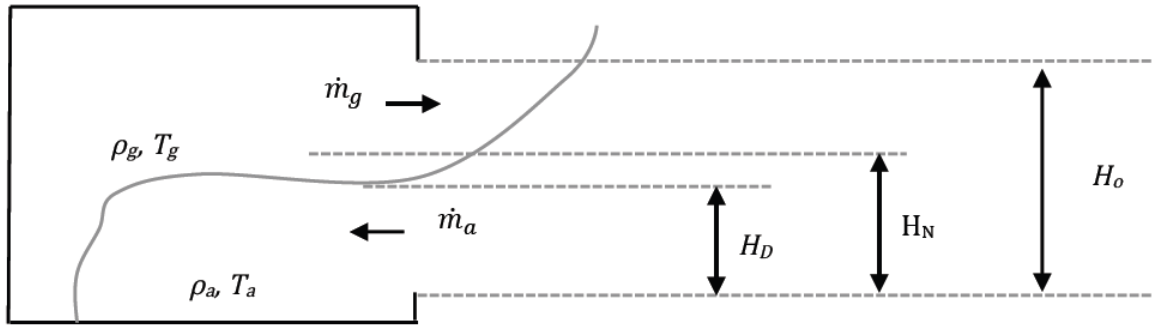

Figure 1. A schematic of the stratified case [14].

In Figure 1 H_o represents the height of the opening, H_N – is the height of the neutral plane and H_D – is the height of the hot gas layer. For the stratified case the room is typically divided into two zones in accordance to the position of the characteristic heights (H_o, H_N and H_D). [15]

3 Experiments

3.1 Experimental Setup

The experimental setup is described in the following sections.

3.1.1 Room dimensions

Experiments were conducted in a 1/3 scale of the standard ISO 9705 fire room with inner dimensions of 120cm (L) x 80cm (W) x 80cm (H). This enclosure had a single vertical opening with dimensions of 65cm (H) x 28.5cm (W) located in the front wall. Position of the vent is presented on the Figure 2. The enclosure was placed under the hood used for extraction of exhaust gases coming from the room through the opening (Figure 2).

3.1.2 Enclosure materials

The enclosure was built with 10 mm thick calcium silicate boards, assembled together into a box by means of metal brackets. These boards had following properties:

Table 2. Property of the material the enclosure is made of.

Material	Density ρ, kg/m^3	Conductivity k, W/mK	Specific heat c, J/kgK	kρc, W^{2}s/m^{4}K^2	Thermal diffusivity α, m^2/s	Thickness δ, m
Calcium silicate board	870	0.175	1130	$1.7 \cdot 10^5$	$1.8 \cdot 10^{-7}$	0.01

3.1.3 Measurements

The temperature in the enclosure was measured by means of 8 type K thermocouples with diameters of 0.51mm. A thermocouple tree was placed at the right corner behind the pool fire (Figure 2). The uppermost thermocouple was located 65mm below the ceiling of the enclosure, the lowest thermocouple was at 35mm above the floor (Figure 3). The spacing between all thermocouples was nearly equal to 100mm. A Servomex 4110 Gas Purity Analyser was used to measure the volume concentration of oxygen and carbon dioxide in the exhaust air in the duct. These parameters are important for HRR calculations. A water cooled heat flux meter SBG01 was installed at the centre of the floor to measure the incident radiative heat flux. The fuel mass loss rate was measured by means of electronic load cell with an accuracy of 0.001kg, placed under the fire source. The schematic depiction of the set-up and the detailed equipment position can be seen in the Figure 2 and Figure 3.

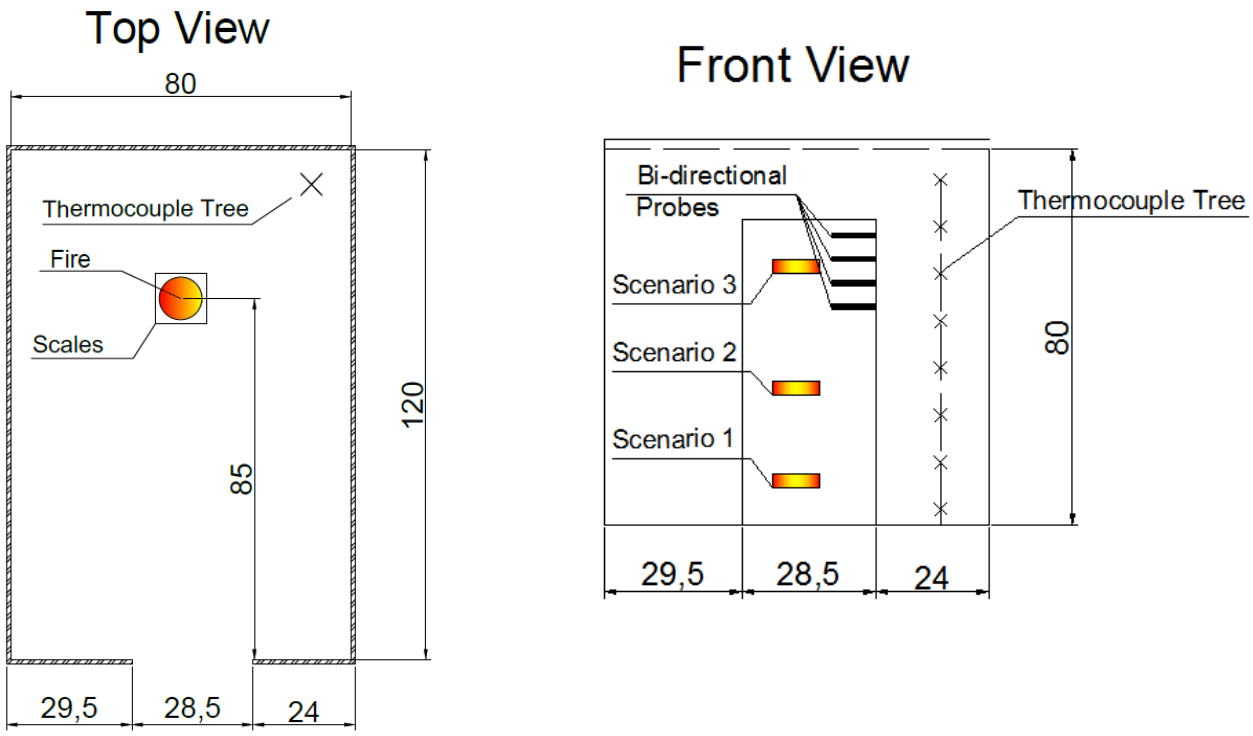

Figure 2.Schematic set-up of the experiment.

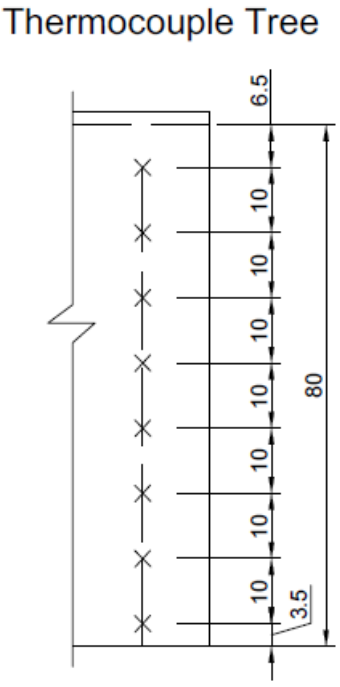

Figure 3.Position of the thermocouples on the thermocouple tree.

3.1.4 Fire source

Heptane was chosen as the fuel for testing. This choice was based on the soot production property of this fuel, which makes its combustion to resemble the actual compartment fire. The size of the pan was chosen to ensure that there was no chance of flashover to occur, as the purpose of this work was to study the developing phase and, possibly, the steady state stages of the fire. It was decided to use pan with a diameter that gives a HRR of around 5 kW. It was guessed that a pool of 10cm in diameter should produce a fire with the desired HRR.

3.1.5 Performance

To represent elevation, the fuel pan was placed on stacked bricks. To measure mass loss of fuel during combustion, a load cell was placed between bricks and the fuel pan. To protect the load cell from heat, a thin layer of thermal insulation was placed between the pan and the load cell. Each brick was 65mm high, the scales with thermal insulation were 80mm high. Three scenarios were tested: fire at the floor level, fire at 1/3 of the room height and fire at 2/3 of the room height. For the first scenario, the fuel pan was placed on the scales that were set directly on the floor of the room, for the second scenario the scales were placed on top of the stack of three bricks and for the last scenario 7 bricks were used under the scales. In this way, elevation in the first scenario is 80mm, in the second – 275mm (3·65+80) and in the last one – 535mm (7·65+80). In each test, the pan was placed at 85cm (horizontally) from the opening. For each test 200ml of heptane was used. The configuration of each scenario is presented below (Figure 4).

For each tested scenario four experimental tests were performed. Additionally, three tests of the free burning of heptane pool were conducted in order to record the open air MLR, HRR and combustion efficiency. To minimize the risk of systematic error, the tests order was alternated so that two similar tests were never performed one after the other. The total number of tests conducted is 15. It was insured that the highest temperature inside the enclosure prior to the beginning of the experiment was not higher than 30^{o}C. Apart from the fuel, 30ml of water was added to the pan each time to prevent heating of the fuel through the bottom of the pan. The duration of the tests varied between 12 and 20 min, the higher the fuel pan was elevated, the faster the fuel was consumed.

Figure 4. Photos made during the experiment; from left to right: Scenario 1, Scenario 2, Scenario 3.

3.2 Experimental Results and Analysis

To minimize the magnitude of error, multiple tests were conducted for each scenario. Further, a mean value equal to the average of all tests was estimated to represent each scenario. In this way, 3 values of every measured parameter were prepared for further comparison: average value of the parameter for scenario 1, scenario 2 and scenario 3. Additional average value of the free burning scenario is available for MLR and volume fraction of $O2/CO_2$ in the duct. The time of ignition was determined from the output results as the time when the measurements by the thermocouples began to show a slight temperature raise. Because of the delay of the gas analyser measurements, different t=0 had to be determined for Oxygen measurements. This was also done manually in the output file, by finding the moment of time when the concentration of O_2 began to notably drop down. Clearly, 4 repetitions of the same tested scenario had different durations due to variable initial conditions and environmental conditions during the test performance. The end of the test was chosen as the time when 2 repetitions out of 4 had completely burnt out. The complete burn out was determined according to the measurements of the load cell. To avoid noisy results and simplify further analysis it was decided to reduce the outputs, leaving averaged values corresponding to every second minute only for all measured or computed parameters. To do so, the averaged values of measurements taken 20 seconds before and 20 seconds after the time point were used.

3.2.1 MLR

In the output file the measured mass of the sample at each second can be found. Mass loss rate can be estimated as the difference of sample mass at subsequent time steps. For simplifications, mass loss rate corresponding to every 2 minutes of the test were taken and plotted for each scenario (Figure 5).

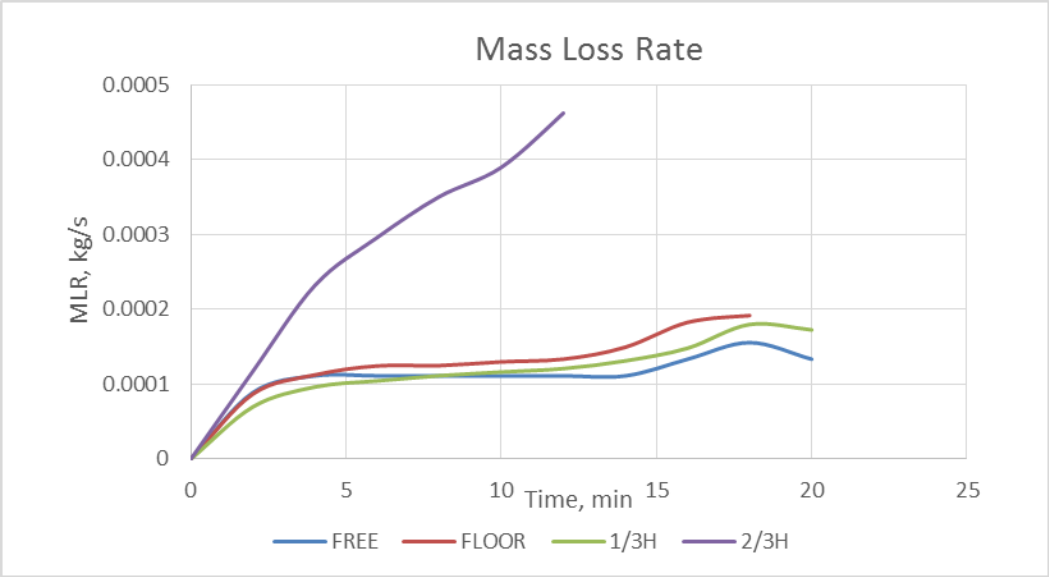

Figure 5. Variation of MLR over time for 3 different elevation scenariosand free burning.

From Figure 5 it can be noticed that the mass loss rate during the free burning of Heptane is smaller than during enclosure fires. That was expected as when the fire is inside the enclosure, it receives radiation from the heated up boundaries and hot gas layer. This radiation leads to additional loss of mass due to release of volatiles, in accordance with the equation below [16] (Eq.(3.1)):

$$\dot{m}'' = \frac{\dot{q}''}{\Delta H_g} \tag{3.1}$$

Where for this case

m'' – additional mass flux or mass burning rate per unit area, kg/(m^{2}s);

$\dot{q}''$ – net heat flux from the boundaries and smoke layer, kW/m^2;

ΔH_g – the heat of gasification (evaporation) of the fuel (Heptane), kJ/kg.

Clearly the closer fuel surface to the smoke layer, the greater is the magnitude of the net heat flux q''. That is why the MLR for the highest elevation scenario (2/3 of the room height) is considerably greater than for all other tested configurations. Yet, the variation of MLR over the time for elevation scenario 2 (fuel is at 1/3 of the height of the room) is below the one for scenario 1 (fuel near the floor), even though it is positioned closer to the source of radiation. There are several factors contributing to such result. First of all, the net heat flux is not linearly dependent on distance to the target, but it is inversely proportional to the distance in power of two [2] (Eq.(3.2)):

$$\dot{q}'' \sim \frac{1}{D^2} \tag{3.2}$$

Where D – is distance from the radiation source to the target.

Because of this relation (Eq.(3.2)) it is likely that the radiation received by the fire base during the scenario 2 is not significant, and comparable to the scenario 1. Another factor that affects the mass loss rate, is the availability of the oxygen around the fuel bed. The higher the fire source, the lesser oxygen concentration around it, due to limited air flow movement. When the fire is near the floor, it gets the maximum amount of available oxygen, but when it is elevated to 1/3 of the room's height, the combustion is limited by the supply of oxygen. This can be the reason that the measured MLR of scenario 1 is higher that one of the scenario 2. It also can be seen that for all 4 tests, at some point in time not long before the complete burnout, a sudden raise of MLR occurred (after 10 minutes for scenario 3,and after 15minutes for others) (Figure 5). This is likely to happen due to the fact that the metal pan containing the fuel, got heated up and this additional heat contributed to the rate of fuel combustion, increasing the total MLR of Heptane.

To sum up, two factors influence the measured differences in rate of mass loss: availability of oxygen and radiation from the smoke layer and boundaries. When the fire is sufficiently close to the ceiling, the second factor dominates, leading to the higher MLR and shorter duration of burning.

3.2.2 HRR

Rate of heat released was not measured directly, however, there are two ways to calculate HRR using experiment's output: by oxygen consumption and by mass loss rate of fuel. The second method involves the use of combustion efficiency, but this parameter is unknown and is likely to change with elevation due to change of available for combustion oxygen. Thus, the Oxygen Depletion method was applied. This method is based on the observation that, for almost all fuels, a reasonably constant amount of energy is released per unit mass of oxygen consumed during combustion. This amount was found to be around 13100 kJ per kilogram of consumed oxygen. [16] This method is well-defined by Janssens [17]. The steps described in his paper were followed in order to determine heat released during the performed experiments. Detailed calculations can be found in Appendix A. Plotted results are presented in the following Figure (Figure 6):

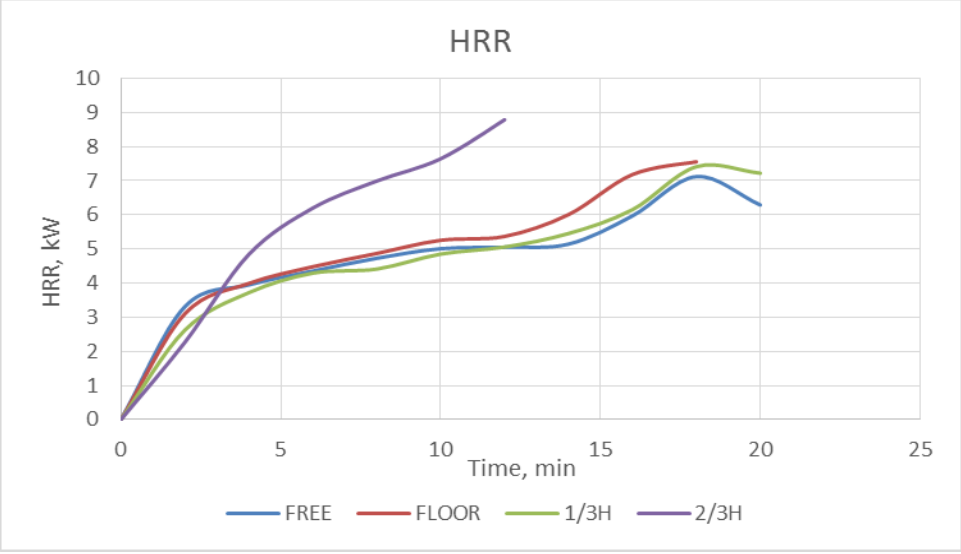

Figure 6. Variation of HRR over time for three elevated scenarios and free burning

During the first minutes of the burning, the heat released by lower positioned fires are greater than by fire elevated closest to the ceiling. It is possible that when the fire located that high the amount of oxygen available for combustion limits the rate of released energy. However, just 5 minutes after ignition, the HRR of the fire that is located near the ceiling surpasses the HRR of all other scenarios and continues rapidly increasing to its peak of 9kW after just 12 minutes. Evidently, the elevation of the fire source at some point starts to significantly affect the heat released rate. The re-radiation from the ceiling and upper parts of the walls enhances the rate of mass being consumed, which is directly related to heat release rate. It is obvious that the closer the fire source is positioned to the source of radiation the higher the impact, this is due to a bigger value of the view factor.

The rates at which energy is released during the combustion of the fuel in the open air, of the fuel positioned on the floor and of the fuel elevated to 1/3 of the height of the enclosure are quite similar. In these scenarios, rate of heat released reached a peak of about 7.1-7.5kW with the average of 5.5kW. Though, the heat release rate when the fuel burned outside of the enclosure is slightly lower. This is again explained by the fact that when fire burns in the open air, all heat that is released is lost to the surrounding air, and no re-radiation is received in the fire bed.

In general, variations of HRR for all 4 scenarios follow similar trends for the corresponding variations of MLR. Although, the difference between MLR of scenario 3 and others is more striking than their differences in HRR.

3.2.3 Combustion Efficiency

According to Babrauskas [18], in case of the well-ventilated fire, the HRR is supposed to be proportional to the MLR, this is shown by the equation that he has developed Eq.(3.3)):

$$\dot{Q} = \dot{m} \cdot \Delta H_{eff} \tag{3.3}$$

where

$\dot{m}$ - mass loss rate, kg/s;

ΔH_{eff} – effective heat of combustion, kJ/kg.

Yet, comparing Mass Loss Rate variations over time (Figure 5) with the graphs of HRR (Figure 6) one can notice that general trends are not absolutely similar. Figure 5 demonstrates stronger dependency on the elevation than Figure 6. MLR corresponding to the scenario 2/3H is much greater comparing to other scenarios, while the difference of HRR relating to different elevations is not so remarkable. Evidently, the effective heat of combustion, ΔH_{eff}, must be also dependent on the source elevation.

Heat of combustion represents the energy released in the form of heat when the fuel undergoes combustion. Complete heat of combustion (ΔH_c) can be measured if the fuel undergoes complete combustion and no char or residues are left. This parameter can be measured in a bomb calorimeter, and values for many fuels are known and can be found in the related literature. Yet, complete combustion rarely occurs, so it is not representative for real fires, therefore, the parameter effective heat of combustion has been introduced. Generally, effective heat of combustion constitutes 70-80% of the complete heat of combustion. Therefore, effective heat of combustion can be found by multiplying complete one by a coefficient, known as combustion efficiency (X_{eff}) (Eq.(3.4)):

$$\Delta H_{eff} = \Delta H_c \cdot X_{eff} \tag{3.4}$$

thus,

$$\dot{Q} = \dot{m} \cdot \Delta H_{eff} = \dot{m} \cdot \Delta H_c \cdot X_{eff} \tag{3.5}$$

Complete Heat of Combustion is not expected to change if the fire position changes, as it is a constant value measured in the open air. Therefore, it must be the global combustion efficiency that gets affected by the fire elevation. The global combustion efficiency depends on the type of fuel and, also, the environment surrounding the fuel, more particularly the oxygen availability [16]. An enclosure restricts the amount of oxygen available for the combustion. The further raise of the fuel source limits the amount of oxygen even more, by decreasing the distance between the fuel bed and the ceiling, the amount of oxygen around the fuel bed becomes lower and also air entrainment gets reduced. Because of that, fires at different elevations can burn with different efficiency, specifically, the higher elevation, the lesser amount of oxygen and smaller the global combustion efficiency.

To find the values of the global combustion efficiency for each elevation, the equation (3.5) can be modified (Eq.(3.6)):

$$X_{eff} = \dot{Q}/(\dot{m} \cdot \Delta H_c) \tag{3.6}$$

HRR and MLR have been found and plotted earlier (Figure 5 and Figure 6), complete heat of combustion of Heptane is assumed to be 44.6 kJ/kg. Thus, if the equation (3.6) is substituted in the spreadsheet, the combustion efficiency versus time dependency can be plotted for each scenario (Figure 7.)

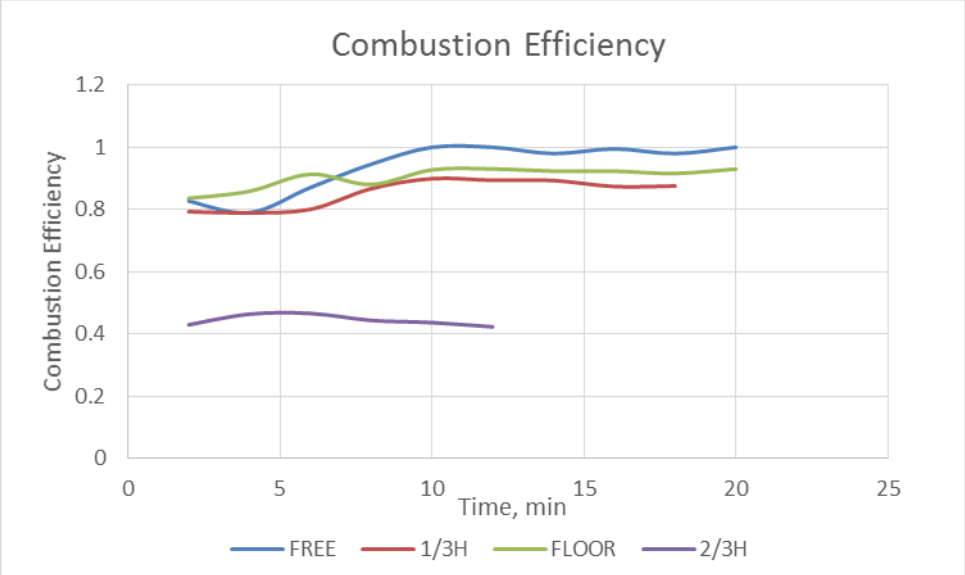

Figure 7. Variation of combustion efficiency over time for three elevation scenarios.

According to obtained results, combustion efficiency of the free burning fire on average is equal to 0.94. According to SFPE [2] the combustion efficiency of Heptane is close to unity and estimated to be

0.92. The found combustion efficiency is believed to be reasonably accurate, as the difference of 0.02 can be caused by imprecision of the experiment or by assumption of the heat of combustion value. The combustion efficiency of the free burning case is also higher than for enclosure fires (Scenario 1, 2 and 3). Which is logical, as there was no air restriction for this case. For the fire located on the floor the averaged over time combustion efficiency is found to be 0.9. This value seems high, but still can be possible, considering the large opening that could provide sufficient amount of air. It can be seen from the graph that when the fire gets elevated combustion process becomes less efficient. The difference is not striking for the 2nd elevation scenario (1/3H), and the achieved averaged value is 0.85. However, when the fire is elevated to the 2/3 of the room's height, and the flame is forced to run over the ceiling, lack of the oxygen causes the drop of the global combustion efficiency below 45%.

3.2.4 Hot Gas Layer Temperature and Interface height

Temperatures at different heights were measured by means of a thermocouple tree. However, in fire engineering practice, for compartment fires, a two-zone model concept is used. This concept assumes that in pre-flashover compartment fires, two distinct layers developed: an upper layer consisting of hot gases and lower layer consisting of cooler air (Two-zone model concept). For further analysis, HGL temperature and interface height for the tested scenarios should be determined from thermocouples measurements. There are several data reduction methods that allow to convert multiple temperature measurements to a single HGL temperature. The chosen one-dimensional analytical method was successfully used in many published papers. [19][20][21] The explanation of the method and the calculation procedure can be found in Appendix B.

After performance of the calculating procedure (App.B), the variation over time of HGL temperature and HGL height can be plotted (Figure 8 and Figure 9).

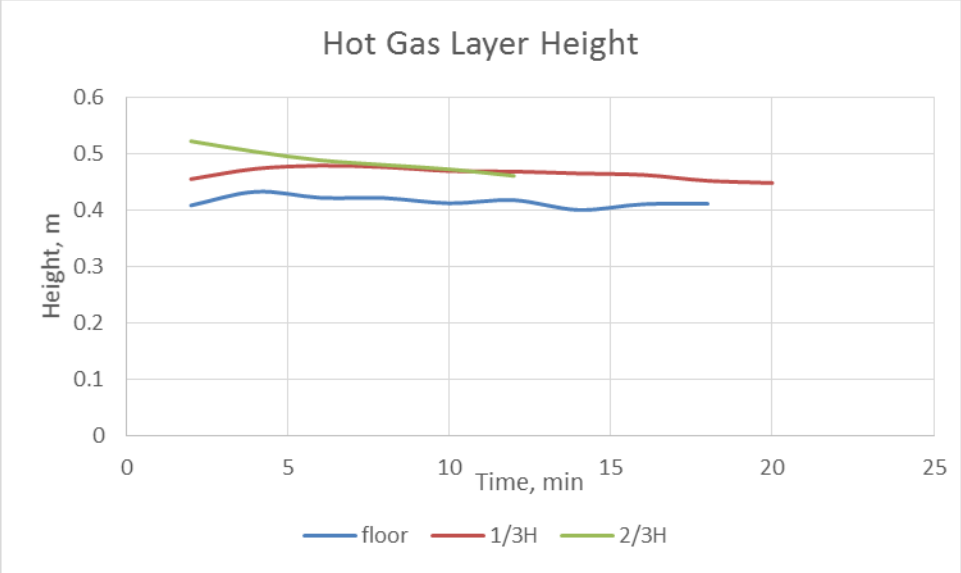

Figure 8. Variation of the hot gas layer height over time for three elevated scenarios.

Figure 8 represents the hot gas layer height fluctuation over the time for three elevation scenarios. For the first scenario the fire source was not exactly placed on the floor, but because of the load cell, fire was slightly lifted by just 0.08 m over the floor. The height of the smoke layer during all

burning periods was slightly fluctuating between 0.4m and 0.425m, raising in the beginning of the tests and going down closer to the end. For the second scenario fire was elevated to 0.275m above the floor. The smoke layer rapidly rose to 0.48m above the floor, and then slowly descended by 3 cm to 0.45m. For the last scenario, the fuel pool was placed 0.535m above the floor which was just 0.265m below the ceiling. In this case the smoke was constantly descending throughout the experiment from 0.52m to 0.46m, and it was below the fuel pan already after 2 minutes.

It can be concluded that the vertical position of the fuel affects the position of the smoke layer. The lower the fire, the lower the smoke can descend. Elevation of the fire source might affect temperature gradient distribution inside the enclosure, which will influence the pressure profiles. Pressure profiles across the room height is a critical factor that determines how the hot air from the enclosure will flow out of the room. Evidently, smoke will be prevented to descend below this height (in FSE known as neutral plane) and will be pushed out instead. It is also possible that the higher elevated fires produce thinner smoke. The closer the fire bed is to the ceiling, the lesser the amount of air entrainment, which leads to a smaller amount of produced smoke.

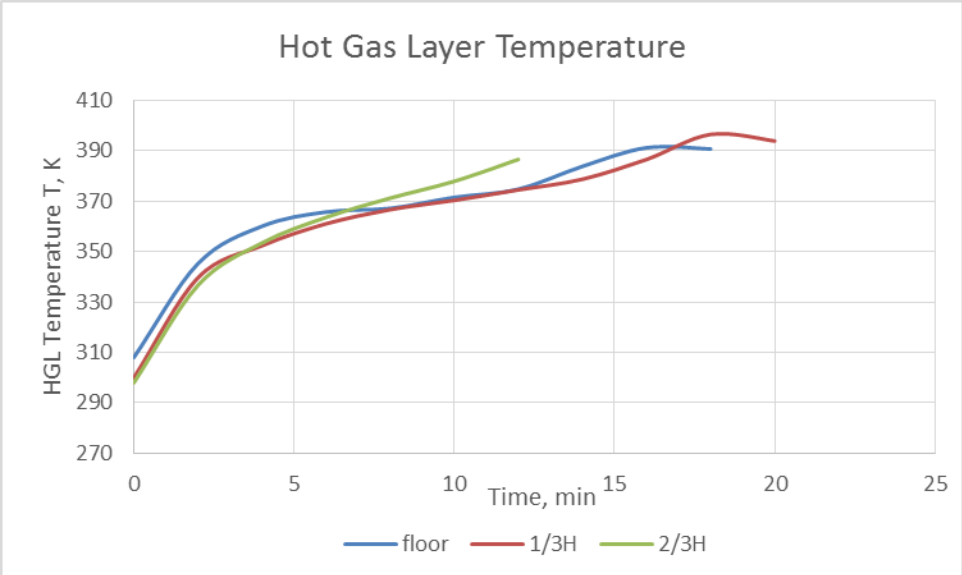

Figure 9. Variation of the hot gas layer temperature over time for three elevation scenarios.

Looking at the experimental results of HGL temperatures (Figure 9) some differences can be noticed with respect to the source elevation. From Figure 9 it can be seen that during the first 5 minutes of the experiment the highest HGL temperatures occurred for the fires positioned on the floor. This, probably, is not caused by the differences in vertical positions of the source, but simply by the fact that initial temperatures inside the enclosure were higher during the tests with source at floor level, due to the inaccuracy of the test performance. Therefore, it is an inaccuracy of the test performance and should not be taken into consideration. 7 minutes after the ignition, the HGL temperature in the tests with the fire placed under the ceiling, started to increase sharply, reaching its peak of 386K just after 12 minutes and burning out afterwards. The HGL temperature in the other two scenarios reached this temperature only 3-4 minutes later. The highest HGL temperature reached during all tests was 396 K and it corresponded to the source being elevated to 27.5 cm above the floor.

After observing results for three elevation scenarios, it is possible to conclude that temperature of the hot gas layer increases faster for the fire source at the highest position (scenario 2/3H). Several possible explanations to this can be named. First of all, according to the energy conservation principle, some part of the energy released from the combustion gets spent for the temperature rise. Consequently, the higher HRR produced by fire, the higher should be the raise of temperature. As it was said, the fire elevated to 2/3 of the enclosure height yielded greater HRR than fires during other scenarios.

Moreover, the closer the fire base is to the ceiling, the lesser heat losses from the plume to the surrounding cooler air and lesser the air entrainment into the plume that cools it down. Thus, smoke produced by the highest elevated fire, looses less heat on its way to the ceiling, resulting in greater temperature of the smoke layer. On the other hand, proximity to the ceiling leads to greater heat losses through the ceiling from the hot gas layer to the outside air. It is not possible to confidently state which losses: from the plume to surrounding or from the smoke layer/ceiling to the outside, are greater. Thus, their combined influence on the HGL temperature is unidentified.

Also, it was visually noticed in course of the experiment that only the very top of the flame sometimes touched the smoke layer when the fire was set near the floor (scenario 1). At the same time, if the fire was elevated to 1/3 of the room's height, a more significant flame-smoke layer interaction has been observed. But, the highest elevated fire (scenario 3) was burning inside the hot gas layer. Below photos made during the tests are presented (Figure 10). If the flame could touch the smoke layer that implies that the layer was directly heated by the flame that was at least 1000°K [22]. It should be expected that scenario 2 and 3 should yield higher HGL temperature than scenario 1, where just little interaction between flame and smoke layer was noticed. Propagation of the flame caused by interaction with the ceiling that was observed during tested scenario 3, possibly lead to the most intensive heat transfer between the flame and the hot gas layer, resulting in such rapid increase of HGL temperature.

Figure 10. Photo made during the experiments depicting the flame – smoke layer interaction.

Overall, if the fire is elevated high enough so that its flames impinges the ceiling, the temperature of the hot gas layer escalates faster than if the fire positioned at the elevation that prevent its flames to

directly interact with the smoke layer. However, the differences in the magnitude of reached temperatures are not that significant – 15K maximum.

3.2.5 Radiative Heat flux

Data on the magnitude of the radiative heat flux received at the floor level can be found directly in the tests output file (Figure 11).

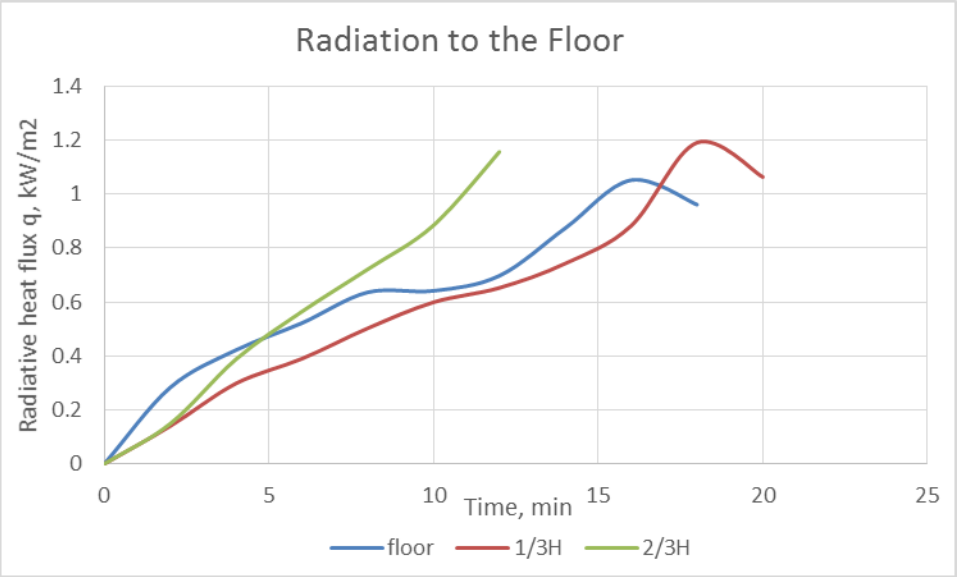

Figure 11. Variation of the received radiative heat flux to the floor over time for three elevation scenarios.

From Figure 11, it can be observed that during the first 5 minutes after ignition the highest radiation registered by the flux-meter corresponded to the first scenario. It should be remembered that the initial temperature for all repetitions of this test was slightly greater. Also, the fire was located closer to the flux-meter and radiation from the flame was greater than when fire source was elevated higher. The total re-radiation from the boundaries and smoke layer was insignificant as the temperatures considerably raised later. Also, coming back to the graphs representing HGL temperatures (Figure 9), one can see that HGL temperature during this period of time was quite similar for all elevation scenarios. However, after 5 minutes, the pattern has changed for the last scenario. The value of received radiation started to increase greatly 5 minutes after the ignition almost reaching 1.2 kW/m^2 only 12 minutes after ignition. For comparison, the same value during the second scenario was reached only 2 minutes later. Once again, the reason for such high measured values for the last elevation case can be explained by radiation of the flame that impinged the ceiling occupying large area of it. When the fire was placed 0.275m above the floor, the radiation that reached the floor was the smallest, as at the same time, source was remote from re-radiating surfaces (boundaries and smoke layer) and its flame was away from the flux meter.

4 Modelling

4.1 Grid Size

An attempt was made to simulate the performed experiment using a computational fluid dynamic software. The Fire Dynamic Simulator, FDS was chosen for this purpose. The grid size selected for the simulation has a big impact on the precision of results. The smaller the grid the closer results will be to the reality. To justify the suitability of the grid size for the buoyant flames there is a method that can be used, which suggests that, the more cells spanning the fire the better the resolution of the calculations. [23] Therefore, the non-dimensional expression (D*/dx), where D* is a characteristic fire diameter of the modelled fire and dx - the selected grid size (dx), was introduced. The characteristic fire diameter, D*, can be found by applying the equation below (Eq.(4.1)):

$$D^* = \left(\frac{\dot{Q}_{fire}}{\rho_\infty c_{p\infty} T_\infty \sqrt{g}}\right)^{2/5} \tag{4.1}$$

Where $\rho_\infty, c_{p\infty}, T_\infty$ - are the density, specific heat and temperature of the ambient air respectively, g is the acceleration due to gravity, m/s^2.

According to the U.S. Nuclear Regulatory Commission, to yield reasonably accurate results, the following should be true: [24]

$$4 \leq \frac{D^*}{dx} \leq 16$$

Another range is used in Danish best practice to valid grid size resolution:

$$10 \leq \frac{D^*}{dx}$$

The grid sized used in the simulation was 0.05m. The characteristic fire diameter, assuming HRR of the fire to be equal to 7kW:

$$D^* = \left(\frac{\dot{Q}_{fire}}{\rho_\infty c_{p\infty} T_\infty \sqrt{g}}\right)^{2/5} = \left(\frac{7}{1.2 \cdot 1 \cdot 298 \cdot \sqrt{9.8}}\right)^{2/5} = 0.14$$

Then

$$\frac{D^*}{dx} = \frac{0.14}{0.05} = 2.8 < 4; \ll 10$$

Apparently, the chosen grid size is unable to accurately resolve calculations for such small fire, especially for the first minutes when the total HRR was even smaller than 7kW. Obtained results should be considered approximate, and in order to get more precise value the grid size has to be reduced. However, the smaller grid size will cause the increase of computational time, which was already quite long. In any case, the main objective of the simulation is to determine whether the FDS is capable to demonstrate the influence of the fire elevation and the enclosure, rather than to provide exact values of different fire parameters. Consequently, it was decided to keep the coarse mesh, but to consider it during the successive analysis.

4.2 Setup

The modelled enclosure had configuration and dimensions similar to the ones used in the experiment (see chapter 3.1). However, due to the mesh used, all dimensions were rounded off to 5 cm. The same is true for elevation distances, for the simulation the following values were used:

Scenario 1: Fire elevated by 0.1m;

Scenario 2: Fire elevated by 0.275m;

Scenario 3: Fire elevated by 0.535m.

The pan was changed from the circular to the square one 10x10cm. The fire was introduced by its mass loss rate per unit area (MLRPUA), the values of which were found by dividing the MLR, measured during the free burning tests (see Figure 5), by the area of the fuel pan (0.00785m^2) (Table 3).

Table 3. MLR and MLRPUA used for the simulations

Time, min	**2**	**4**	**6**	**8**	**10**	**12**	**14**	**16**	**18**	**20**
MLR, 10^{-4} kg/s	0.89	1.11	1.11	1.11	1.11	1.11	1.11	1.33	1.56	1.42
MLRPUA, kg/(sm^2)	0.011	0.014	0.014	0.014	0.014	0.014	0.014	0.017	0.02	0.019

To reproduce the developing fire, the time-based ramp function of the mass loss was used. The similar values from the Table 3 were united to shorten the ramp (Table 4)

Table 4. Values and fraction of MLRPUA used for ramp function.

Time, s	**MLPUA, kg/sm^2**	**Fraction**
0	0	0
120	0.011	0.6
240	0.014	0.7
960	0.017	0.85
1080	0.02	1.0

In order to recreate the experimental setup the following devices were used in FDS:

Upper Layer Temperature – to provide the time history of the HGL temperature, assuming two-zone model. In FDS the same data reduction principle is applied for the upper temperature calculations than the one used for processing experimental results (Appendix B. Hot Gas Layer Temperature and Height, Reduction Method). Therefore, the following further comparison can be made directly without accounting for any methodological differences.

Layer Height – this device allows calculations of the smoke layer position along the specified vertical line at any moment of time. In order to reduce the calculation time, this line was appointed to start 0.2m above the floor and finish 0.05m below the ceiling. FDS uses the same data reduction method that was applied in this study (see section 3.2.4).

Radiometer – this device represents the measurements of the flux meter similar to one used in the experiment, therefore, it was positioned in the centre of the modelled enclosure.

The most challenging part of this model is to represent the effect of the actual elevation. It is apparent that such function is not included into the existing version of FDS. However, J. Wahlqvist have developed a simplified environmental feedback model that serves for that purpose [25]. This sub-model takes into account two important fire behaviour phenomenon: the reduction of the mass loss rate resulting from the decrease of the oxygen concentration near the fire base (Eq.(4.2)) and the increase of the mass loss rate due to the re-radiation from the heated boundaries and hot gas layer (Eq.(4.3)).

$$\dot{m}''_{O2} = \dot{m}''_{\infty} \cdot (0.1 \cdot O_2[\%] - 1.1) \tag{4.2}$$

$$\dot{m}''_{rad} = \frac{\dot{q}''_{rad\ in,external} - \dot{q}''_{rad\ out,fuel}}{\Delta h_{v,fuel}} \tag{4.3}$$

Then, the total mass loss rate:

$$\dot{m}''_{O2} = \dot{m}''_{\infty} \cdot (0.1 \cdot O_2[\%] - 1.1) + \frac{\dot{q}''_{rad\ in,external} - \dot{q}''_{rad\ out,fuel}}{\Delta h_{v,fuel}} \tag{4.4}$$

More detailed description of the development of this simplified sub-model can be found in the referenced paper [25]. The model proposed by J.Wahlqvist has been implemented into FDS (version 6.1), the inputs needed to use the model are mass loss rate per unit area (MLRPUA), total fuel mass, surface temperature (f.e. boiling temperature of the liquid fuel) and heat of vaporization. One weakness of the simplified environmental feedback model for this particular study is that it cannot reproduce the ceiling impingement by flames, which might be a crucial factor for scenario 3.

Example of the FDS input file for scenario 1 can be found in Appendix E.

4.3 FDS Results

Three simulations representing the three scenarios tested in the fire laboratory were simulated in FDS. The simulations provided results on HRR, Mass Loss Rate, HGL temperature and height and radiative heat flux on the floor.

4.3.1 Mass Loss Rate

Equal Mass Loss Rate per unit area was input for every simulated scenario. However, the total mass loss rate calculated by the FDS was also influenced by Oxygen concentration and received radiation from the boundaries and a smoke layer. The Figure 12 below shows the variation of the total mass loss rate over the time for every elevated scenario.

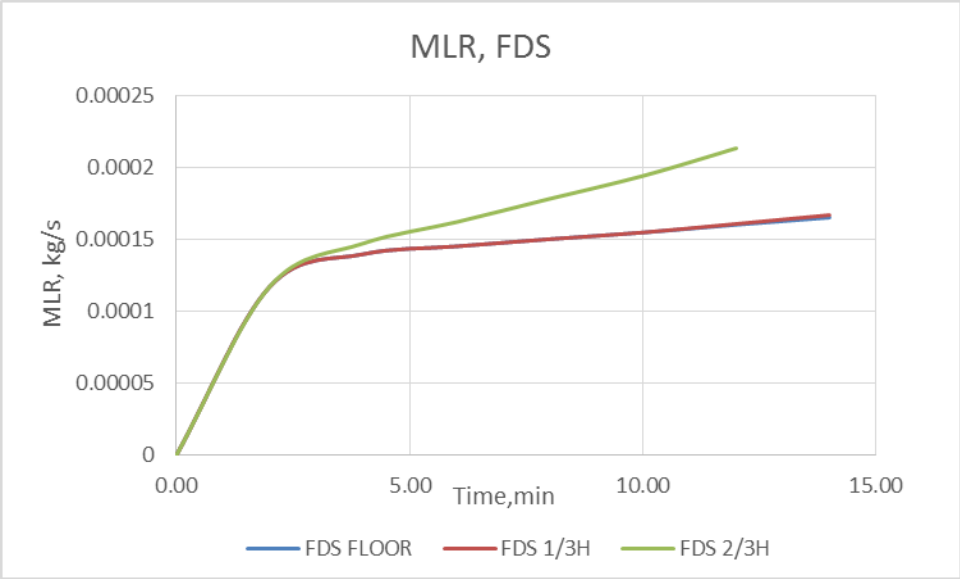

Figure 12. Total MLR calculated in FDS

It can be seen from the graph (Figure 12) that all three simulations give the same results for the first 2 minutes of burning. It can be assumed that during this period of time the concentration of oxygen near the fire source is stable, the temperature in the enclosure does not raise sufficiently high to significantly heat up the walls and the smoke layer is still rather weak. However, after 2 minutes some differences between simulations can be observed. Yet, for the fire near the floor and the fire elevated by (1/3H) over the floor, the predicted total mass loss rate, by FDS, is almost the same through all period of burning. It can be guessed that fire near the floor has more oxygen available for combustion, while fire elevated to 1/3H receives greater fraction of radiation from the walls and a smoke layer, overall this results in quite similar total MLR for both elevations. It can be seen from the Figure 12 that the highest source elevation (2/3H) leads to the highest MLR, most likely it is caused by the proximity of the fire source to the hot gas layer and to the hottest part of the boundaries. Thus, the amount of received radiation well compensates for the lesser amount of oxygen, yielding greater burning rate.

To see how accurate the values are predicted by FDS, they are compared to the MLR that was measured in course of the experiment (Figure 13).

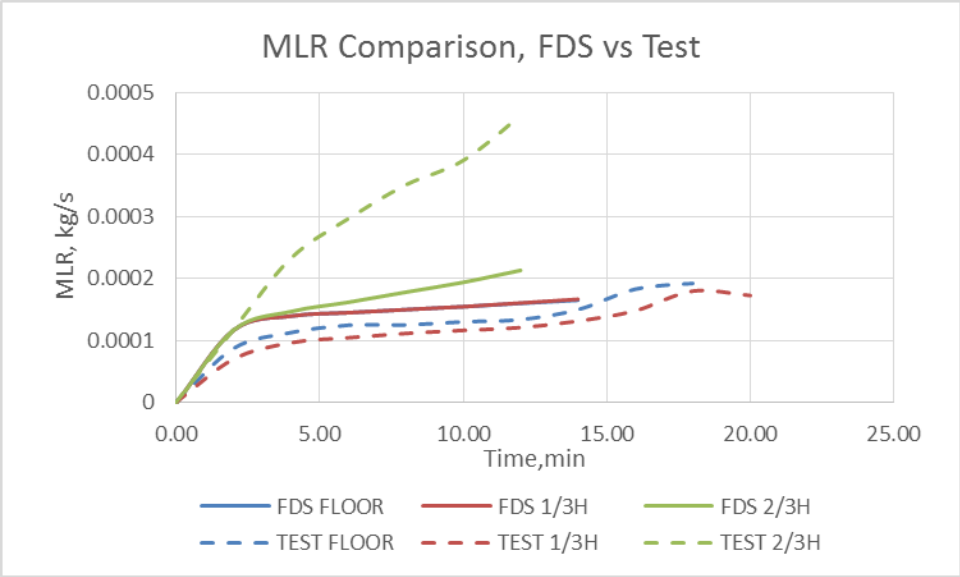

Figure 13. Comparison of the MLR calculated in FDS and measured experimentally.

The interesting observations can be made from the graphs (Figure 13), MLR calculated by FDS for the two lowest elevations are greater than the experimentally measured ones, while the MLR for the scenario 3 is much lower than the measured one. The high values of MLR for scenarios 1 and 2 can be explained by inaccuracy of the input parameters. In section 4.2 the process of specifying MLR per unit area was described. As it was said, the experimental MLR for free burning case was divided by actual area of the pan of 0.0078m^2. It was overlooked, that due to the square grid, the Heptane pool in simulation has a rectangular shape with area 0.1x0.1=0.01m^2, and not 0.00785m^2. Because of that oversight, the total MLR calculated by FDS should be greater than the experimental by 27%:

However, the input mistake does not explain why FDS underestimated the MLR for the scenario 3 (2/3H). Perhaps, FDS does not consider all sources of external radiation or underestimates them. But most likely, such difference with experimental results is caused by the fact that in the test, for the scenario 3, the ceiling impingement by flames occurred and FDS is not capable to account for that. The flames, extended across the ceiling, is a critical component of the total radiative heat flux received by the fuel surface, ignorance of which leads to gross underestimates.

4.3.2 HRR

Rate of heat released by fire was calculated using the specified mass loss rate per unit area of the fuel. Because of that, the overall pattern of HRR variation over time plotted on the Figure 14 is quite similar to the pattern of MLR variation on Figure 12. All three simulations behave identically for the first 2 minutes of the simulation, then the two lowest fires keep producing similar results, while the fire closest to the ceiling releases energy with greater rate.

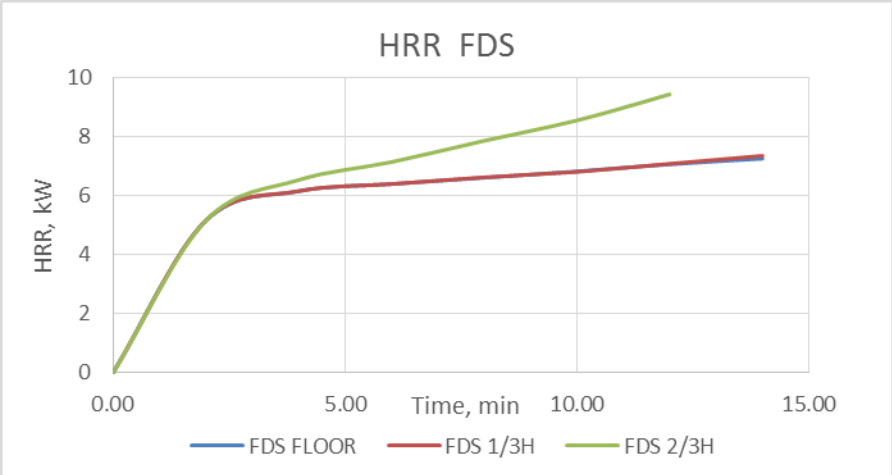

Figure 14. HRR calculated during the FDS simulation

Comparing to the experimental results (Figure 15), it can be noticed that the rate of energy released calculated by FDS for all three simulations is higher than HRR found from the experimental results. The first reason for that, is certainly, the higher MLR calculated by FDS due to inaccurate inputs. Another reason, is that the global combustion efficiency, as appeared, has to be specified for FDS simulations. This was deliberately not done to test the assumptions of the calculations involved in the Environmental feedback model of J.Wahlqvist [25]. It turned out that only chemical combustion efficiency was applied by FDS, equal for all simulated scenarios. Because of that, there is no difference in HRR calculated for scenarios 1 and 2.

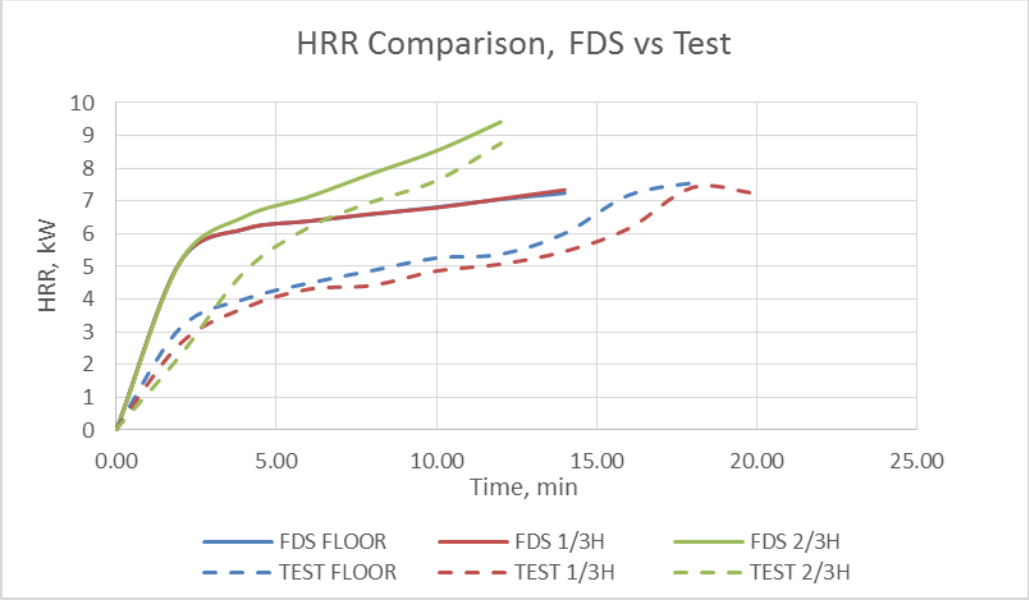

Figure 15.Comparison of the HRR calculated in FDS and measured experimentally.

4.3.3 HGL Temperature and Height

According to results calculated by FDS, the higher the elevation of the fire the greater is the temperature of the hot gas layer (Figure 16) and the lesser the smoke layer can descend (Figure 17). Yet, the predicted raise of temperature is not linear to the raise of the fire position. The difference between the first and the second elevation, and the second and the third is about 260mm, while the differences in HGL temperatures between these pairs of scenarios are far from being equal (Figure 16). This can be explained by the fact that the radiation is proportional to the distance in power of 2, which has been earlier discussed in the section 3.2.4. Thus, the fire located closer to the ceiling is supposed to receive heat flux in power of 2 of the heat flux received by the fire at 1/3 of the room's height.

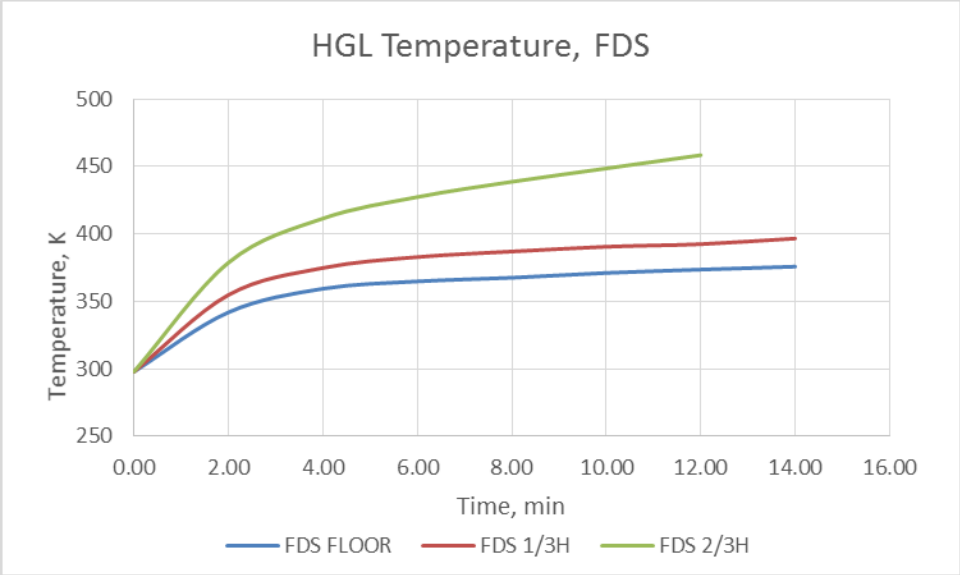

Figure 16. HGL Temperature calculated by FDS

On the figures representing the position of the smoke layer (Figure 17), additional lines indicating fire position are plotted, so it could be seen that FDS does not allow the descending of the smoke below the fire source. Also, the position of the HGL stays constant trough all burning time.

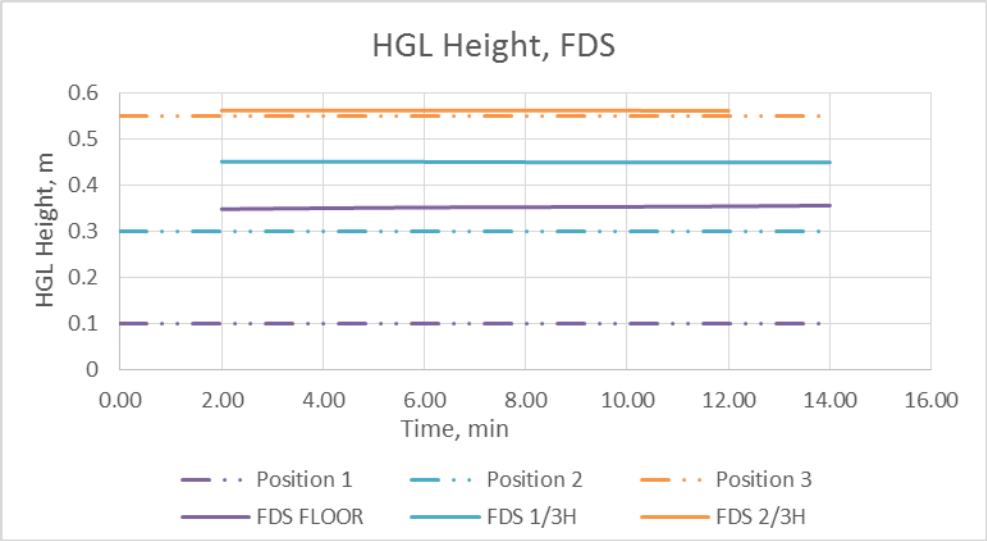

Figure 17. HGL Height calculated by FDS

The two figures below (Figure 18 and Figure 19) present the comparison of HGL properties calculated by FDS and found from experimental measurements by using data reduction method. Temperatures calculated by FDS for the fires raised above the floor, appeared to be higher than experimental ones (Figure 18). Obviously, the higher values of HRR and MLR could cause this. It is also possible that FDS does not account for all heat losses from the system or entrainment of cooler air.

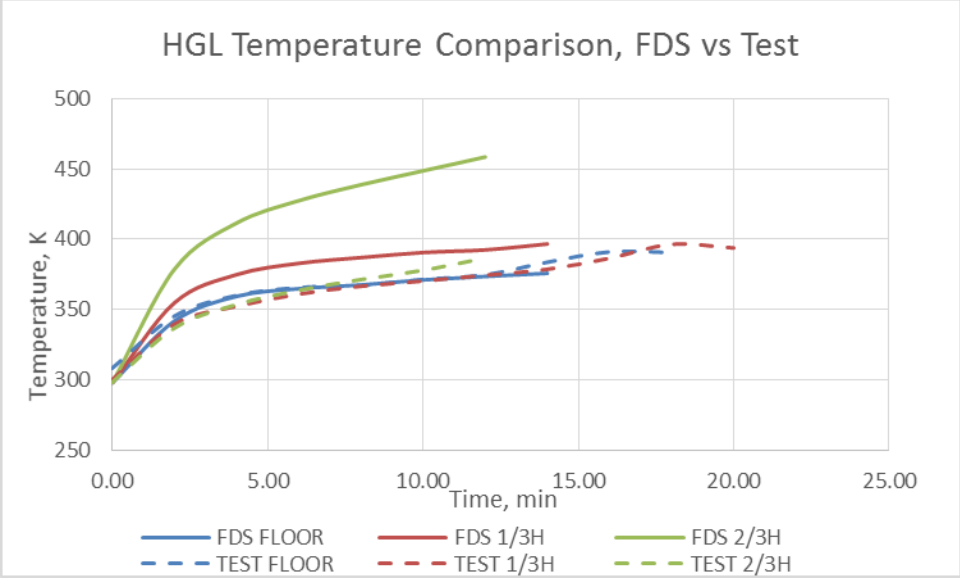

Figure 18. Comparison of the HGL Temperatures calculated in FDS and measured experimentally.

FDS assumption that smoke layer cannot reach the fuel base is not supported by the experimental results, where smoke layer in test of the scenario 3 descended at least 10cm lower than the fuel pan (Figure 19). Moreover, through the duration of the tests, the smoke layer was gradually lowering and slightly fluctuating, but not staying constant.

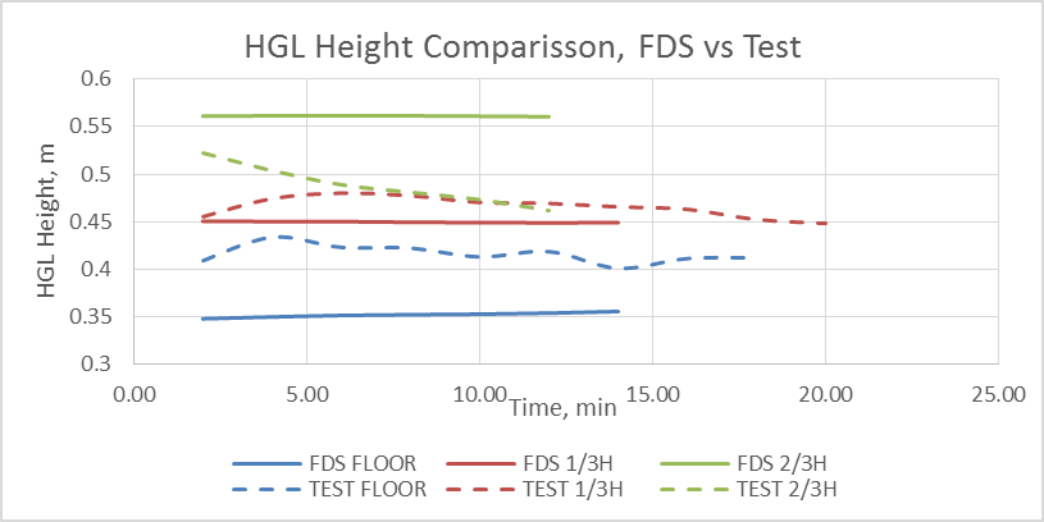

Figure 19. Comparison of the HGL Height calculated in FDS and measured experimentally.

4.3.4 Heat Flux

In the graph below, the calculated heat flux received at the centre of the floor is plotted (Figure 20). From this image one can see that the closer fire is positioned to the flux meter the higher heat flux it detects. Thus, the flame by itself is the main source of radiation that reaches the floor, at least in the beginning of the room burning. The fire located near the floor resulted in the greatest heat flux. The second highest value for the first 11 minutes, was yield by fire elevated to 1/3 of the room's height. But after 11 minutes the fire near the ceiling produced greater heat flux than the one below it. If the fire of scenario 3 did not burn out so rapidly, it could reach the values of heat flux yielded by fire near the floor. Therefore, if the fire is positioned high enough, the boundaries and smoke layer can reach such temperatures that the total radiation (from flame, layer and surfaces) surpasses the radiation from the less elevated fire.

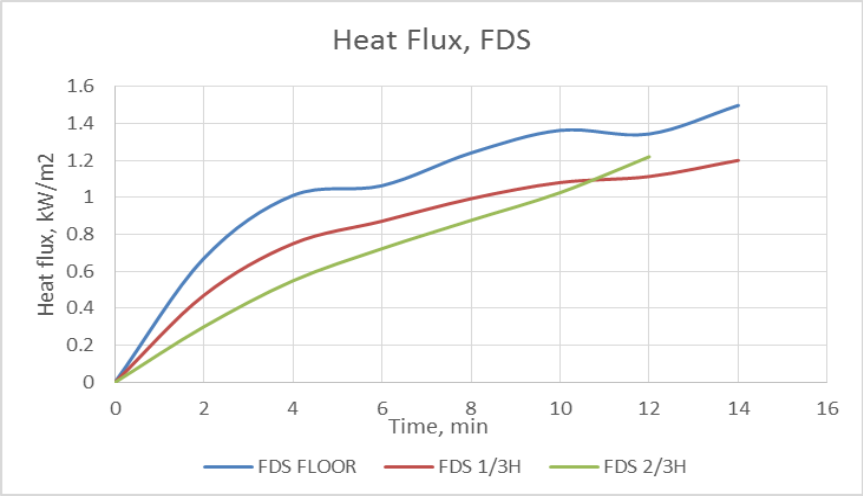

Figure 20. Radiative Heat Flux at floor calculated by FDS

The Figure 210 and Figure 201 gives an idea of how far the FDS results are from the experimental measurements, as it can be seen the heat flux calculated by FDS is nearly twice as high as the measured one, except for the scenario 3, where the difference is less striking. Though, it is not entirely appropriate to compare these two methods. As the dissimilarity between experimental HRR and HRR calculated by FDS make it impossible to justify weather the difference in heat flux measurements are caused by FDS assumptions or by HRR values.

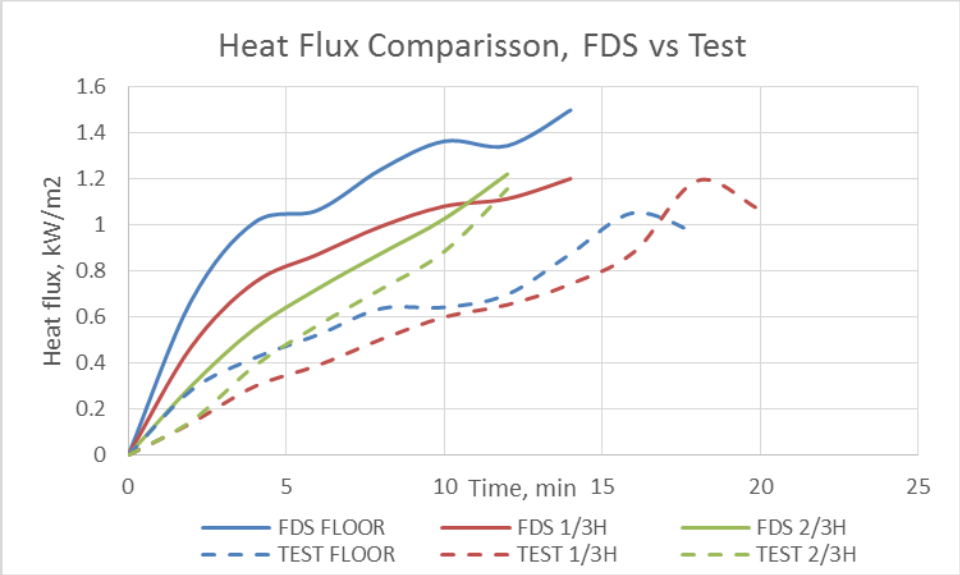

Figure 21. Comparison of the Heat flux calculated in FDS and measured experimentally.

Overall, the accuracy of the calculations of FDS or any other simulation tool is ensured by the precision of the input parameters. Attention should be paid when introducing these parameters, how the model will implement computations is should also be taken into consideration.

5 Analytical Methods

In this part of the work, parameters of interest are going to be estimated analytically using methods and equations found in the available literature.

5.1.1 MLR

After performing a large number of free burning experiments with fuel pools of various diameters the following equation for the mass loss rate per unit area was arrived at (Eq.(5.1)). This equation implies that mass loss rate is influenced by the diameter of the pool and, also, by two empirical constants, *k* and β, that depends on the fuel type. k – is the extinction-absorption coefficient of the flame and β – is the mean beam length corrector. These parameters present a function of radiative heat flux from the flame toward the fuel.

$$\dot{m}'' = \dot{m}''_{\infty}\left(1 - e^{-k\beta D}\right) \tag{5.1}$$

It is possible to find in available literature data for different fuels. [16] For the Heptane found values are:

$$\dot{m}''_{\infty} = 0.101$$

$$k\beta = 1.1.$$

It is important to remember that equation 5.1 and experimental data are valid for fuel pools with the diameter of 0.2m and larger. Yet, in this work a pan with diameter of 0.1m was used, this means, it is not absolutely correct to apply equation 5.1, however, there is no other alternative.

Then, for D=0.1m;

$$\dot{m}'' = \dot{m}''_{\infty}\left(1 - e^{-k\beta D}\right) = 0.101\left(1 - e^{-1.1\cdot 0.1}\right) = 0.01052 kg/m^2 s$$

In order to compare an analytical value with experimental ones, the calculated value has to be multiplied by the area of the pool to obtain the same units as the measured mass loss rates have.

$$\dot{m} = \dot{m}'' \cdot A_f \tag{5.2}$$

Where m – mass loss rate of the fuel, kg/s;

$\dot{m}''$ – mass loss rate of fuel per unit area, kg/m^{2}s;

A_f – area of the pool, m^2;

for the round pan: $A_f = \pi D^2/4 = 0.00785 m^2$.

Finally,

$$\dot{m} = \dot{m}'' \cdot A_f = 0.01052 \cdot 0.00785 = 8{,}3 \cdot 10^{-5} kg/s.$$

It should be highlighted that the applied analytical method is valid for the pools with diameters larger than 0.2m, using these equations for the smaller pool size does not provide with realistic results. The average value of experimentally found MLR of the free burning case is $1.18 \cdot 10^{-4} kg/s$. This value is bigger than analytical one by 40%. MLR of enclosure fires are greater that of free fire, consequently, the difference with analytical value is also higher.

5.1.2 HRR

As it has been discussed earlier, in case of fuel controlled fires only, for many materials a relation exists between rate of heat released and mass loss rate [18] (Eq.(5.3)):

$$\dot{Q} = \dot{m} X \Delta H_c \tag{5.3}$$

Where m – mass loss rate of the fuel, it was previously estimated as $8.3*10^{-5}$ kg/s;

X – combustion efficiency, generally assumed 0.7 for compartment fires [16];

ΔH_c – complete heat of combustion, for heptane ΔH_c = 44.6MJ/kg.

Therefore,

$$\dot{Q} = \dot{m} X \Delta H_c = 8.3 \cdot 10^{-5} \cdot 0.7 \cdot 44.6 \cdot 10^3 = 2.6 kW$$

The obtained value is likely to be underestimated due to the improper value of the mass loss rate used for the calculations. It was decided to repeat these calculations using MLR values measured in the course of the experiment for every 2 minutes time-step for all three scenarios and the free burning case (Figure 5).

Resulting values of HRR are presented in the graph below (Figure 22).

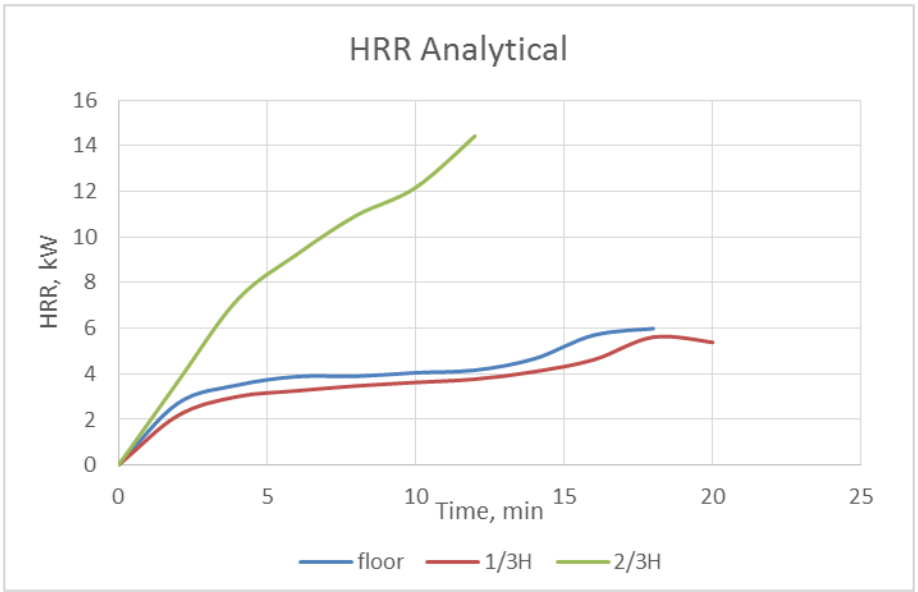

Figure 22. Variation of analytically found HRR over time for three elevation scenarios.

According to the tendency of graphs presented on the figure (Figure 22), for the assumed combustion efficiency of 0.7 and experimentally measured mass loss rate, the rate of energy released during the fires at floor and half-elevated (scenarios 1 and 2) is lower that the HRR of the free burning. Thus, the HRR of the maximum elevated fire is extremely greater than energy released for all other tests, nearly 3 times greater at its peak. To assess the error that one might expect when implementing calculations of HRR using measured MLR and assumed efficiency of 0.7, the graphs of analytically estimated HRR were plotted against experimentally found HRR (Figure 23).

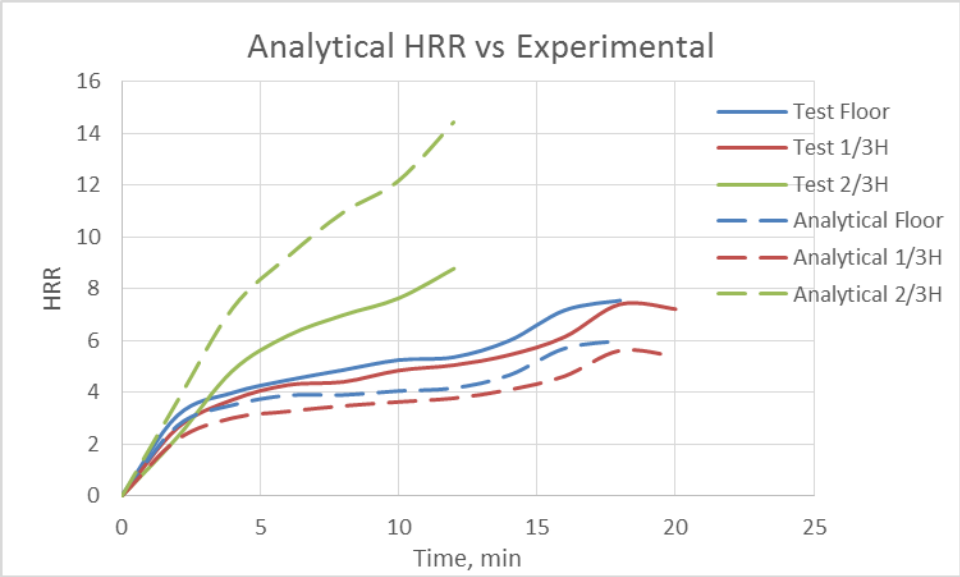

Figure 23.Comparison of the HRR calculated analytically and measured experimentally.

From the collation of the two sets of graphs (Figure 23), it can be noticed that the analytical method underestimates HRR for low positioned fires, but greatly overestimates HRR of the fire elevated to 2/3 of the room's height. To assess the quantative error analytical values can be divided by experimental one. This calculation was performed for every scenario and every time step. The found error was then averaged over time, final result is presented below:

$$Scenario\ 1\ (floor)\colon \dot{Q}_{a,1} = 0.81\dot{Q}_{e,1};$$

$$Scenario\ 2\ (1/3H)\colon \dot{Q}_{a,2} = 0.77\dot{Q}_{e,2};$$

$$Scenario\ 3\ (2/3H)\colon \dot{Q}_{a,3} = 1.57\dot{Q}_{e,3}$$

Indexes *a* and *e* denote "analytical" and "experimental" respectively.

All in all, performed analytical calculations results in error of about 20% when applied to first and second scenarios. For the highest elevated fire the analytical value is overestimated by more than 50%.

5.1.3 HGL Temperature and Interface Position

Two methods different in their approach have been chosen for estimating hot gas layer temperature. In this study these methods are addressed as Method 1 and Method 2. The Method 1 is known in fire safety engineering as the MQH Method, because of the scientist who worked on developing this approach: McCaffrey, Quintiere and. [26] Method 2 is based on the simplified energy balance. Both methods assume that fire compartment can be represented as two-zone model. Detailed description of each method and following calculations suitable for the studied case can be found in Appendix C (Method1) and Appendix D (Method 2). Below the results only are presented

5.1.3.1 Method 1

The MQH formula for temperature increase is given below (Eq.(5.4)):

$$\Delta T = 6.85 \left(\frac{\dot{Q}^2}{A_0 \sqrt{H_o} h_k A_t} \right)^{1/3} \tag{5.4}$$

After performance of all calculations described in Appendix C, the temperature of the hot gas layer was found for each configuration scenario. Results are gathered and depicted on the Figure 24. First two minutes of fire were deliberately ignored as the used method is valid only when a smoke layer of sufficient depth has been formed so mass flow out of the enclosure is possible.

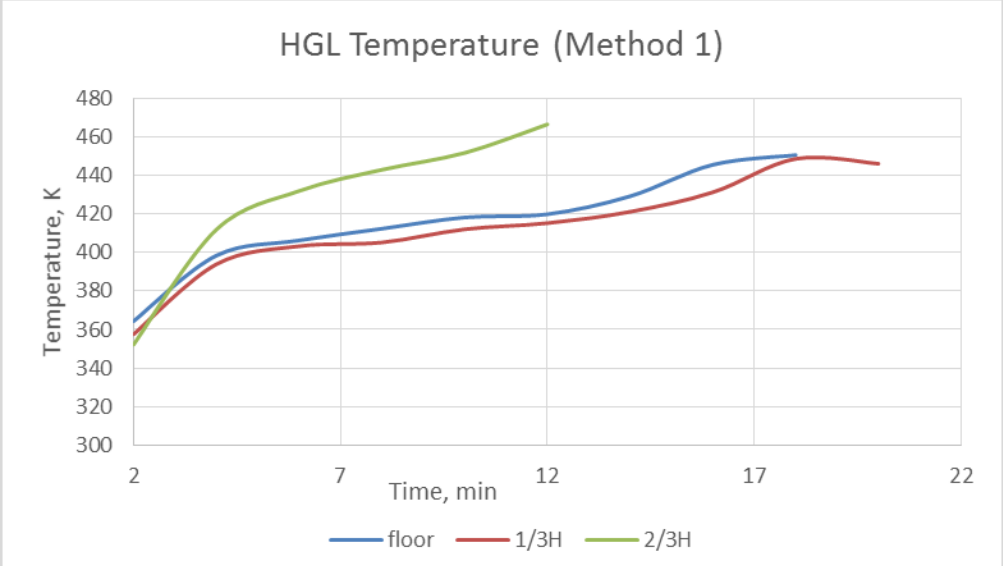

Figure 24. Hot gas layer temperature estimated using Method 1 for every elevation scenario.

From the graph above it can be seen that during the first 4 minutes of the burning the highest temperatures of hot gas layer are reached when the fire is positioned on the floor (Figure 24). Yet, after 4 minutes the temperatures corresponding to the scenario 3 (2/3H) sharply increases reaching 466K. The lowest temperatures relate to the scenario 2, fire at 1/3 of the room's height, though, the scenario 2 values do not significantly differ from those of the floor case. It should be noticed that the general pattern of the HGL temperature graphs resemble a lot the pattern of the HRR graphs presented in the Section

3.2.2, Figure 6. This is not unexpected as experimentally obtained HRR was a key input parameter for MQH calculations.

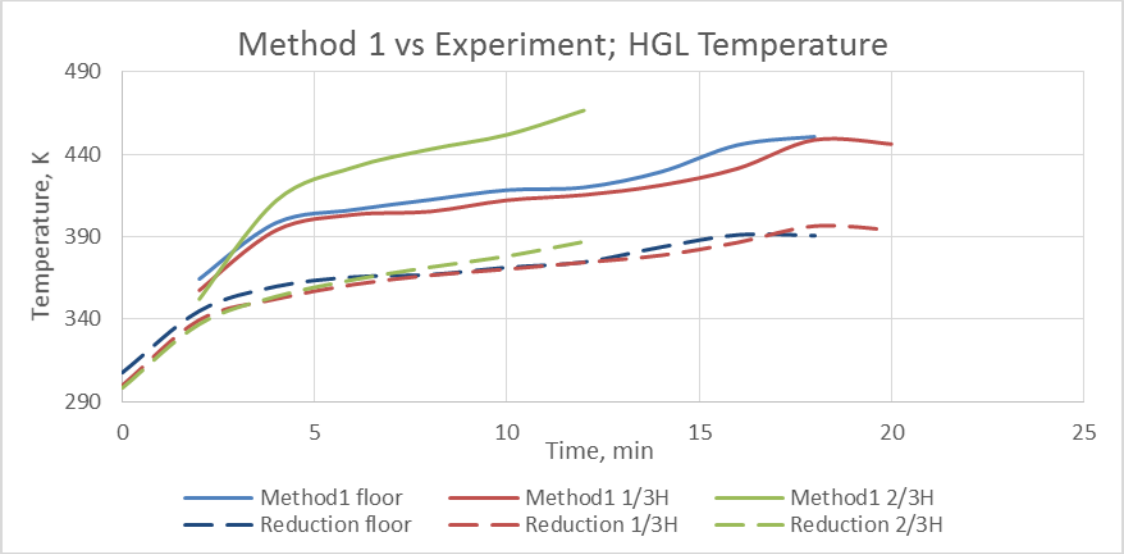

Figure 25. Comparison of the HGL Temperatures calculated from Method 1 and measured experimentally.

Comparing temperatures calculated with Method 1 with temperatures obtained from experiments, it is clear that Method 1 generally overestimates temperatures of hot gas layer (Figure 25). The quantative difference was found to be:

$$Scenario\ 1\ (floor)\colon T_{M1,1} = 1.12T_{e,1};$$

$$Scenario\ 2\ (1/3H)\colon T_{M1,2} = 1.11T_{e,2};$$

$$Scenario\ 3\ (2/3H)\colon T_{M1,3} = 1.17T_{e,3};$$

Indexes *M1* and *e* denote "Method 1" and "experiment" respectively.

Interesting observations can be made if HGL temperatures based on the experimental measurements are compared to HGL Temperature estimated in accordance to Method 1, but with the use of HRR values measured in the free burning test (Figure 26).

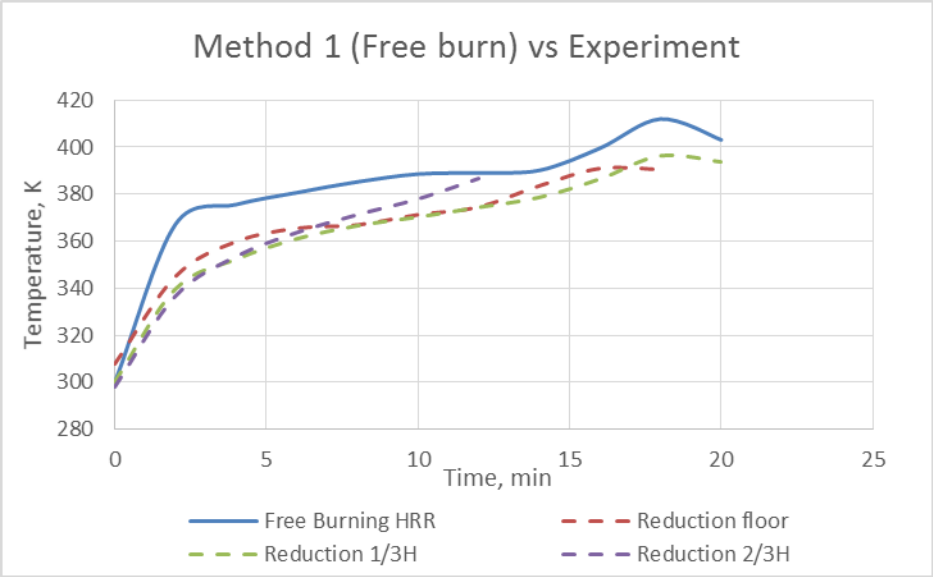

Figure 26. Comparison of the HGL Temperatures calculated from Method 1 using HRR of free burning Heptane with measured experimentally.

In this case only one single time dependent value of HGL temperature can be found using Method 1. The differences between this value and temperatures based on tests for every elevations are:

$$Scenario\ 1\ (floor)\text{: } T_{M1,free} = 1.039 T_{r,1};$$

$$Scenario\ 2\ (1/3H)\text{: } T_{M1,free} = 1.042 T_{r,2};$$

$$Scenario\ 3\ (2/3H)\text{: } T_{M1,free} = 1.036 T_{r,3};$$

Overall, if the experimentally measured HRR of each elevation are used as an input for MQH method of HGL temperature estimation, the error for the low positioned fires should be expected to be just above 10%, and for highly raised fires – of about 15%. However, if the HRR from the free burning test is used, the error for each elevation is about 4% only.

5.1.3.2 *Method 2*

The equation for the hot gas layer temperature that came out of the energy balance principle is found in the Appendix D to be (Eq.(5.5)):

$$T_g = T_{amb} + \Delta T = T_{amb} + \frac{\dot{Q}}{(\dot{m}_g c_p + h A_t)} \tag{5.5}$$

The HGL temperature was found for each time step, though, all values prior to the first 2 minutes are ignored due to the absence of the mass flow out. Visual presentation of the results can be found in the Figure 27.

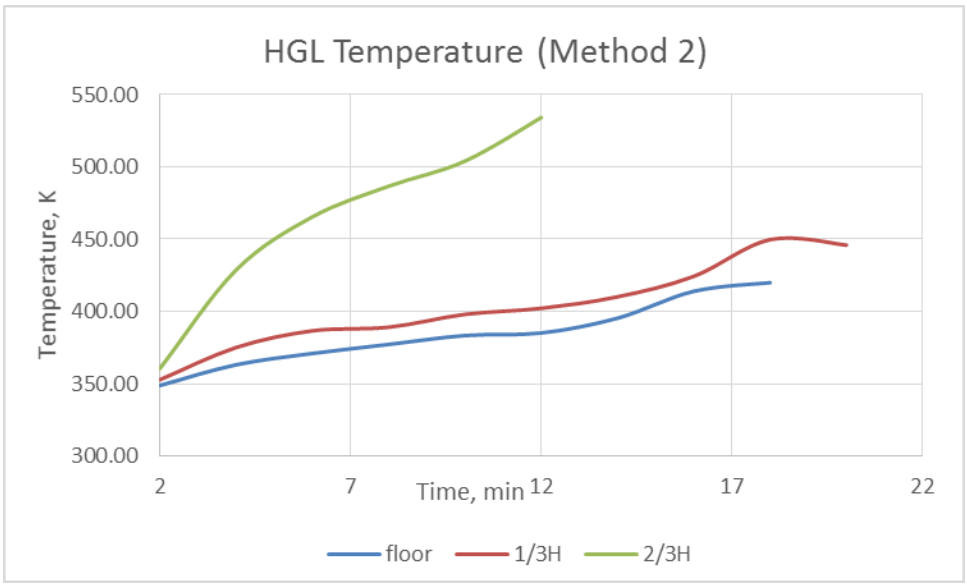

Figure 27. Hot gas layer temperature estimated using Method 2 for every elevation scenario.

Graphs that are presented above (Figure 27) are again very similar in their trends to the HRR variation over time found experimentally and used as the input parameter. The highest overall temperature corresponds to the scenario 3. And temperatures found for scenarios 1 and 2 are very similar in their magnitude.

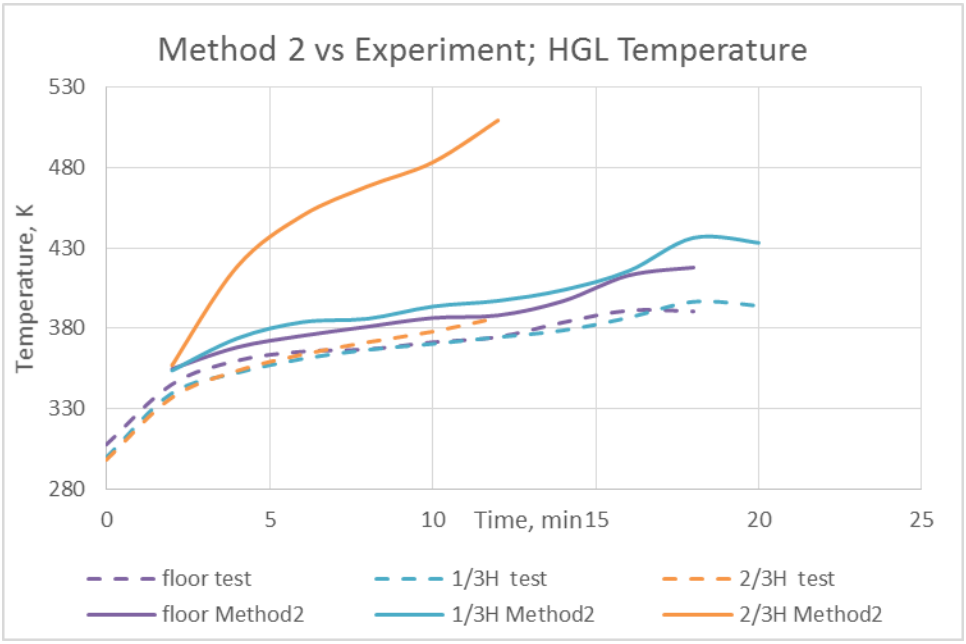

Figure 28. Comparison of the HGL Temperatures calculated from Method 2 and measured experimentally.

Again comparing the values of temperature estimated with analytical method (2) with values found through the data reduction, following relations were estimated:

$$Scenario\ 1\ (floor): T_{M2,1} = 1.03T_{r,1};$$

$$Scenario\ 2\ (1/3H): T_{M2,2} = 1.08T_{r,2};$$

$$Scenario\ 3\ (2/3H): T_{M2,3} = 1.27T_{r,3};$$

Indexes *M2* and *r* denote "Method 2" and "reduction" respectively.

Instead of using HRR values from tests with elevations, only HRR from the free burning test can be used for Method 2 calculations. The differences between analytical values and experimentally based temperatures take following form (Figure 29):

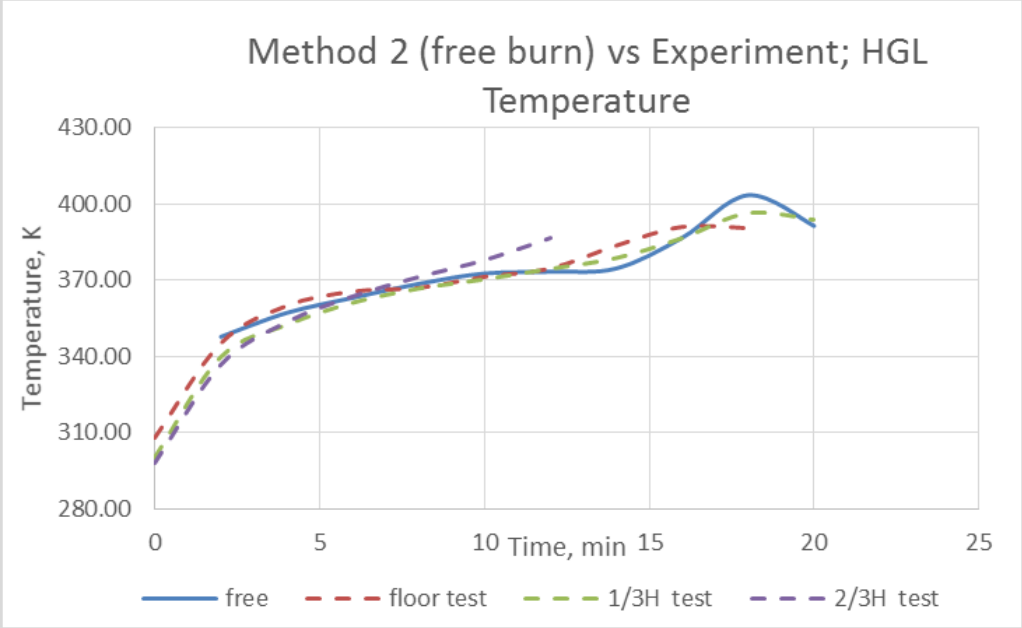

Figure 29. Comparison of the HGL Temperatures calculated from Method 2 using HRR of free burning Heptane with measured experimentally.

Numerically the difference between an analytical value and experimental can be expressed as:

$$Scenario\ 1\ (floor): T_{M2,free} = 0.99T_{r,1};$$

$$Scenario\ 2\ (1/3H): T_{M2,free} = 1.01T_{r,2};$$

$$Scenario\ 3\ (2/3H): T_{M2,free} = 0.99T_{r,3};$$

From the expressions above, it can be concluded that using HRR, measured in free burn test, provides results with an error of just 1% for every elevation, while using HRR from elevated tests leads to the increase of the error.

In general, Method 2 allows for more accurate estimates of HGL Temperature than Method 1. Relatively accurate results can be achieved only if the HRR obtained from the free burn test is used.

Another parameter that was estimated applying Method 2 is the height of the smoke layer (Figure 30). It can be seen that estimated height of the smoke layer is directly related to the elevation of the fire source, meaning that the higher the location of fire, the lesser is the descent of the smoke.

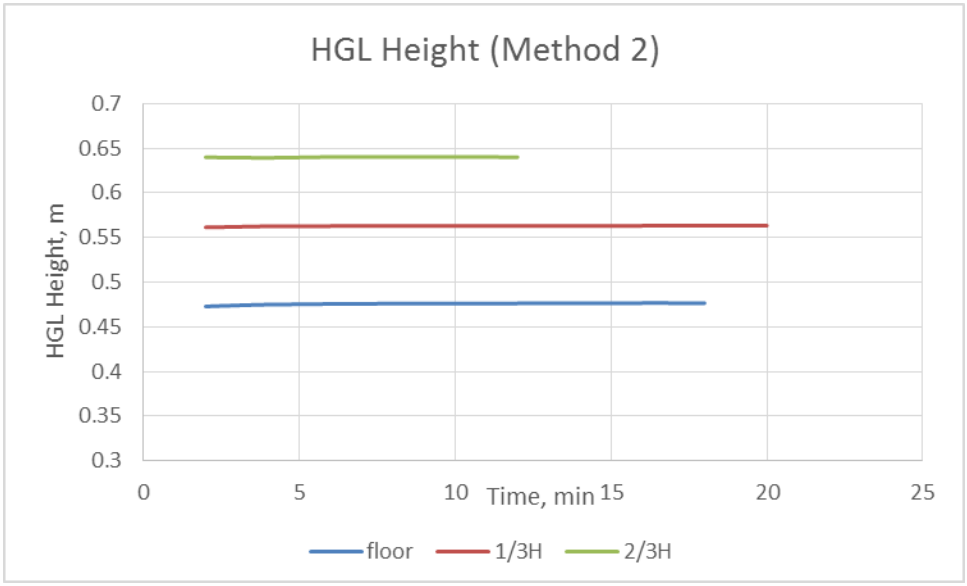

Figure 30. Hot gas layer height estimated using Method 2 for every elevation scenario.

Comparing analytical results to the ones obtained by data reduction (Figure 31), it can be seen that Method 2 predicted position of the smoke layer that are higher than the experimentally found ones.

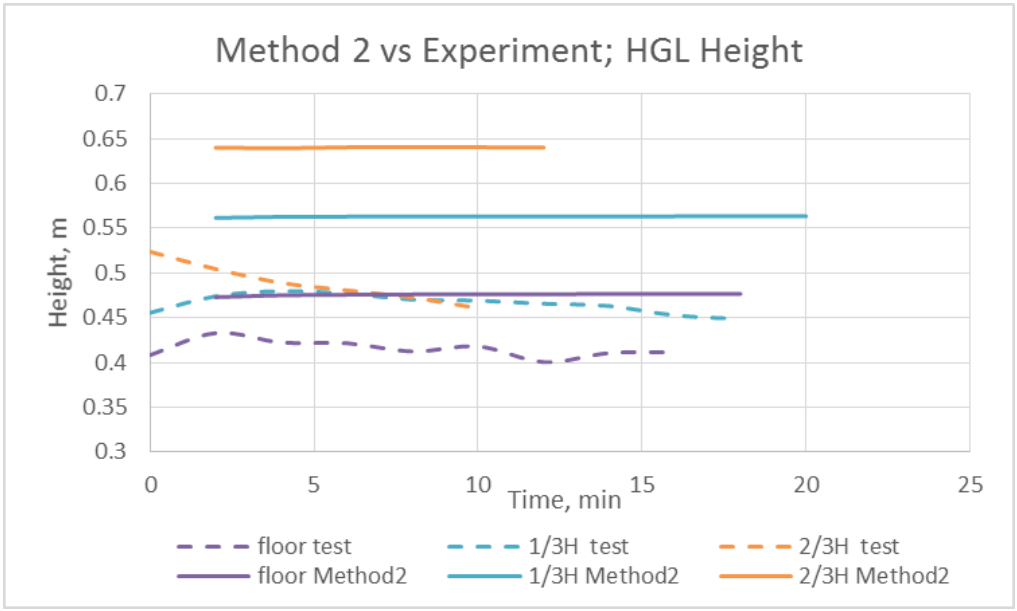

Figure 31. Comparison of the HGL Height calculated from Method 2 and measured experimentally.

This method overestimated HGL height by 14% for the Scenario 1, by 20% for the scenario 2 and by 31% for the Scenario 3. Consequently, the higher the elevation, the greater the error produced by Method 2.

$$Scenario\ 1\ (floor)\text{: } Z_{M2,1} = 1.14 Z_{r,1};$$

$$Scenario\ 2\ (1/3H)\text{: } Z_{M2,2} = 1.20 Z_{r,2};$$

$$Scenario\ 3\ (2/3H)\text{: } Z_{M2,3} = 1.31 Z_{r,3}$$

Figure 32 compares experimentally based values of HGL height to the analytical one found using Method 2 and applying HRR for free burning case.

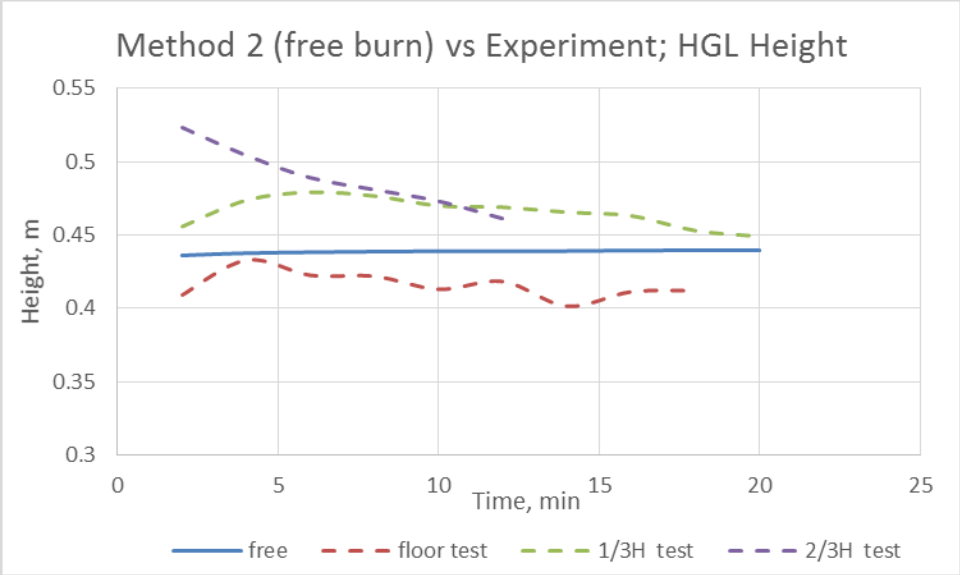

Figure 32. Comparison of the HGL heights calculated from Method 2 using HRR of free burning Heptane with experimentally measured ones.

$$Scenario\ 1\ (floor)\text{: } Z_{M2,free} = 1.06 Z_{r,1};$$

$$Scenario\ 2\ (1/3H)\text{: } Z_{M2free2} = 0.94 Z_{r,2};$$

$$Scenario\ 3\ (2/3H)\text{: } Z_{M2,free} = 0.90 Z_{r,3};$$

One can notice that the analytical value is higher than HGL height during Scenario 1, but lower than HGL height for elevated Scenarios 2 and 3. But the difference between this analytical result and experimental ones is smaller when using HRR from free burn test, than HRR from enclosure tests with elevations.

Altogether, both methods used could not provide results that accurately resemble experimental findings. The reasons of that could be approximations and assumptions applied to develop analytical models, and, also, the fact that both models were derived from the experimental studies with the fire

located near the floor. Nevertheless, the distinction between analytical and experimental results is relatively small, especially if the HRR from the free burn test is used as the input parameter. Thus, Method 1 and Method 2 can serve to provide an idea of the values that can be reached in real fire with uncertainty of about 10%. Still, like for any other analytical method, accuracy of the results predicted by Method 1 and Method 2 greatly depends on the precision of the inputs.

6 Discussions

In this chapter the answers for the research questions listed in the chapter 1.2 will be analysed and discussed. Different scientific methods are applied in order to analyse the different questions (Table 1). Only data from the experimental study is used to analyse and discuss the first four questions, while experimental data together with FDS simulations and analytical calculations will be used to analyse RQ5 and RQ6, respectively. The main assumption of this study is that the results obtained during the experiments (measurements and processed data) reasonably well represent reality.

To assess the influence of the fire elevation on development of a certain parameter, this parameter will be plotted against the height of the elevation. As the fire in this study is in its growth phase, all parameters are time dependent, thus, the separate graph for every time step should be analysed. The last time step is chosen to be t=12 minutes, due to the fact that fires elevated by 2/3 of the room's height, completely burnt out, shortly after 13 minutes from the ignition.

In order to provide a quantative impact on the change of the certain parameter caused by the source elevation, the mean values of this parameter corresponding to the elevated case (scenario 2 and 3) will be divided by the mean value for scenario 1 (floor). These simple calculations will clearly demonstrate by how much the fire parameter will be changed in the studied setup, if elevated by 1/3 or 2/3 of the room's height. The calculation will be done for every time step to provide the range of expected differences. The maximum and minimum values will be used for comparison with results provided by other methods, applied in this study.

RQ1. How will the heat release rate be affected by the elevation of the fire source?

To answer this question the HRR can be plotted against the height of elevation (Figure 1).

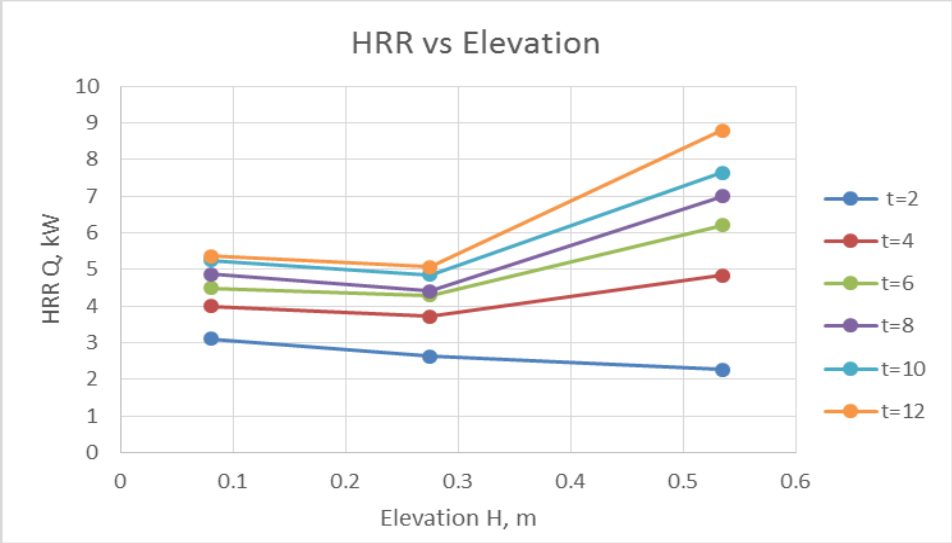

Figure 33. Relations between HRR and fire elevation.

Except first 2 minutes, the highest elevated fire released greatest amount of energy, and the fire elevated to 1/3H – the lowest. The only exception is the first 2 minutes, when the HRR was inversely proportional to increased elevation of the fire. This can be explained by the availability of oxygen be also

inversely proportional to the elevation. During all the period of burning, the HRR of scenario 2 (1/3H) was smaller than HRR of scenario 1 by 5-16%. The difference was greater during the first minutes after ignition. When the HRR of scenario 3 is compared with HRR of scenario 1, the dissimilarity between two values was also growing in time, and if 4 minutes after ignition the HRR of scenario 3 was greater by 17%, just before the burn out this number changed to over 60%.

Auxiliary graphs were plotted to demonstrate the influence of elevation on the MLR of fuel (Figure 34).

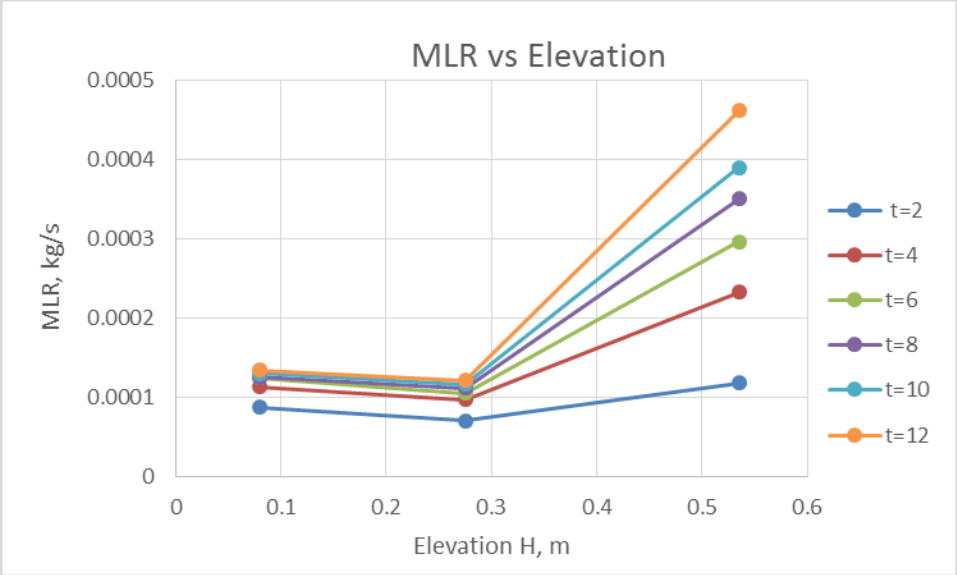

Figure 34. Relations between MLR and fire elevation.

The distinction of MLR between Scenarios 1 and 2 was 10-20%. However, the fire elevated to 2/3H yielded MLR that was 1.4-3.5 times higher than the MLR of the scenario 1.

From the plotted graphs (Figure 33 and Figure 34) it can be seen that mass loss rate is more sensitive to the elevation than heat release rate. On average, the elevation to 1/3 of the room's height caused decrease in Mass loss rate by 14%, but HRR lowered just by 8%. The elevation to the 2/3 of the height led to the vast increase of the MLR as for the scenario 3 it is 2.5 times greater than for the floor case (average). While on average the HRR grew just by 30% when it got elevated to that height. Moderate raise in HRR with elevation can be explained by the global combustion efficiency that gets lower if the fire lifted higher. The summary of changes caused by fire elevation can be found in the table below (Table 5).

Table 5. Extreme values of differences in values of HRR and MLR between Scenario 1 and Scenarios 2 and 3.

Parameter	**Difference with 1/3H**		**Difference with 2/3H**	
	min	max	min	max
MLR	-20%	-10%	+35%	+246%
HRR	-16%	-5%	-17%	+63%

RQ2. How will hot gas layer properties (such as temperature and hot gas layer height) be affected by the elevation of the fire source?

The Figure 35 and Figure 36 show the dependency of hot gas layer properties on the fire source elevation. For the first 4 minutes of fire, the highest temperatures of the hot gas layer correspond to the case with fire near the floor (Figure 35). It was mentioned earlier in the text, that initial temperatures in the enclosure were slightly greater for tests of scenario 1. From the HRR graph (Figure 6) it was also observed that fire placed close to the floor released greater amount of energy during the first minutes of the combustion.

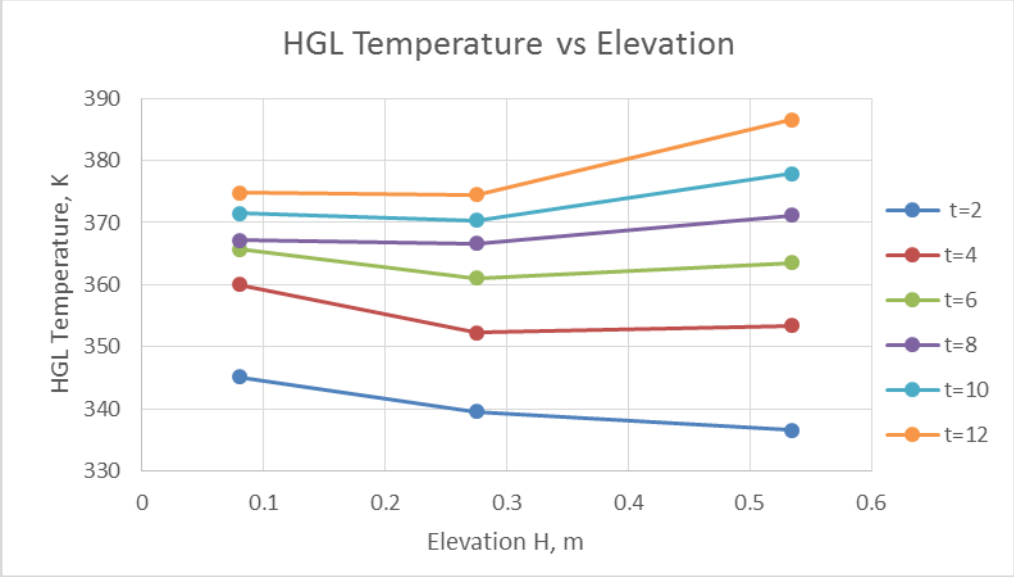

Figure 35. Relations between HGL Temperature and fire elevation.

Over the burning period the difference between HGL Temperatures reached during the test of scenario 1 and scenario 2 was never over 3%. The same is true when likening scenario 1 and scenario 3. Thus, the Temperatures reached when the fire was elevated to 1/3H are smaller than those for fire near the floor, and the temperatures corresponding to elevation of 2/3H are higher. The summary of changes in the HGL temperature values caused by the elevation can be found in Table 6.

Table 6. Extreme values of differences in values of HGL Temperatures between Scenario 1 and Scenarios 2 and 3.

Parameter	**Difference with 1/3H**		**Difference with 2/3H**	
	min	max	min	max
HGL Temperature	-2%	<-1%	-2%	+3%

Observing the graphs for HGL height (Figure 36), it can be seen that during the first minutes of fire, the smoke was thin and unstable, therefore, the graphs corresponding to t=2 min and t=4 min look somehow different from later ones. It was expected that the higher the fire is elevated the lesser smoke it can produce due to reduced amount of air entrainment into the plume. Thus, the smoke layer height should be greater for the higher positioned fires. While the smoke layer from the elevated fires (1/3H and 2/3H) was indeed never as deep as smoke produced by floor fire, the smoke from the scenario 3 in the end of the burning, descended lower than smoke from the scenario 2. There can be several possible

reasons of why the smoke of the scenario 3 could get that low. First of all, when fire was elevated right under the ceiling, its flames occupied the space where hot gas layer usually forms, driving smoke away from the centre closer to the walls. Moreover, the height of the opening and formed pressure profile across the enclosure due to increased temperatures, could also force the smoke to go lower.

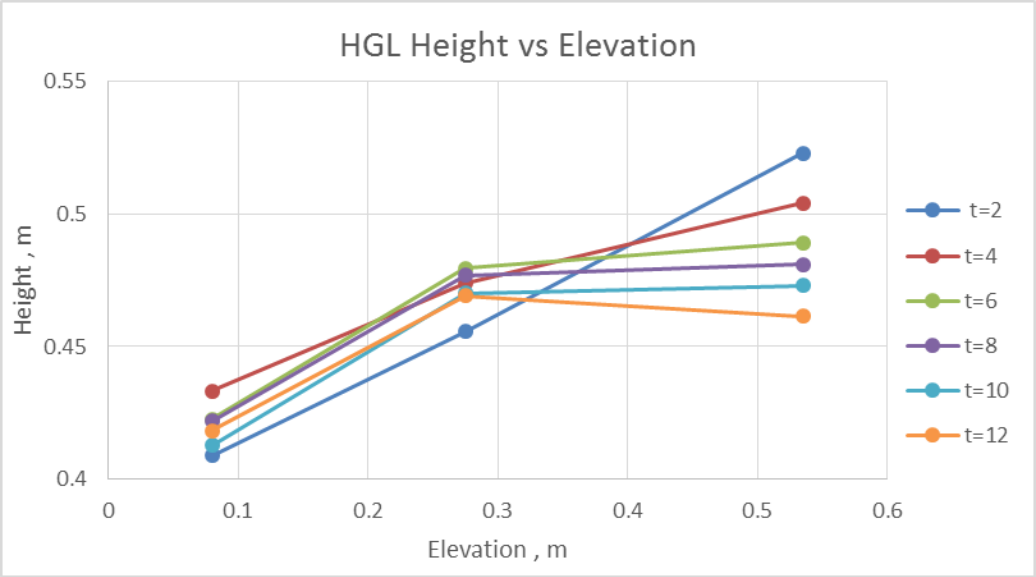

Figure 36. Relations between HGL Height and fire elevation.

Comparing actual heights of the hog gas layer position, it can be said that if the fire is elevated to 1/3H of the room, its smoke is 9-14% higher than smoke from the floor fire. The hot gas layer from the 2/3H elevated fire is 10-30% higher than the smoke corresponding to the floor case. From these observations one can conclude that the effect of elevation on temperature of hot gas layer can be neglected for this experimental setup, as the average difference between values for different scenarios is about 1%. Yet, the elevation is a substantial factor for the smoke layer position, the significant difference can be expected for the lifted up fire. The summary of changes in the HGL temperature values caused by the elevation can be found in Table 7.

Table 7. Extreme values of differences in values of HGL height between Scenario 1 and Scenarios 2 and 3.

Parameter	**Difference with 1/3H**		**Difference with 2/3H**	
	min	max	min	max
HGL Height	+9%	+14%	+10%	+28%

RQ3. How will radiative heat flux to the floor be affected by the elevation of the fire source?

The graphs, representing effect of elevation on heat flux measured on the floor (Figure 37), demonstrate similar trend to all previous graphs: the second scenario yields lower value than the floor one (by 7-50% of scenario 1), but the values corresponding to scenario 3 become the greatest after 4 minutes of burning (by 10-65% of scenario 1).

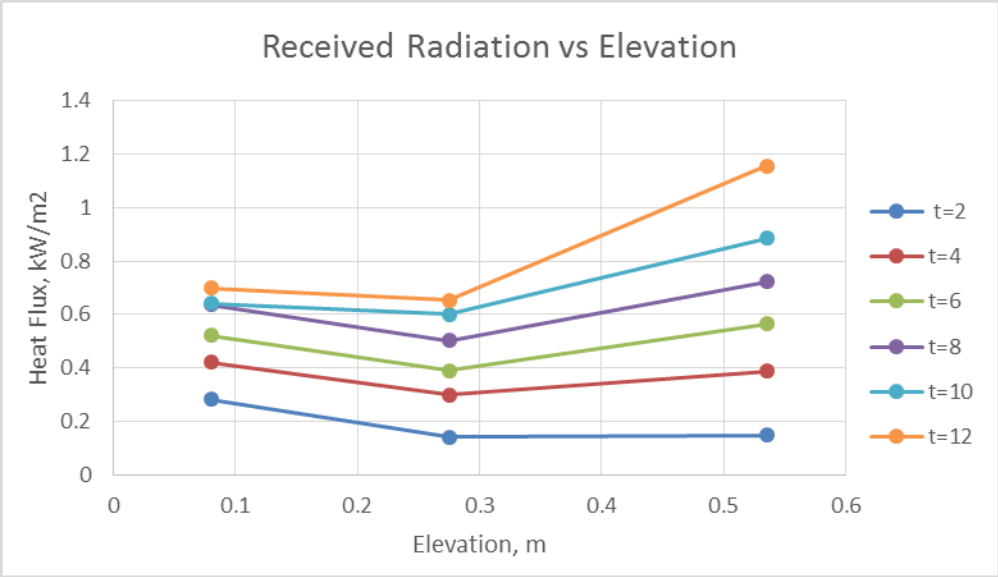

Figure 37. Relations between Heat fluxes received at floor and fire elevation.

Consequently, fire elevated to 1/3 of the room's height contributes to lesser amount of radiation than the fire on the floor, and fire closest to the ceiling results in the raise of the heat flux reaching the floor. It should be remembered, that the longer the highly raised fire burns, the bigger the difference from the floor case is, the increase by 65% can be possible (Table 8).

Table 8. Extreme values of differences in values of received heat flux between Scenario 1 and Scenarios 2 and 3.

Parameter	**Difference with 1/3H**		**Difference with 2/3H**	
	min	max	min	max
Heat Flux	-50%	-7%	-50%	+65%

RQ4. Does elevation of the fire source influences the speed of the growth of the fire parameters (HRR, HGL Temperature and height, heat flux etc.)

The time to reach a certain reference value for each parameter and elevation is determined, in order to provide an answer to this question. A HRR of 7kW, HGL temperature of 380K and heat flux of 1 kW/m^2 were selected as reference values as these values were reached in every test. The time to arrive to these values was found for every elevation by application of the interpolation method. The time to reach reference points versus fire elevation was plotted and can be found below (Figure 38).

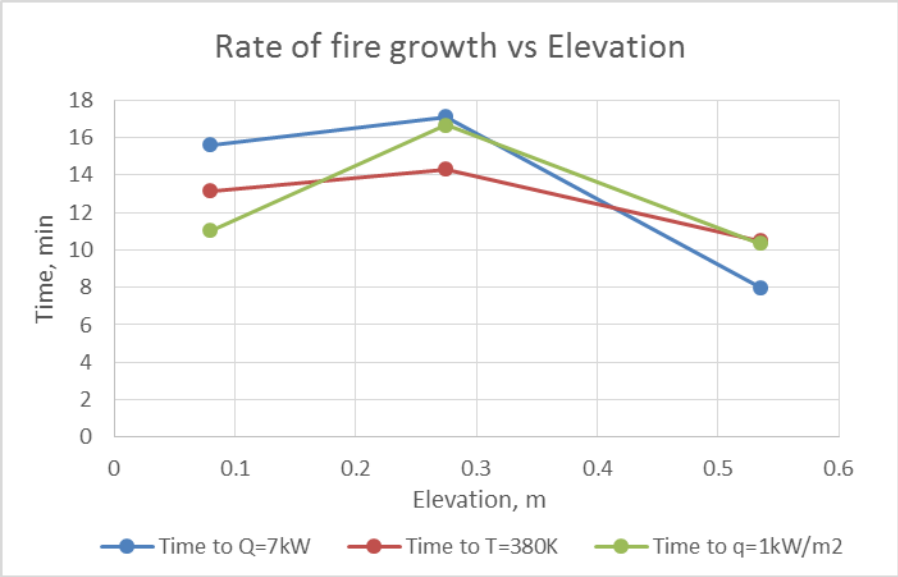

Figure 38. Relations between fire growth and fire elevation.

The graphs indicate that reference points are reached faster if the fire is in the proximity to the ceiling, but lower if it is elevated to 1/3 of the room's height (Figure 38). The correlations describing the change in time to reach certain values of HRR, HGL temperature and heat flux, depending on fire position are presented below:

$$t_1^{7kW} = 1.1t_2^{7kW} = 0.5t_3^{7kW} \quad (6.6)$$

$$t_1^{380K} = 1.09t_2^{380K} = 0.8t_3^{380K} \quad (6.7)$$

$$t_1^{1kW/m2} = 1.5t_2^{1kW/m2} = 0.94t_3^{1kW/m2} \quad (6.8)$$

For the fires at 1/3 of the height, a delay of 10% is expected to reach both certain values of HRR and HGL T, and 50% to reach a heat flux of 1 kW/m^2, which makes this case to be less hazardous in terms of occupants' safety. On the other hand, if the fire is elevated as high as 2/3 of the room height, the HRR of 7kW is reached in half of the time compared to the fire near the floor. Also, a HGL temperature of 380K is reached 20% faster. The 6% difference in time to 1kw/m^2 heat flux is relatively small and can be ignored, although, it should be remembered that if the duration of fire is prolonged, the difference can get bigger. Overall, while the effect of the elevation to 1/3H can be ignored, the fire elevated to 2/3 of the room's height grew much faster than the fire near the floor, so it is a much bigger threat for occupants' safety.

Summary: Experimental results

To sum up first four research questions, all studied fire parameters demonstrated dependence on the vertical position of the fire. Some, like MLR and HRR, are considerably affected by elevation of the fire, thus, ignoring the fire position and assuming that it is located near the floor, will likely to lead to gross underestimates of these parameters. Then again, HGL temperature changes so little with the source elevation that it can be easily ignored. Other parameters, heat flux to the floor and HGL height, tend to fluctuate moderately with the source elevation. The found dependency on elevation height are not simply

linear, for all parameters it was noticed, that elevation to 1/3 of the room height produces slightly less hazardous conditions compared to when the fire is on the floor. However, the 2/3H scenario causes a more rapid growth of the fire. For this reason, it is believed that more than one factor must contribute to changes of fire parameters when elevation varies.

The factor responsible for the delay of fire development in scenario 2 is likely to be the decrease in the oxygen concentration around the fire base. Oxygen concentration is directly related to the mass loss rate, which in its turn contributes to HRR and HGL properties. The lower the quantity of available oxygen, the slower the development of the fire parameters. The factor that is most likely causing the more intense fire in scenario 3 is the radiation from the heated surfaces and smoke layer to the fire base. As it was discussed earlier, this factor contributes to additional rate of mass loss, resulting in higher total MLR, HRR, HGL temperature and heat flux to the floor.

The least obvious but still essential factors that also contribute to the conditions in the room, are the heat losses, air entrainment, combustion efficiency, flame-smoke and flame-ceiling interactions. In the scenario when the fire is placed on the floor the smoke needs to travel a longer distance before it reaches the smoke layer. On its way part of the heat will be lost to the surrounding cooler air. At the same time, if the fire located closer to the ceiling, so little heat is lost during the smoke transportation, it still will get lost but through the ceiling directly outside. The greater the distance between fire base and smoke layer, the more air can entrain the smoke, which through the mixing will cool down the smoke, but contribute to the larger production of it. When fire is in proximity to the ceiling, practically no fresh air entrainment is possible, consequently, smoke production will be limited. The oxygen deficiency as it was shown earlier, results in decrease of the combustion efficiency. Less efficient fires produce more unburnt particles. These particles cause denser smoke, additionally, they radiate greater than smaller particles. If the flames interact with the smoke layer, the last will increase its temperature more rapid. Ceiling impingement by the flame results in that the flame propagates horizontally underneath the ceiling. This results in a high temperature underneath the ceiling that heats the smoke layer and the ceiling, which causes the greater heat flux being emitted.

As it now can be seen, there are many different factors contributing to the outcomes of elevated fires for this particular set-up. That makes the problem quite complex, so no simple recommendation of the safety factor or correction coefficient that can account for the elevation of the source, can be made at this point. More tests of different elevation positions are required to assess the importance of each factor independently. Still, one interesting observation was made, turned out that the elevation of the fire does not cause essential changes in fire development, unless the fire is elevated to such point, where flame penetrates the smoke layer, impinging the ceiling. Therefore, not the actual physical elevation should be considered, but more fire size – enclosure size ratio and flame-smoke interactions.

RQ5. Is it possible to account for the elevation of the fires source in existing fire modelling softwares?

To analyze and discuss this question, results of FDS simulations will be plotted versus elevation and differences in values with respect to different elevations will be computed. Than these findings can be compared to experimental ones found in the answers to RQ1-RQ3.

MASS LOSS RATE AND HEAT RELEASE RATE

MLR and HRR in FDS calculations assumed to be directly dependent, therefore, both parameters follow the same trend. Because of that, they are put in the same discussion section. FDS predicted MLR and HRR were plotted against the height of elevation over the floor (Figure 39 and Figure 40).

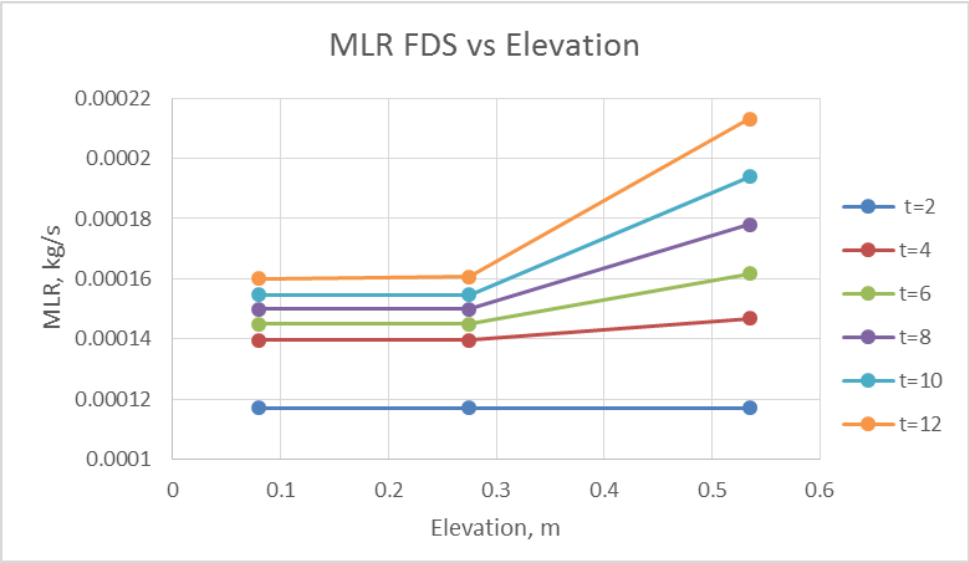

Figure 39. Relations between MLR calculated in FDS and fire elevation.

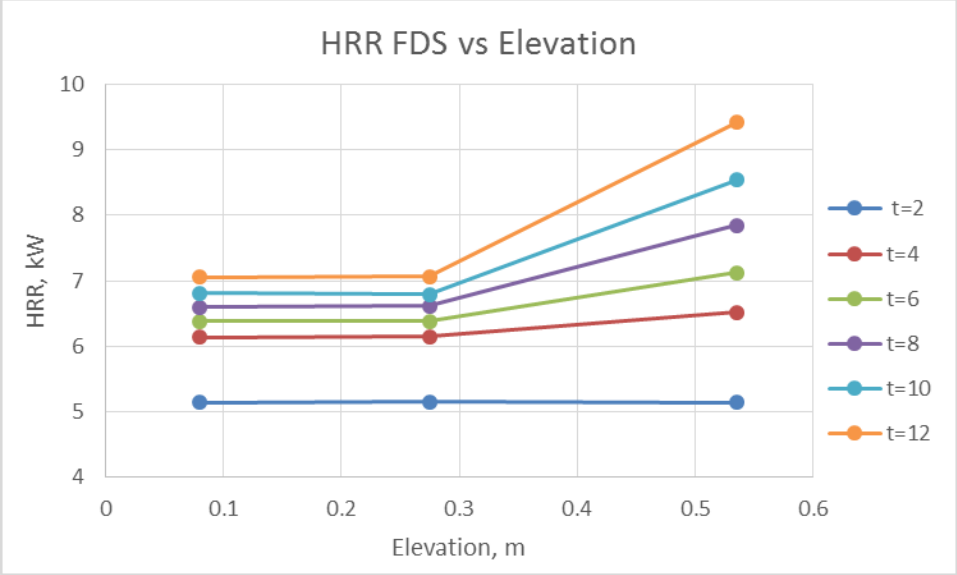

Figure 40. Relations between HRR calculated in FDS and fire elevation.

As it can be seen from graphs (Figure 39 and Figure 40) that according to FDS principles and assumptions, HRR and MLR both depend on the source elevation in the similar manner. These parameters

do not change at all if they are lifted from the floor to the 1/3 of the room's height. Yet, the further raise to the 2/3 of the room's height causes increase in MLR and HRR, and this increase gets bigger with the time. In this way, in the beginning of the combustion there is no difference, but just 12 minutes after ignition, MLR/HRR of 2/3H scenario is greater than same parameters of the floor case by 33%.

To see if this corresponds to what was observed during the experiment, the minimum and maximum differences between floor case and each elevation case computed from FDS are confronted to those found from experiments (Table 5) in the Table 9 below.

Table 9.Comparison of the effect of elevation on HRR found experimentally and predicted by FDS.

Parameter		**Difference with 1/3H**		**Difference with 2/3H**	
		min	max	min	max
MLR	Experimental	-20%	-10%	+35%	+246%
	FDS	0	0	0	+33%
HRR	Experimental	-16%	-5%	-17%	+63%
	FDS	0	0	0	+33%

Signs "-" and "+" implies: smaller or bigger than the values found for the floor case (Scenario 1).

From the comparison in Table 9, one can see that FDS seems to be not able to account for the lowering effect of the elevation to 1/3H on the HRR and MLR. Though, this is not a serious issue, as it will lead to more conservative (safe) solution. On the other hand, FDS underestimates the impact of the high elevation which might lead to inappropriate design. According to FDS results the maximum difference between MLR (HRR) yielded by floor fire and highly elevated one is just 33%, while experiment showed that this maximum difference is 246% for MLR and 63% for HRR. It is possible that FDS does not consider all sources of radiation that enhance the total MLR of the fuel.

HGL TEMPERATURE

Plotting HGL temperature against the elevation of the fire shows that FDS predicts nearly linear dependency of these two parameters (Figure 41).

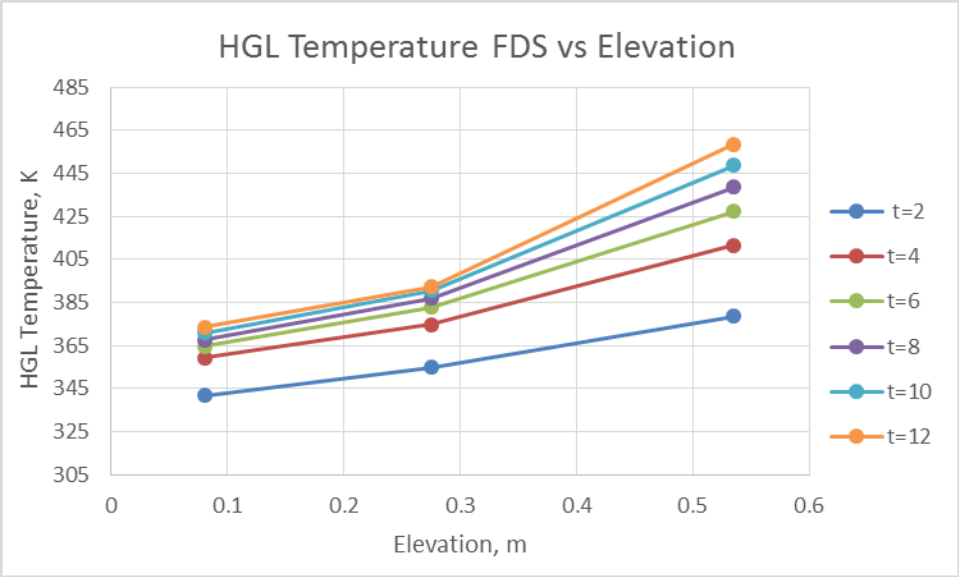

Figure 41. Relations between HGL Temperature calculated in FDS and fire elevation.

The temperatures reached when the fire was lifted to 1/3H are in general 5% higher than temperatures corresponding to the floor fire. The temperatures predicted for 2/3H elevation scenario are at least 10% higher than those for floor fire in the beginning of the simulation, but this values grows with time, making up 22% after 12 minutes.

Comparing extreme differences from FDS outputs to the experimental ones (Table 6), it can be spotted that FDS overrates the influence of elevation on HGL temperature, providing much higher change in values that those measured experimentally (Table 10).

Table 10. Comparison of the effect of elevation on HGL temperature found experimentally and predicted by FDS.

HGL Temperature	**Difference with 1/3H**		**Difference with 2/3H**	
	min	max	min	max
Experimental	-2%	<-1%	-2%	+3%
FDS	+4%	+5%	+11%	+23%

HGL Height

From the graphs of HGL height plotted against the fire elevation, a conclusion can be drown that smoke layer position is practically linear to the fire position, and does not change over the burning period (Figure 42). The smoke layer produced by the fire from scenario 2 is higher by 30% than the smoke from the floor fire, and the smoke from the scenario 3 is higher by 60%.

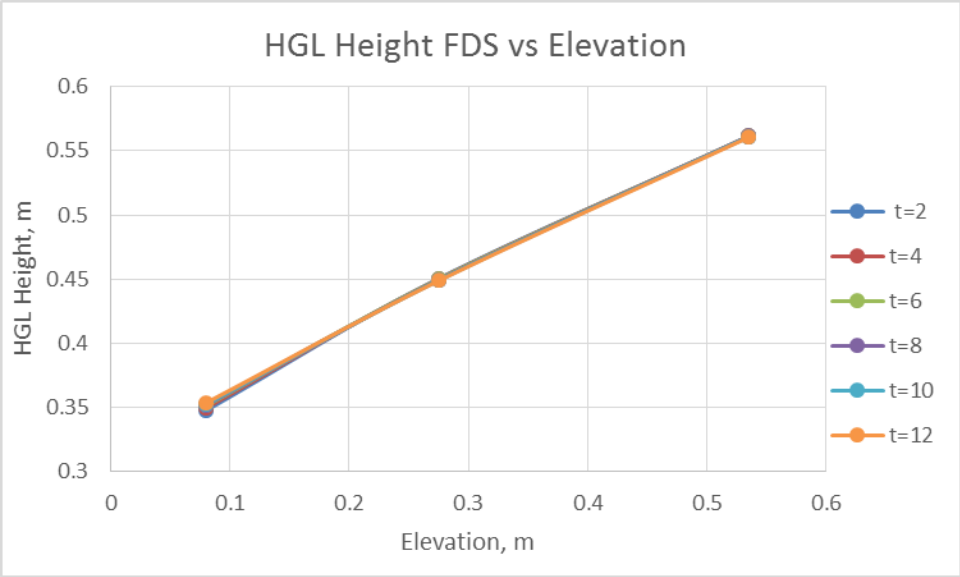

Figure 42. Relations between HGL heights calculated in FDS and fire elevation.

The Table 11 summaries minimum and maximum differences in HGL height caused by fire elevation predicted by FDS and found experimentally (Table 7). According to the data in the Table 11, FDS calculations give higher HGL heights of elevated fires in relation to the floor case.

Table 11. Comparison of the effect of elevation on HGL height found experimentally and predicted by FDS.

HGL Height	Difference with 1/3H		Difference with 2/3H	
	min	max	min	max
Experimental	+9%	+14%	+10%	+28%
FDS	+27%	+30%	+59%	+61%

RADIATIVE HEAT FLUX

The graphs of the heat flux change with elevation (Figure 43) show evidence that in FDS the closer the fire to the flux meter, the higher the measurements it detects. Yet, this is true only for the first 10 minutes of fire, as at the last time step, t=12min, the measured heat flux of scenario 3 surpasses the heat flux of scenario 2. This means that after sufficiently long period of time, the radiation from the smoke and boundaries could exceed the radiation from the flame.

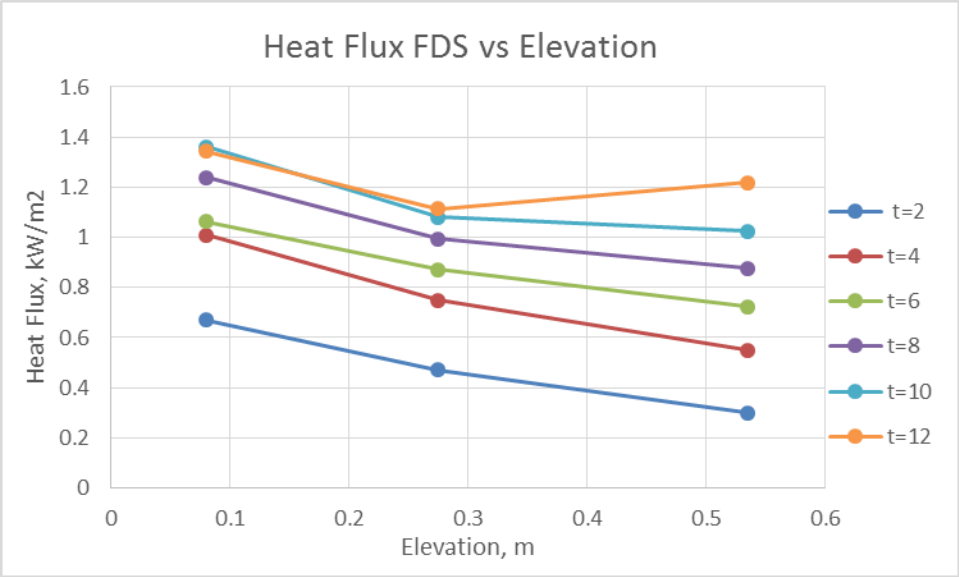

Figure 43. Relations between Heat Flux to the floor calculated in FDS and fire elevation.

By comparing the minimum and maximum differences between heat flux values caused by the source elevation calculated by FDS and from experimental results (Table 8), one can note that generally, values obtained from FDS outputs for elevation to 1/3H is similar to the extreme values found from experimental results. However, the second set of values (for 2/3H) is absolutely incorrect. Experimentally it was discovered that the fire at highest elevation yielded more intensive heat flux than the floor fire (reaching 65%), while FDS predicted decrease of heat flux if the fire got raised to 2/3H (Table 12).

Table 12. Comparison of the effect of elevation on heat flux found experimentally and predicted by FDS.

Heat Flux	**Difference with 1/3H**		**Difference with 2/3H**	
	min	max	min	max
Experimental	-50%	-7%	-50%	+65%
FDS	-30%	-11%	-5%	-9%

Summary: FDS results

All in all, FDS even with the auxiliary environmental feedback model, is not a very effective tool to use for the design of elevated fires. It was discovered that FDS calculations underestimate influence of source elevation on the growth of the most critical fire parameters – MLR, HRR and heat flux. The under prediction of these parameters is significant, which can lead to the false FSE design. Moreover, FDS overrates the raise of HGL temperature with fire elevation, presumably, due to overlooking some heat exchange processes inside the system. Lastly, the simulation tool applies several assumptions to its computations that limit the smoke layer descent to the fire position, resulting in non-realistic position of the hot gas layer.

Some modifications of the FDS calculation methods are required to adapt the software for the elevated fire problems. Additional computations accounting for the re-radiation from the boundaries, smoke and large soot particles, heat losses through the ceiling, flame-smoke interaction, flame-ceiling interaction, decrease of the global combustion efficiency due to the lack of oxygen, decrease of produced smoke due to lesser air entrainment in the plume, pressure differentiation across the compartment and other factors that arise when fire is elevated should be supplemented in the FDS.

RQ6. Is it possible to account for the elevation of the fires source using existing hand-calculations methods for fire safety engineering?

To be able to judge how reliable existing analytical methods used in fire safety engineering are, the analytically found parameters will be later plotted versus elevation and changes in values of these parameters due to elevation will be computed in relation to the floor case. Then, these results can be compared to experimental ones found in the answers to RQ1-RQ3.

MASS LOSS RATE

In the equation used for calculating mass loss rate for the pool fires (Eq.(5.1)) the only variable input parameter was a diameter of the pool, which is obviously independent of the vertical position of the source. Consequently, the Equation 5.1 cannot account for the elevation, and most likely is valid only for the case with the fire being near the floor. No conclusive comparison can be made with the experimental results, as this equation is meant to be applied for the pools with diameter of at least 0.2m, but the pan used in the experiment was 0.1m in diameter. The estimated value for the Heptane pool of 0.1m in diameter was found to be $0.8 \cdot 10^{-4}$kg/s, while measured free burn mass loss rate was approximately $1.3 \cdot 10^{-4}$kg/s and larger for the enclosed fires. Overall, equations Equation 5.1 gives a steady state value for pools with diameter greater than 0.2m only, with no possibility to account for elevation.

HRR

The HRR rate was analytically found using Equation 5.3 for generally assumed combustion efficiency of 0.7 and mass loss rate measured during the tests. Analytical HRR was plotted against the height of elevation over the floor (Figure 44) and changes of the HRR due to the elevation were found too.

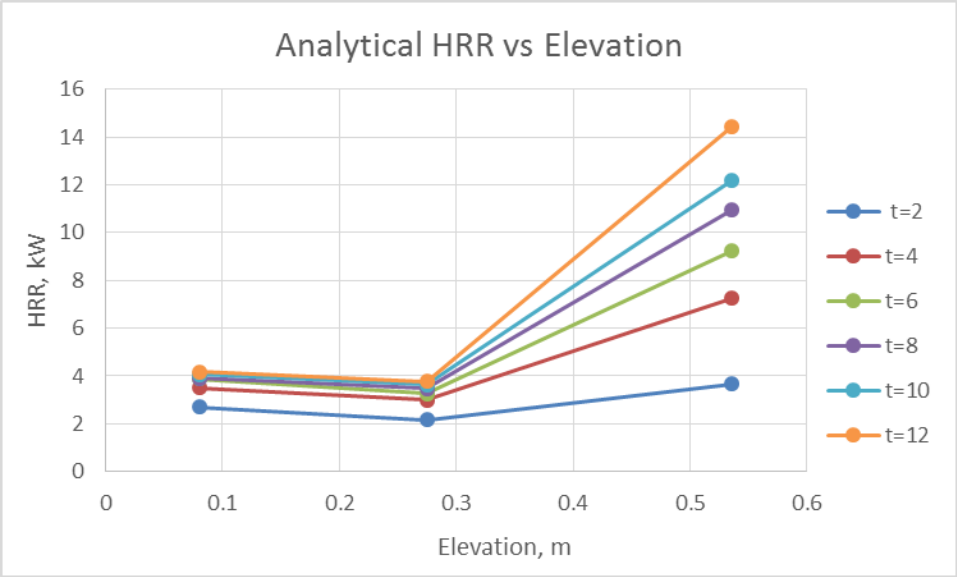

Figure 44. Relations between analytically found HRR and fire elevation.

The found extreme differences due to the elevation to 1/3H and to 2/3H are confronted to those that were found for experimental HRR in RQ1 (Table 5) in Table 13 below.

Table 13. Comparison of the effect of elevation on HRR found experimentally and predicted analytically.

HRR	Difference with 1/3H		Difference with 2/3H	
	min	max	min	max
Experimental	-16%	-5%	-17%	+63%
Analytical	-20%	-10%	+35%	+246%

As any other analytical calculations, the one for HRR mostly depends on the input parameters. Uncertainty of one can essentially affect final results. In this case, the use of assumed combustion efficiency of 0.7, led to the slight underestimates of HRR for scenario 2 and gross overestimates of HRR for scenario 3. Therefore, when performing a Fire Safety Engineering design for fire that is possible to be elevated, attention should be paid to the choice of combustion efficiency value.

Hot Gas Layer Temperature

Two analytical methods have been used to calculate the hot gas layer temperature in the room. Method 1 is known as the MQH Method as it was developed by McCaffrey, Quintiere and Harkleroad . [26] Method 2 is based on the principal of energy balance and includes equation developed by N. Johansson and P. van Hees [14] and by Heskestad [27].

To evaluate the capability of both models to account for the source elevation, provided by those methods temperatures were plotted against the elevation (Figure 45 and Figure 46) and differences between floor scenario and elevation scenarios were computed.

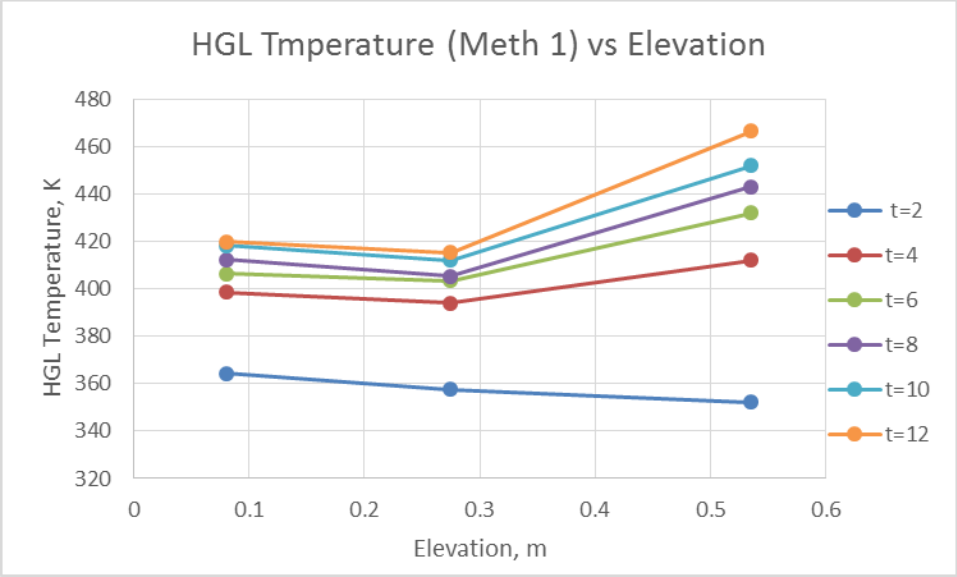

Figure 45. Relations between HGL temperatures calculated using Method 1 and fire elevation.

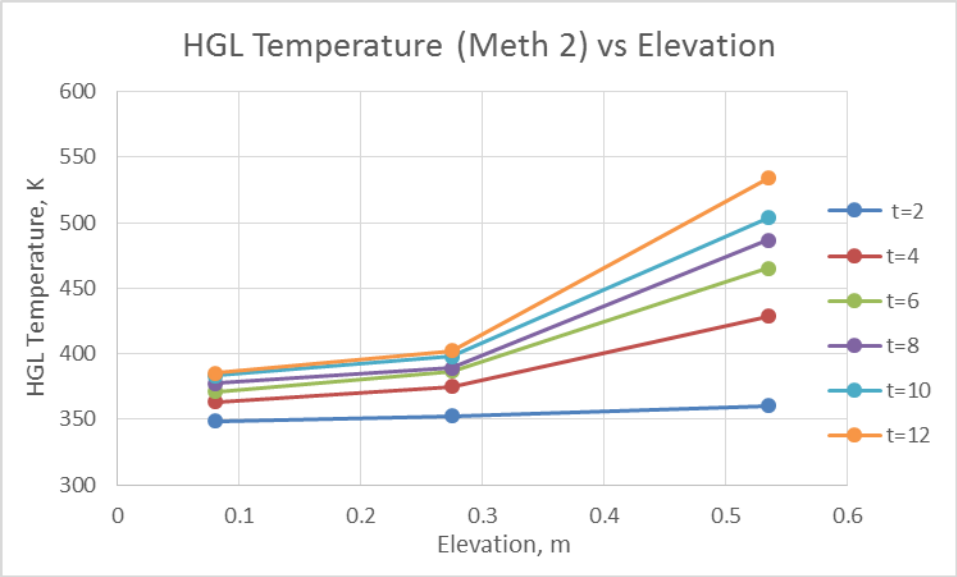

Figure 46. Relations between HGL temperatures calculated using Method 2 and fire elevation.

Method 1 predicts that if the fire is elevated from the floor to 1/3H, the temperature of the smoke layer will get lower by 1-2%. While Method 2 gives that such change of fire position will result in the raise of temperature by 1-4%. Both Methods forecast that the raise of the fire from the floor to the 2/3H of the room will lead to the significant raise of the HGL temperature. The Method 1 gives the maximum increase of 11%, and Method 2 – of 39%.

In the Table 14 the comparison of extreme changes predicted by analytical methods are compared with experimentally found ones (Table 6).

Table 14.Comparison of the effect of elevation on HGL temperature found experimentally and predicted analytically by Methods 1 and 2.

HGL Temperature	Difference with 1/3H		Difference with 2/3H	
	min	max	min	max
Experimental	-2%	<-1%	-2%	+3%
Method 1	-2%	-1%	-3%	+11%
Method 2	+1%	+4%	+3%	+39%

Analytical Method 1 can account for the elevation reasonably well, as found differences are not much different from those found for experimental temperatures. However, the Method 2 overestimates the effect of elevation. Nevertheless, one should keep in mind, that the magnitudes of temperatures found analytically were not similar to the experimental ones, as it was early discussed in Section 5.1.3. Moreover, analytical methods are critically dependent on the input parameters. In this case, the exact values of HRR from every elevation test were used, because of that the effect of elevation was so close to experimental findings. However, in real practice a single HRR value from free burning test is usually used, but this cannot provide any effects of fire elevation.

HOT GAS LAYER HEIGHT

In the course of HGL temperature calculations in accordance with the Method 2, the vertical position of the smoke layer was also found. To see if the mass and energy conservation method can be used to estimate the influence of the elevation on the magnitude of the HGL height, a graph of calculated HGL versus elevation is presented (Figure 47).

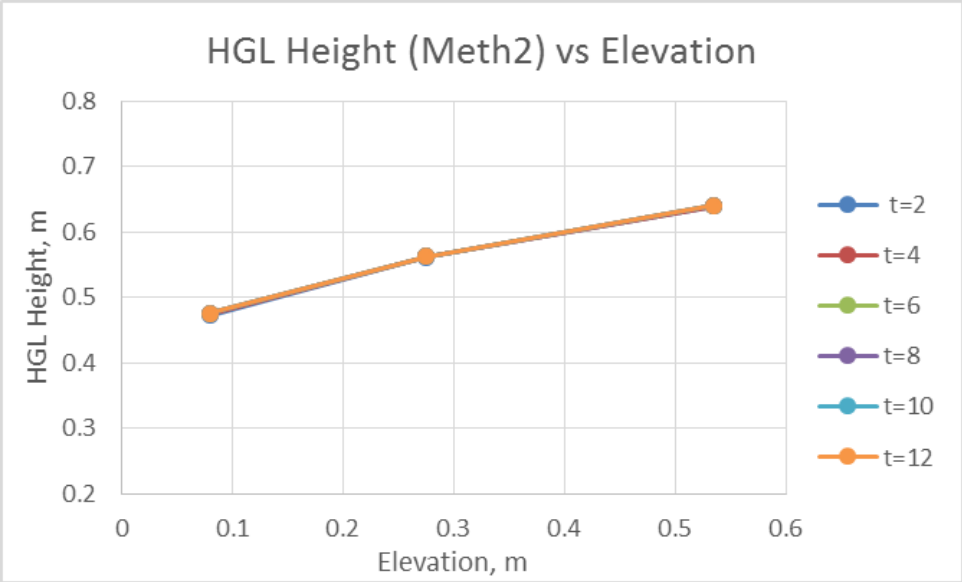

Figure 47. Relations between HGL heights calculated using Method 2 and fire elevation.

From the Figure 47 it can be seen that a position of the smoke layer is practically linear to the fire position, and does not change over the burning period. The smoke layer produced by the fire from scenario 2 is higher by 19% than the smoke from the floor fire, and the smoke from the scenario 3 is higher by 35%.

To decide whether the Method can account for elevation, found extreme differences are collated to those found for experimental results (Table 7) in following Table 15:

Table 15. Comparison of the effect of elevation on HGL height found experimentally and predicted analytically by Methods 2.

HGL Height	Difference with 1/3H		Difference with 2/3H	
	min	max	min	max
Experimental	+9%	+14%	+10%	+28%
Method 2	+18%	+19%	+34%	+35%

From the Table it can be seen, that the analytical method for estimating the smoke layer height, slightly overestimates the impact of the source elevation. The higher the elevation, the greater the error of analytical prediction.

Summary: analytical methods

All in all, analysis of the analytical results showed that reliability of the theoretical models depends greatly on the input parameters used for calculations. Averaged value of combustion efficiency and calculating using tabular values of MLR, will certainly lead to inability of predicting correct fire parameters for the elevation cases. Use of the experimental values of HRR in HGL temperature calculations can provide relatively accurate results and even account for the elevation of the source. However, if the approximate value of HRR is used, the results are likely to contain a significant uncertainty. In order to adjust existing calculation methods to be suitable for scenarios with elevated fire source, a database of experimentally obtained MLR and HRR for different elevations should be collected for most common fuels. It is possible that new methods for estimating for combustion efficiency, MLR or HRR can come in the future.

It can be finally concluded, that elevation of the source does affect the development of almost all fire parameters. Ignorance of this phenomena most definitely will lead to the inappropriate fire safety engineering design, endangering the occupants' life. Existing analytical calculations methods and simulation softwares are not capable of reliable prediction of the elevated fire effects, because there are some phenomena involved that at the moment just cannot be modelled correctly. Most of the theoretical methods used for hand or FDS calculations are based on HRR, until the way is found to predict HRR for elevated fires, the existing analytical methods will not be of any use.

7 Uncertainties and Validity of the Study

7.1 Uncertainties and Sources of Error

The performed earlier analysis and discussions assumed that results obtained during the experiments (measurements and processed data) are by default trustworthy. Basing on this assumptions, discussions were carried out to answer the research questions, and corresponding conclusions were formed. Yet, there are uncertainties associated with the experiment and the experimental measurements. Numerous imprecisions were allowed during the tests, therefore, there is likely to be a number of possible sources of error that could affect the experimental results or the following analysis. Some of them could considerably affect the results.

The first inaccuracy noticed was that the initial temperature in the enclosure was different for every test. Higher temperature in the beginning of the experiment could lead to greater peak temperature, higher magnitude of the computed hot gas layer temperature and also of the heat flux measured by flux meter, as radiation is proportional to the temperature in the power of four. Rate of heat released and mass loss rate can also be slightly increased as gasification of the fuel occurs faster at higher temperatures and heat fluxes.

The pool fire was placed 10 cm away in horizontal direction from the flux meter. It was meant that only the radiation from the hot smoke layer and boundaries would get measured by the flux meter. However, it is likely that radiation from the flame could also get in the range of flux meter. If it were true, then heat flux measurement would be higher for the first scenario with the pool fire on the floor, because the flame was closer to the flux meter, so the view factor was greater.

Calibration of the gas analyser and supporting software was not done before every test or even once a day; instead an earlier estimated approximate correction coefficients were applied to all measurements. This is likely to cause imprecision of the results, as parameters that are important for HRR measurements change throughout a day. To have the precise results, calibration ought to be done prior each test, which would be time consuming, and that is why this was not implemented.

It was also not possible to measure the volume fraction of the carbon monoxide in the exhaust air with the gas analyser. Consequently, without this parameter the followed calculation of the HRR was less precise. Still, in the experiment a complete combustion took place; therefore, it is reasonable to assume that CO products could be negligible.

As it was mentioned in a set-up description, a stack of bricks was used to recreate different elevations. That means, that for different scenarios uneven number of bricks was present in the room: 0, 3 or 7. Bricks, as a solid, were absorbing some amount of heat and, afterwards, they reradiate it back to the room. Naturally, conditions in the room during the test were not similar for scenario for which no bricks were needed, and scenarios with 3 or 7 stacked bricks placed under the fuel pan.

Some uncertainties could arise because of the human factor. For example, even though the amount of the water and fuel for each test was tried to be carefully measured, some liquid was spilled during the placing of the pan inside the room. Moreover, the position of the fuel pan was not absolutely the same for each repeated test, as it was dark inside the enclosure, and not much could be seen, an error of 1-2 cm is expected.

To analyse experimental results, data for each scenario was compared between each other from ignition to when the fire went out. Yet, the exact moment of the ignition was not easy to record. Instead it was selected later by analysing output file, as the moment when certain parameter has started to change. Clearly, such approach is user dependent, thus, unprecise. Each device used had a delay in measurements processing. It was expected that the difference in initial time for load cell and gas analyser should be around 45 seconds. However, this difference was later found to be dissimilar for every test, fluctuating between 20 and 70 seconds. Thus, the error of about 10-25 seconds is possibly to be expected.

As it was stated earlier, four repetitions were conducted for every scenario. Yet, only averaged values were used for further analysis. If one or several repetitions were imprecise, the following averaging of all outputs could lead to great divergence with true values. Usually, this is avoided by executing a great number of repetitions. The larger the number the lesser the expected random error. It can be guessed, four repetitions are not a sufficient number, thus, expected random error should be great. To have an idea of the actual extent of the error from the experimental performance, the variation of the extreme values (maximum or minimum) from mean can be calculated.

The difference of the extreme from the mean is found by dividing minimum and maximum measured value by the mean. This was done for every time step, and averaging over the time was performed. The maximum values are selected as the representative of the expected error due to averaging for every scenario (Table 16, Table 17 and Table 18). The spread in the values caused by the multiple repetitions was found for HRR and MLR measurements and calculations.

Table 16.The variation of values due to averaging, scenario 1.

Scenario 1: fire on the floor

Measured Parameter	Max/Mean	Min/Mean	Maximum Variation
HRR	0.072	0.067	7.2%
MLR	0.191	0.109	19.1%

Table 17.The variation of values due to averaging, scenario 2.

Scenario 2: 1/3H

Measured Parameter	Max/Mean	Min/Mean	Maximum Variation
HRR	0.142	0.094	14.2%
MLR	0.068	0.056	6.8%

Table 178.The variation of values due to averaging, scenario 3.

Scenario 3: 2/3H

Measured Parameter	Max/Mean	Min/Mean	Maximum Variation
HRR	0.158	0.114	15.8%
MLR	0.12	0.152	14%

The Tables (16-18) above provide a visual comprehension of the accuracy and trustworthy of the experimentally achieved results. For every tested scenario expected variation is greater than 5%, which implies that they cannot be simply neglected. On the other hand, the variations are less than 20%, which in Fire Safety Engineering practice is sometimes considered to be not a critical error. In any case, the obtained experimental results should be carefully used for the analysis, and one shall always keep in mind the possibility of the significant inaccuracy.

7.2 Validity

In course of this study several observations were made that gave rise to some conclusions regarding dependency of the fire parameters on the elevation of the fire source. However, the recently discussed uncertainties of the performed experiments and limitations stated in the section 1.3 evidence that achieved findings are likely to be limited and cannot be considered to be trustworthy and suitable for any fire scenarios. In research practice two type of validity are recognized: internal validity and external validity.

Internal validity implies the level of confidence in the achieved outcomes of the performed work. It can be evaluated based on the significance of the sources of error present in the study. This was talked over in the previous section (7.1) a definite number of the uncertainty is hard to give. Yet, a value of at least 20% is expected. Internal validity of other two research methods used in the study: FDS simulations and hand calculations should be also discussed.

Regarding the performance of FDS simulations, it can be stated that due to the inaccuracy of the MLR per unit area inputs, the results were compromised. Additionally, the chosen grid was too coarse to implement precise calculations. While, the imprecision of the input data should not have an impact on the prediction of the elevation effect on fire development, the course grid could cause averaging of some parameters that could reduce the display of the changes caused by fire elevation. Therefore, the validity of the FDS outputs is disputable.

Internal validity of the hand-calculated results depends on the choice of the input parameters and initial conditions. Initial temperature was approximated, used HRR values were measured experimentally and could differ by 15%. The attempt to account for elevation in application of the Method 2 (Appendix D. Method 2) was used in this work for the first time, thus, there is a chance that these calculation are not appropriate. Furthermore, the used models include an uncertainty due to the assumptions made in the process of their development. In their work N. Johansson et al [19] provides values of uncertainties for the Method 1 and Method 2. According to this study the model uncertainty of the Method 1 is 8%, and of the Method 2 – 15%. All in all, the total uncertainty of the conducted calculations can exceed 20%.

External validity is the extent to which the results of a study can be generalized to other situations. [28] Considering the experimental set up and other specifics of the study, some restrictions of the application can be already defined. First of all, the findings are not applicable for the fires in under ventilated conditions. Available oxygen and combustion efficiency were the key factors in performed analysis, thus, any drastic changes of these parameters are likely to change the outputs entirely. Secondly, due to the geometry of the fire room used, it is uncertain whether results can be appropriate for fires in long corridors or extremely high enclosures. Moreover, a single Heptane pool fire might not be entirely representative for the real room fire with multiple objects. Lastly, the fires during the test burned out before the steady state was reached.

Altogether, accomplished study was limited by its configuration and choice of fuel. Due to restricted time given for this work, the number of performed scenarios and their repetition was insufficient. Substantial uncertainties are also present in the outcomes. For these reasons, it is impossible to express obtained results in terms of absolute values that could be applied to any other situation. Nevertheless, some general trends were observed that can give rise to the future work.

8 Conclusions

The experimental study of elevated fires in a single compartment was conducted to investigate the influence of the fire source elevation on the development of conditions hazardous for life safety. Additionally, Fire Safety Engineering analytical methods and fluid dynamics softwares were examined to determine their ability to account for effects of fire elevation. It was discovered that elevation of the fire up to the area of the smoke layer formation, accelerates the fire growth, causing greater risks than general floor fires. While the elevation of fuel to the height, where no significant smoke-flames interaction occurs, results in the retardation of the fire development and reduction of the hazardous risks. The analytical Fire Safety Engineering methods and FDS simulations did not provide dependency of vertical fire position similar to the experimental findings, yet, it gave relatively similar general trends. Therefore, it was established that these means of Fire Safety Engineering design cannot exactly estimate the impact of the fire elevation, but still can be used as a guidance.

This study was unable to provide any quantative solutions for design of elevated fires. Neither could it suggest specific modifications that could be applied to analytical calculation methods and simulation softwares. Yet, the study showed that the use of existing computational methods can provide mostly good trends and values with uncertainties of no more than 25%. In order to achieve better results, sufficient to resolve this problem, the study has to be continued in the future, covering more fire scenarios. In the future it is advised to conduct more experiments for other elevation positions, different type of fuels, multiple fuels, enclosures of diverse size and configuration and longer duration of fire. Besides experimental studies, additional simulations in FDS with better grid resolutions and modified configurations and inputs should be conducted. Deeper literature search and application of other analytical models to the elevation fire problem can bring more comprehension of the issue.

9 Acknowledgement

I would like to express my gratitude to people who provided valuable guidance and assistance throughout this work. Firstly, I want to thank my promoter and supervisor Associate Lecturer Nils Johansson for his endless support, valuable advices and infinite patience. Associate Professor Stefan Svensson for his assistance with the performance of experiments and equipment setup. Jonathan Wahlqvist for sharing his knowledge and for his assistance with FDS input writing and simulations running. My husband Jonathan Vallee for sharing this unique experience with me.

10 References

[1] B. McCaffrey, "Flame Heigh," *SFPE Handb. Fire Prot. Eng.*, no. 2nd ed., pp. 2–1–2–8, 1995.

[2] SFPE, *SFPE Engineering Guide to Performance-Based Protection*. Bethesda, MD, USA: Society of Fire Protection Engineers, 2007.

[3] M. Ahrens, "HOME STRUCTURE FIRES, NFPA Database," 2015. [Online]. Available: http://www.nfpa.org/research/reports-and-statistics/fires-by-property-type/residential/home-structure-fires.

[4] L. Staffansson, "Selecting design fires," pp. 1–105, 2010.

[5] B. Evarts, "FIRES IN U.S. INDUSTRIAL AND MANUFACTURING FACILITIES, NFPA," 2012. [Online]. Available: http://www.nfpa.org/research/reports-and-statistics/fires-by-property-type/industrial-and-manufacturing-facilities/fires-in-us-industrial-and-manufacturing-facilities.

[6] I. O. O. Sugawa, K. Kawagoe, Y. Oka, "Burning Behavior in a Poorly-Ventilated Compartment Fire-Ghosting Fire," *Fire Sci Technol*, vol. 9(2), p. 5–14, 1989.

[7] E. E. Zukoski, "Development of a stratified ceiling layer in the early stages of a closed-room fire," *Fire Mater.*, vol. 2, no. 2, pp. 54–62, 1978.

[8] L. Mounaud, "A parametric study of the effect of fire source elevation in a compartment," Virginia polytechnic institute and state university, 2004.

[9] J. Backovsky, K. Foote, N.J. Alvares, "Temperature profiles in forced-ventilation enclosure fires," *Fire Saf. Sci*, vol. 315–324, 1989.

[10] J. Zhang, S. Lu, Q. Li, R. Yuen, M. Yuan, and C. Li, "Impacts of elevation on pool fire behavior in a closed compartment: A study based upon a distinct stratification phenomenon," *J. Fire Sci.*, vol. 31, no. 2, pp. 178–193, 2012.

[11] J. Zhang, S. Lu, Q. Li, C. Li, M. Yuan, and R. Yuen, "Experimental study on elevated fires in a ceiling vented compartment," *J. Therm. Sci.*, vol. 22, no. 4, pp. 377–382, 2013.

[12] J. Wang, S. Lu, Y. Hu, H. Zhang, and S. Lo, "Early Stage of Elevated Fires in an Aircraft Cargo Compartment: A Full Scale Experimental Investigation," *Fire Technol.*, vol. 51, no. 5, pp. 1129–1147, 2015.

[13] A. Purser, "Amendment to the General Laws, Health and Safety," *Compr. Fire Saf. Act 2003*, p. Chapter 23–28, 2003.

[14] N. Johansson and P. van Hees, "A Simplified Relation Between Hot Layer Height and Opening Mass Flow," *11th Int. Symp. Fire Saf. Sci.*, vol. 60, no. m, pp. 432–443, 2014.

[15] J. Quintiere and B. Karlsson, "Pressure Profiles and Vent Flows for Well-Ventilated Enclosures," in *Enclosure fire dynamics*, 1999.

[16] J. Quintiere and B. Karlsson, "Energy Release Rates," in *Enclosure fire dynamics*, 1999.

[17] M. L. Janssens, "Measuring rate of heat release by oxygen consumption," *Fire Technol.*, vol. 27, no. 3, pp. 234–249, 1991.

[18] V. Babrauskas, "Heat Release Rates," in *SFPE Handbook of Fire Protection Engineering*, 2007, pp. 799–823.

[19] N. Johansson, S. Svensson, and P. van Hees, "An evaluation of two methods to predict temperatures in multi-room compartment fires," *Fire Saf. J.*, vol. 77, pp. 46–58, 2015.

[20] M. Janssens and H. C. Tran, "Data Reduction of Room Tests for Zone Model Validation," *J. Fire Sci.*, vol. 10, no. 6, pp. 528–555, 1992.

[21] I. Collaborative, "International Collaborative Project to Evaluate Fire Models for Nuclear Power Plant Applications : Proceedings of International Collaborative Project to Evaluate Fire Models for Nuclear Power Plant Applications : Proceedings of Meeting Held at National In," 2002.

[22] B.J. McCaffrey, "Purely Buoyant Diffusion Flames: Some Experimental Results," *NBSIR 79–1910, Natl. Bur. Stand.*, 1979.

[23] K. Mcgrattan and R. Mcdermott, "Fire Dynamics Simulator User ' s Guide," 2013.

[24] K. McGrattan, S. Hostikka, R. McDermott, J. Floyd, C. Weinschenk, and K. Overholt, "Fire Dynamics Simulator User's Guide (Sixth Edition)," *Natl. Inst. Stand. Technol.*, 2014.

[25] J. Wahlqvist and P. van Hees, "Implementation and validation of an environmental feedback pool fire model based on oxygen depletion and radiative feedback in FDS," *Fire Saf. J.*, pp. FISJ–D–15–00136R3.

[26] B. J. McCaffrey, J. G. Quintiere, and M. F. Harkleroad, "Estimating room temperatures and the likelihood of flashover using fire test data correlations," *Fire Technol*, vol. 17, pp. 98–119, 1981.

[27] G. Heskestad, "Fire Plumes, Flame Height, Air Entrainment, Flame height and air entrainment," in *SFPE Handbook of Fire Protection Engineering, 5th edition*, 2016, pp. 415–416.

[28] Wikipedia, "External validity." [Online]. Available: https://en.wikipedia.org/wiki/External_validity.

Appendices

Appendix A. HRR Calculations

Equation for HRR, taking into consideration O_2 consumption and CO_2 production can be seen bellow (Eq.A.1):

$$\dot{Q} = E \frac{\phi}{1+\phi(\alpha-1)} \dot{m}_e \frac{M_{O_2}}{M_a} (1 - X^{o}_{H_2O} - X^{o}_{CO_2}) X^{A^o}_{O_2} \qquad (A.1)$$

Where

Q – heat release rate;

E –amount of energy released by complete combustion per unit mass of oxygen consumed;

α – expansion factor;

ϕ –oxygen depletion factor;

m_e – mass flow rate in the duct;

M_{O2} – molecular weight of O_2 (32kg/kmol)

M_a – molecular weight of the incoming air

$X^{o}_{H_2O}$ - mole fraction of H_2O in the incoming air;

$X^{o}_{CO_2}$ - mole fraction of CO_2 in the incoming air;

$X^{A^o}_{O_2}$ - measured mole fraction of O_2in the incoming air

As it can be noticed many components of Eq.(A.1) are unknown at the moment and thus, have to be calculated.

a) E and α calculations.

Stoichiometric equation for the combustion of heptane is:

$C_7H_{16} + 11O_2 + 41.4N_2 \rightarrow 8H_2O + 7CO_2 + 41.4N_2$

$$E = \Delta H_c \frac{M_{C_7H_{16}}}{M_{O_2}} \qquad (A.2)$$

Where ΔH_c - complete heat of combustion of heptane (44.6 MJ/kg);

$M_{C_7H_{16}}$ - molecular weight of heptane

$M_{C_7H_{16}} = 7 \cdot 12 + 16 \cdot 1 = 100$ kg/kmol

M_{O_2} - molecular weight of oxygen (32 kg/kmol)

$$E = \Delta H_c \frac{M_{C_7H_{16}}}{M_{O_2}} = 44.6 \frac{100}{11 \cdot 32} = 12.67 MJ / kg$$

$$\alpha = \frac{n_{product}}{n_{react}} = \frac{8 + 7 + 41.4}{11 + 41.4} = 1.076 \qquad (A.3)$$

a) Oxygen depletion factor, φ

As only O_2 and CO_2 were measured, the equation for oxygen depletion factor is:

$$\emptyset = \frac{X_{O_2}^{A^o}\left(1 - X_{CO_2}^{A}\right) - X_{O_2}^{A}\ (1 - X_{CO_2}^{A^o})}{(1 - X_{O_2}^{A}\ - X_{CO_2}^{A}) X_{O_2}^{A^o}} \qquad (A.4)$$

Where

$X_{O_2}^{A^o}$ and $X_{CO_2}^{A^o}$ - measured mole fraction of O_2 and CO_2 in the incoming air. They can be found from the output file as the average value of O_2 and CO_2 mole fractions for the time before ignition.

$X_{CO_2}^{A}$ and $X_{O_2}^{A}$ - measured mole fraction of O_2 and CO_2 in the exhaust gases. Those values can be found directly in the results document. Value of φ can be calculated using spread-sheet for each second of experiment.

b) Mass flow rate in the duct

$$\dot{m}_e = 26.54 \frac{A k_c}{f(\mathrm{Re})} \sqrt{\frac{\Delta P}{T_e}} \qquad (A.5)$$

Where

A - cross-sectional area of the duct;

k_c – velocity profile shape function (0.875);

f(Re) – Reynolds number correction (1.08);

ΔP – pressure difference in the duct (given in output file);

T_e – Temperature of the gasses in the duct (given in output file).

Area of the duct can be found knowing that diameter of the duct is 20cm.

$$A = \frac{\pi D^2}{4} = 0.0314 m^2$$

$$\dot{m}_e = 26.54 \frac{0.0314 \cdot 0.875}{1.08} \sqrt{\frac{\Delta P}{T_e}} = 0.675 \sqrt{\frac{\Delta P}{T_e}}$$

Value $\sqrt{\frac{\Delta P}{T_e}}$ is known but changes with time, thus, it can be found in the output file.

c) Molecular weight of the incoming air, M_a

$$M_a = M_{dry}(1 - X^0_{H_2O}) + M_{H_2O} X^0_{H_2O} \qquad (A.6)$$

Where M_{dry} – molecular weight of the dry air (29 kg/kmol);

M_{H2O} – molecular weight of H_2O (18 kg/kmol);

$X^0_{H_2O}$ - mole fraction of H_2O in the incoming air, which can be calculated using the equation bellow:

$$X^0_{H_2O} = \frac{RH}{100} \frac{p_s(T_a)}{p_a} \qquad (A.7)$$

Where RH – relative humidity (30%);

p_a – air pressure at a temperature T_a;

T_a – temperature of air at time t=0s, changes for every test, can be found in the output file as an average temperature inside the enclosure prior the ignition;

$p_s(T_a)$ – saturation pressure of water vapour at T_a, can be estimated using formula:

$$\ln(p_s) = 23.2 - \frac{3816}{(T_a - 46)} \qquad (A.8)$$

Lastly,

$$M_a = M_{dry}(1 - X^0_{H_2O}) + M_{H_2O} X^0_{H_2O} = 29(1 - X^0_{H_2O}) + 18 \cdot X^0_{H_2O}$$

d) Finally all components of the Eq.(A.1) have been found and it is possible to determine HRR (Eq.(A.2)):

$$\dot{Q} = E \frac{\phi}{1 + \phi(\alpha - 1)} \dot{m}_e \frac{M_{O_2}}{M_a} (1 - X^o_{H_2O} - X^o_{CO_2}) X^{A^o}_{O_2} = 12670 \frac{\phi}{1 + \phi(1.076 - 1)} \dot{m}_e \frac{32}{M_a} (1 - X^o_{H_2O} - X^o_{CO_2}) X^{A^o}_{O_2}$$

All unknown values can be calculated from the measured values found in the output +spread sheet file. Graphical illustration of results are presented in the Section 3.2.2.

Appendix B. Hot Gas Layer Temperature and Height, Reduction Method

The chosen method presents a temperature in the room as a continuous function that depends on the height of the room. The Figure 48 could assist in understanding the development of this method.

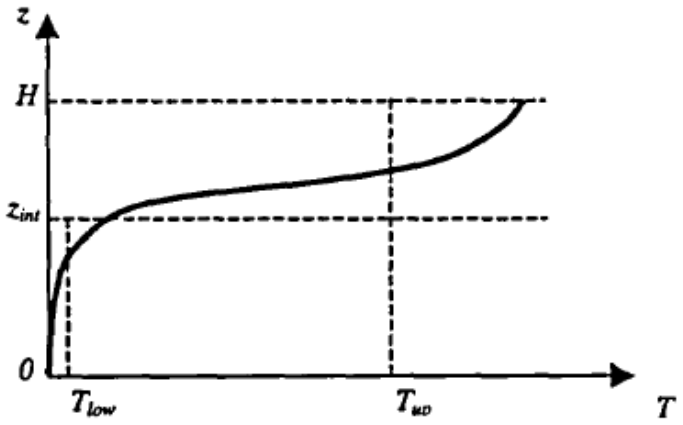

Figure 48. Schematic depiction of two zone model concept.

From the two zone model concept and the conservation of mass the equations (Eq.(B.1) and Eq.(B.2)) can be derived:

$$(H - z_{int})T_{up} + z_{int} \cdot T_{low} = \int_0^H T(z)dz = I_1 \qquad (B.1)$$

$$(H - z_{int})\frac{1}{T_{up}} + z_{int}\frac{1}{T_{low}} = \int_0^H \frac{1}{T(z)}dz = I_2 \qquad (B.2)$$

Then,

$$z_{int} = \frac{T_{low}(I_1 I_2 - H^2)}{I_1 + I_2 T_{low}^2 - 2T_{low}H} \qquad (B.3)$$

$$T_{up} = \frac{1}{H - z_{int}} \int_{z_{int}}^H T(z)\,dz \qquad (B.4)$$

Here, T_{low} – is taken as a temperature measured by the lowest thermocouple, K;

z_{int} – vertical position of the interface between two layers or HGL height, m;

T_{up} – HGL temperature, K;

H – vertical position of the highest thermocouple, m;

I_1 and I_2 can be calculated in a spread-sheet from the discrete data obtained during the experiments. For the time saving reasons, HGL temperature and position of the interface between two layers were found only for every second minute of the tests.

Appendix C. Method 1

McCaffrey, Quintiere and Harkleroad independently had developed an expression that allowed to estimate the temperature rise for known HRR and enclosure characteristics (Eq. (C.1)). [26]

$$\Delta T = 6.85 \left(\frac{\dot{Q}^2}{A_0 \sqrt{H_o} h_k A_t} \right)^{1/3} \quad (C.1)$$

Where $\dot{Q}$- is HRR of the fuel, kW;

H_o – the opening height, 0.65 m;

A_o – the opening area, m^2;

$A_o = 0.65 \cdot 0.285 = 0.18525\ m^2$;

h_k – effective heat conduction coefficient of the solid enclosure's boundaries, kW/m^2K;

A_t – total internal surface area in the enclosure, m^2;

$A_t = (1.2 \cdot 0.8 + 2 \cdot 0.8 \cdot 0.8) - 0.18525 = 2.0548\ m^2$.

In order to calculate the temperature rise, the conduction coefficient should be determined first. McCaffrey and colleagues proposed following manner to do that (Eq. (C.2) and (C.3)).

$$\text{For } t < t_p: \ h_k = \sqrt{\frac{k\rho c}{t}}; \quad (C.2)$$

$$\text{For } t \geq t_p: \ h_k = \frac{k}{\delta} \quad (C.3)$$

Where t_p – is a thermal penetration time, s;

k - conductive of the compartment surface material, kW/mK;

ρ – density of the compartment surface material, kg/m^3;

c – specific heat of the compartment surface material, kJ/kgK.

Thermal penetration time can be given as (Eq. (C.4)):

$$t_p = \frac{\delta^2}{4\alpha} \quad (C.4)$$

where δ – is a thickness of the boundary, m;

$\alpha = k/\rho c$ – thermal diffusivity of the compartment surface material, m^2/s.

Thermal properties of the boundaries' material are: (Table 18)

Table 18. Properties of the boundaries' material

Material	Density ρ, kg/m³	Conductivity k, W/mK	Specific heat c, J/kgK	kρc, W^2s/m^4K^2	Thermal diffusivity α, m^2/s	Thickness δ, m
Calcium silicate board	870	0.175	1130	$1.7 \cdot 10^5$	$1.8 \cdot 10^{-7}$	0.01

Than thermal penetration time:

$$t_p = \frac{\delta^2}{4\alpha} = \frac{0.01^2}{4 \cdot 1.8 \cdot 10^{-7}} = 138.8s$$

Thus, during the first 139 seconds, the Equation C.2 should be used to find effective conduction coefficient for the transient case. As it is dependent on the time, it is better to compute this parameter in excel spread sheet. After 139 seconds, the constant given by Equation C.3 should be used:

$$h_k = \frac{k}{\delta} = \frac{0.175}{0.01} = 17.5\, W/m^2K$$

The variation over time of the effective conduction coefficient is presented on the graph below (Figure 49). In this study it was decided that for parameters that changes with time, the values corresponding to every 2nd minute only should be considered, in order to simplify observations. In this way, only for the first 2 minutes different conduction coefficient is found (0.0378 kW/m²K), as for later time steps this parameter stays constant at 0.017 kW/m²K.

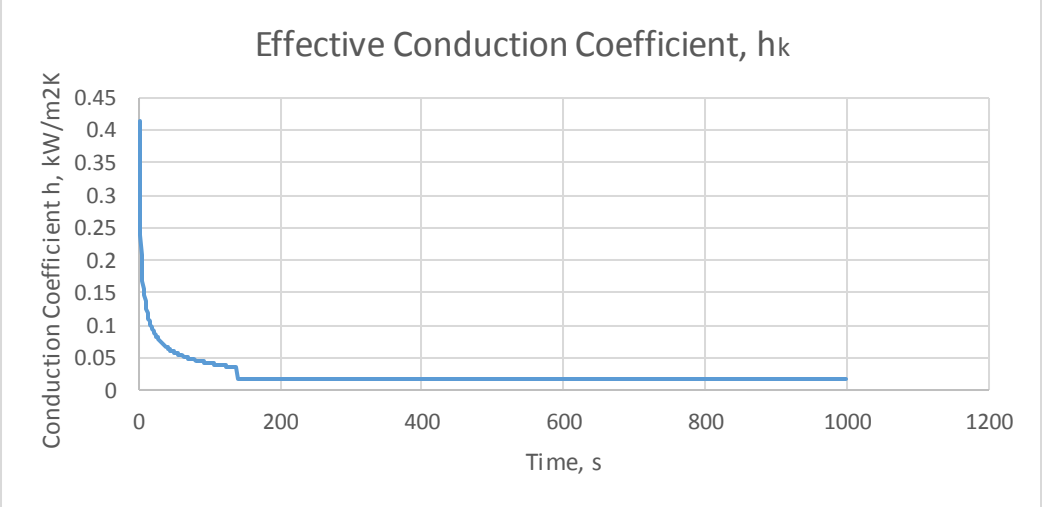

Figure 49. Variation of the effective conduction coefficient over time.

The last unknown parameter for the Equation C.1 is the heat release rate. The estimated HRR of 2.6kW is likely to be incorrect, therefore, it was decided to use rather the values of HRR obtained experimentally for every scenario and for every two minutes of tests.

For the first elevation scenario (fire near the floor), the heat release rate after 2 minutes of combustion was 3.1kW (Table 19). Therefore, the rise of hot temperature in the room:

$$\Delta T = 6.85\left(\frac{\dot{Q}^2}{A_0\sqrt{H_o}h_k A_t}\right)^{1/3} = 6.85\left(\frac{3.1^2}{0.18525\sqrt{0.65}\cdot 0.0378\cdot 2.0548}\right)^{1/3} = 64K$$

The initial temperature in the room prior each test was slightly different. The averaged value for 4 repetitions was found to be equal: $T_{amb} = 27^oC = 300^0K$.

Then, the hot gas layer temperature at 2 minutes after ignition was:

$$T_g = T_{amb} + \Delta T = 300 + 64 = 364K$$

The similar calculations were implemented in excel work sheet for every time step and for every elevation scenario, by using HRR values (for every 2nd minute) obtained from the experimentally measured Oxygen depletion. Results can be found in the Table 19, 17 and 18, graphical results are in the Section 5.1.3.1, Figure 24.

Table 19. Results of the Method 1 calculation for scenario 1

Scenario 1 (Floor)		
Time, min	HRR (test 1), kW	HGL Temperature, K
2	3.10	364.36
4	3.99	398.43
6	4.48	406.31
8	4.87	412.40
10	5.26	418.24
12	5.37	419.92
14	6.01	429.26
16	7.18	445.59
18	7.56	450.62

Table 20. Results of the Method 1 calculation for scenario 2

Scenario 2 (1/3H)		
Time, min	HRR (test 2), kW	HGL Temperature, K
2	2.62	357.54
4	3.72	393.92
6	4.29	403.31
8	4.41	405.23
10	4.85	412.11
12	5.06	415.28

14	5.45	421.18
16	6.15	431.32
18	7.41	448.69
20	7.22	446.15

Table 21. Results of the Method 1 calculation for scenario 3.

Scenario 3 (2/3H)		
Time, min	HRR (test 3), kW	HGL Temperature, K
2	2.27	352.20
4	4.84	411.92
6	6.20	431.98
8	6.99	443.01
10	7.64	451.77
12	8.79	466.57

In real Fire Safety Engineering practice it seldom happens that HRR for particular scenario was experimentally found prior the calculations. More often just HRR from the free burning experiment is determined. Therefore, to assess the impact of this assumption, HGL temperature was computed using HRR from the free burning test (Table).

Table 22. Results of the Method 1 calculation using HRR of free burn test for all elevation scenarios.

All Scenarios		
Time, min	HRR (free burning), kW	HGL Temperature, K
2	3.31	367.20
4	3.95	375.60
6	4.35	380.68
8	4.73	385.25
10	5.01	388.59
12	5.05	389.10
14	5.14	390.16
16	5.97	399.58
18	7.12	412.01
20	6.29	403.12

Appendix D. Method 2

This method performs as a simple two-zone model. A simple energy balance for the pre-flashover fire in the enclosure similar to the one on the figure below (Figure 50) is: energy released during the fire is spend for losses due to air flow out through the vents and for heat losses to compartment boundaries. Mathematically this can be expressed as (Eq.(D.1)):

$$\dot{Q} = \dot{m}_g c_p \Delta T + h_k A_T \Delta T, \qquad (D.1)$$

where Q – rate of heat released in the compartment, kW;

m_g – airflow out through the vents, kg/s;

c_p – specific heat of gases, generally taken as 1.0 kJ/kgK;

$\Delta T = T_g - T_a$ – temperature increase in the compartment, K;

h – effective conduction heat transfer coefficient for the boundaries, kW/m^{2}K;

A_T – total area of the boundaries, m^2.

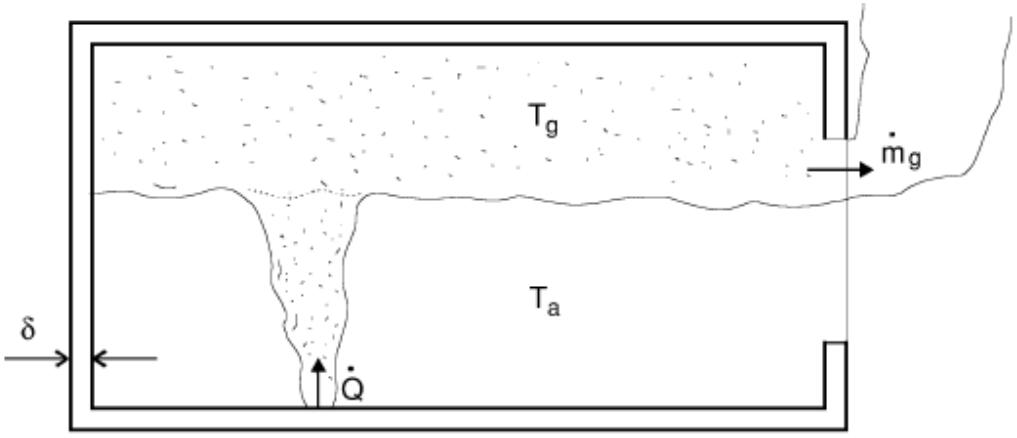

Figure 50. Schematic depiction of the stratified case.

Equation D.1 can be rewritten in terms of the temperature increase (Eq.(D.2)):

$$\Delta T = \frac{\dot{Q}}{(\dot{m}_g c_p + h_k A_t)} \qquad (D.2)$$

It should be pointed out, that the equation D.2 is valid only from the moment when hot gases from the enclosure begin to flow out through the vent. Otherwise, the component m_g cannot be introduced.

The effective conduction heat transfer coefficient for this case can be found as:

$$For\ t < t_p = 139s:\ \ h = \sqrt{\frac{k\rho c}{\pi t}}; \qquad (D.3)$$

$$or\ t \geq t_p = 139s:\ \ h = \frac{k}{\delta} \qquad (D.4)$$

The properties of the enclosure boundaries are given in the Table 18. The graph representing variation of the effective heat transfer coefficient over the time can be found below (Figure 51):

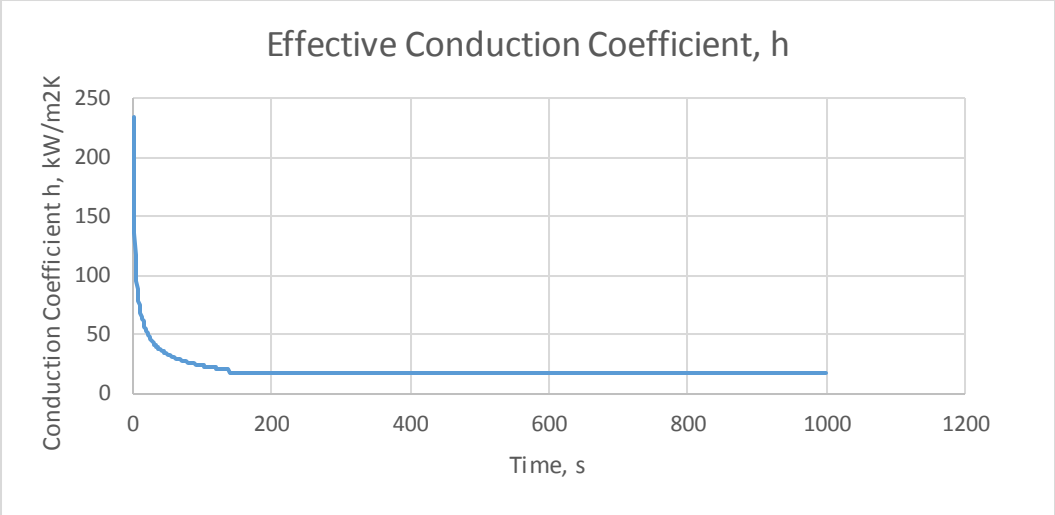

Figure 51. Variation of the effective conduction coefficient over time.

Now, to solve the Equation D.2 and find temperature increase, and, then, hot gas layer temperature, the outflow of hot gases through the vent (m_g) has to be determined first.

N. Johansson and P. van Hees in their paper [14] proposed an equation for the outflow for

$(z_{int}/H_o) > 0.3$:

$$\dot{m}_g = 0.68 A_o \sqrt{H_o}\left(1 - \frac{z_{int}}{H_o}\right) \qquad (D.5)$$

Unfortunately, this equation (Eq.(D.5)) cannot be simply used as the height of the hot gas layer (z_{int}) is also unknown. More complicated approach has to be applied.

Heskestad [27] gives equation for entrainment below mean flame height, L_f, for pool fires of diameter 0.13m and 0.1m:

$$\dot{m}_{ent} = \dot{m}_{ent,L}\left(\frac{z}{L_f}\right)^2 \qquad (D.6)$$

where z – the distance between fuel surface and smoke layer, m:

$z = z_{int} - H_{elev,}$

H_{elev} – elevation of the fire, m

m_{ent} – air entrainment at the height z, kg/s;

$m_{ent,L}$ – air entrainment at mean flame height L_f, kg/s;

According to Heskestad [27] the equation for entrainment at mean flame height, L_f, for pool fires of any diameter, for normal atmospheric conditions takes form of:

$$\dot{m}_{ent,L} = 0.0058\dot{Q}_c \qquad (D.7)$$

Q_c – convective part of the rate of energy release, generally assumed to make up 70% of the total HRR (0.7Q), kW;

L_f – mean flame height, m.

To find the mean flame height the formula developed by Heskestad [27] can be applied (Eq.(D.7):

$$L_f = 0.235\dot{Q}^{2/5} - 1.02D \qquad (D.8)$$

As it can be seen from the Equation D.8 the mean flame height depends on the rate of heat released. Similar to the Method 1, it is chosen to use experimental values of HRR, which are time dependent. Thus, the parameter L_f will be also found for every time step. In this way, for the fire source at floor level and t=2min, Q=3.1kW.

Then,

$$L_f = 0.235\dot{Q}^{2/5} - 1.02D = 0.235 \cdot 3.2^{2/5} - 1.02 \cdot 0.1 = 0.27m.$$

Values for other time steps and other scenarios can be found in the tables that will follow (Table 23, 21 and 22)

From the conservation of mass law, at $z = z_{int}$:

$m_{ent} = m_g$

Consequently,

$$0.0058\dot{Q}_c\left(\frac{(z_{int} - H_{elev)}}{L_f}\right)^2 = 0.68A_o\sqrt{H_o}\left(1 - \frac{z_{int}}{H_o}\right) \qquad (D.9)$$

Solving Equation D.9 for z_{int} gives a quadratic equation (Eq.(D.10)):

$$\left(\frac{0.0058 \cdot 0.7 \cdot Q}{L_f^2}\right) z_{int}^2 - \left(\frac{0.0058 \cdot 0.7 \cdot Q \cdot 2 \cdot H_{elev} \cdot \sqrt{H_o} - 0.68 \cdot A_o L_f^2}{L_f^2 \sqrt{H_o}}\right) z_{int} + \left(\frac{0.0058 \cdot 0.7 \cdot Q \cdot H_{elev}^2 - 0.68 A_o \sqrt{H_o} L_f^2}{L_f^2}\right) = 0 \qquad (D.10)$$

According to the Equation D.10 the height of the hot gas layer is dependent on two variable with time parameters: HRR and mean flame height. Therefore, the position of the hot gas layer has to be found for every time step. This has been done and can be found in the tables below. (Table 23, 21 and 22)

Now when z_{int} is known, it is possible to find flow out of hot gases, m_g for every time step. This was done in a spread-sheet.

$$\dot{m}_g = 0.68 A_o \sqrt{H_o} \left(1 - \frac{z_{int}}{H_o}\right)$$

Finally, assuming that the initial room temperature was 300°K, the temperature of the hot gas layer (Eq.(D.9)):

$$T_g = T_{amb} + \Delta T = T_{amb} + \frac{\dot{Q}}{(\dot{m}_g c_p + h A_t)} \qquad (D.11)$$

Table 23, Table 24 and Table 25 below demonstrate estimated results for every scenario. Graphical visualizations can be found in the Section 5.1.3.2.

Table 23. Results of the Method 2 calculation for scenario 1.

Scenario 1 (Floor)				
Time, min	HRR (test 1), kW	Mean flame height L_f, m	HGL height Z_{int}, m	HGL Temp, K
2	3.10	0.27	0.47	348.78
4	3.99	0.31	0.48	363.09
6	4.48	0.33	0.48	370.94
8	4.87	0.34	0.48	377.18
10	5.26	0.35	0.48	383.33
12	5.37	0.36	0.48	385.12
14	6.01	0.38	0.48	395.32
16	7.18	0.42	0.48	413.97
18	7.56	0.43	0.48	419.91

Table 24. Results of the Method 2 calculation for scenario 2.

Scenario 2 (1/3H)				
Time, min	HRR (test 2), kW	Mean flame height L_f, m	HGL height Z_{int}, m	HGL Temp, K
2	2.62	0.24	0.56	352.68
4	3.72	0.30	0.56	375.01
6	4.29	0.32	0.56	386.61

8	4.41	0.32	0.56	389.06
10	4.85	0.34	0.56	397.98
12	5.06	0.35	0.56	402.18
14	5.45	0.36	0.56	410.15
16	6.15	0.38	0.56	424.30
18	7.41	0.42	0.56	449.76
20	7.22	0.42	0.56	445.94

Table 25. Results of the Method 2 calculation for scenario 3.

Scenario 3 (2/3H)				
Time, min	HRR (test 3), kW	Mean flame height L_f, m	HGL height Z_{int}, m	HGL Temp, K
2	2.27	0.22	0.64	360.37
4	4.84	0.34	0.64	428.64
6	6.20	0.39	0.64	465.40
8	6.99	0.41	0.64	486.64
10	7.64	0.43	0.64	503.98
12	8.79	0.46	0.64	534.21

In real situation fire safety engineer is likely to use values of HRR found from the free burning tests. Thus, HGL temperatures were also calculated using HRR of free burning Heptane (Table 26).

Table 26. Results of the Method 2 calculation using HRR of free burn test for all elevation scenarios.

All Scenarios				
Time, min	HRR (free burning), kW	Mean flame height L_f, m	HGL height Z_{int}, m	HGL Temp, K
2	3.31	0.28	0.44	347.73
4	3.95	0.31	0.44	357.15
6	4.35	0.32	0.44	363.10
8	4.73	0.34	0.44	368.60
10	5.01	0.35	0.44	372.71
12	5.05	0.35	0.44	373.35
14	5.14	0.35	0.44	374.67
16	5.97	0.38	0.44	386.76
18	7.12	0.41	0.44	403.52
20	6.29	0.39	0.44	391.44

Appendix E. FDS inputs for scenario 1.

```
&HEAD CHID='FLOOR'/
&MESH ID='MESH',IJK=24,32,24,XB=0.0,1.2,-0.8,0.8,0.0,1.2/
&TIME T_END= 1200.0/
&MISC TMPA=25. /
&DUMP DT_DEVC=1/
&RADI RADIATION=.TRUE.,
RADIATIVE_FRACTION=0.35,
NUMBER_RADIATION_ANGLES=200,
EXTERNAL_RADIATION_MODEL=.TRUE./
&REAC FUEL = 'N-HEPTANE',
C= 7.0,
H = 16.0,
O=0.0,
N=0.0,
SOOT_YIELD =0.015,
CO_YIELD =0.006,
HEAT_OF_COMBUSTION=44600.0,
IDEAL=.TRUE./
&SURF ID='FIRE',COLOR='RED',
TMP_FRONT=98.0,
RAMP_T='FIRE_RAMP_T',
EMISSIVITY=1.0,
MLRPUA=0.02,
RAMP_Q='FIRE_RAMP_Q',
HEAT_OF_VAPORIZATION=318.0,
PEATROSS_BEYLER=.TRUE.,
FUEL_MASS=0.135,/
```

&RAMP ID='FIRE_RAMP_Q', T=0.0, F=0.0/

&RAMP ID='FIRE_RAMP_Q', T=120.0, F=0.6/

&RAMP ID='FIRE_RAMP_Q', T=240.0, F=0.7/

&RAMP ID='FIRE_RAMP_Q', T=960.0, F=0.85/

&RAMP ID='FIRE_RAMP_Q', T=1080.0, F=1.0/

&RAMP ID='FIRE_RAMP_T', T=0.0, F=0.0/

&RAMP ID='FIRE_RAMP_T', T=120.0, F=0.6/

&RAMP ID='FIRE_RAMP_T', T=240.0, F=0.7/

&RAMP ID='FIRE_RAMP_T', T=960.0, F=0.85/

&RAMP ID='FIRE_RAMP_T', T=1080.0, F=1.0/

&OBST XB=0.55,0.65,0.15,0.25,0.1,0.15, SURF_IDS='FIRE','INERT','INERT'/ Fire

&DEVC ID='PB_O2_FRAC',QUANTITY='VOLUME FRACTION', SPEC_ID='OXYGEN', STATISTICS='MEAN', DRY=.TRUE., XB=0.45,0.75,0.05,0.35,0.05,0.15/

&DEVC ID='PB_O2_TMP', QUANTITY='TEMPERATURE', STATISTICS='MEAN', XB=0.45,0.75,0.05,0.35,0.05,0.15/

&DEVC ID='PB_EXT_RAD', QUANTITY='EXTERNAL RADIATION FUEL', STATISTICS='MEAN', XB=0.55,0.65,0.15,0.25,0.15,0.15,/

&MATL ID='CALCIUM_SELICATE_BOARD', CONDUCTIVITY=0.175, SPECIFIC_HEAT=1.13, DENSITY=870. /

&SURF ID='ROOM_BOUNDARY', MATL_ID='CALCIUM_SELICATE_BOARD', COLOR='RED', BACKING='VOID',

THICKNESS=0.10,TRANSPARENCY=0.1/

&OBST XB=0.15,0.2,-0.65,0.65,0.05,0.85, SURF_ID='ROOM_BOUNDARY' /

&OBST XB=1.0,1.05,-0.65,0.65,0.05,0.85, SURF_ID='ROOM_BOUNDARY' /

&OBST XB=0.2,1.0,-0.6,-0.65,0.05,0.85, SURF_ID='ROOM_BOUNDARY' /

&OBST XB=0.2,1.0,0.6,0.65,0.05,0.85, SURF_ID='ROOM_BOUNDARY' /

&OBST XB=0.15,1.05,-0.65,0.65,0.0,0.05, SURF_ID='ROOM_BOUNDARY' /

&OBST XB=0.15,1.05,-0.65,0.65,0.85,0.9, SURF_ID='ROOM_BOUNDARY' /

&HOLE XB=0.45,0.75,-0.6,-0.65,0.05,0.7/

&VENT XB=0.0,1.2,0.8,0.8,0.0,1.2, SURF_ID='OPEN'/

&VENT XB=0.0,1.2,-0.8,-0.8,0.0,1.2, SURF_ID='OPEN'/

&VENT XB=0.0,0.0,-0.8,0.8,0.0,1.2, SURF_ID='OPEN'/

```
&VENT XB=1.2,1.2,-0.8,0.8,0.0,1.2, SURF_ID='OPEN'/
&PROP ID='BIG_TC',BEAD_DIAMETER=0.0005 /
&DEVC ID='TC_1',XYZ=0.95,0.55,0.1, QUANTITY='THERMOCOUPLE',PROP_ID='BIG_TC'/
&DEVC ID='TC_2',XYZ=0.95,0.55,0.2, QUANTITY='THERMOCOUPLE',PROP_ID='BIG_TC'/
&DEVC ID='TC_3',XYZ=0.95,0.55,0.3, QUANTITY='THERMOCOUPLE',PROP_ID='BIG_TC'/
&DEVC ID='TC_4',XYZ=0.95,0.55,0.4, QUANTITY='THERMOCOUPLE',PROP_ID='BIG_TC'/
&DEVC ID='TC_5',XYZ=0.95,0.55,0.5, QUANTITY='THERMOCOUPLE',PROP_ID='BIG_TC'/
&DEVC ID='TC_6',XYZ=0.95,0.55,0.6, QUANTITY='THERMOCOUPLE',PROP_ID='BIG_TC'/
&DEVC ID='TC_7',XYZ=0.95,0.55,0.7, QUANTITY='THERMOCOUPLE',PROP_ID='BIG_TC'/
&DEVC ID='TC_8',XYZ=0.95,0.55,0.8, QUANTITY='THERMOCOUPLE',PROP_ID='BIG_TC'/
&DEVC XB=0.6,0.6,-0.2,-0.2,0.2,0.8, QUANTITY='LAYER HEIGHT', ID='LAYER' /
&DEVC XB=0.6,0.6,-0.2,-0.2,0.2,0.8, QUANTITY='LOWER TEMPERATURE', ID='LOW_T' /
&DEVC XB=0.6,0.6,-0.2,-0.2,0.2,0.8, QUANTITY='UPPER TEMPERATURE', ID='HGL_T' /
&DEVC ID='FLUX', XYZ=0.6, 0.0, 0.05, QUANTITY='RADIOMETER',IOR=3/
&SLCF PBY=0.0, QUANTITY='TEMPERATURE'/
&SLCF PBY=0.0, QUANTITY='PRESSURE'/
&SLCF PBY=0.0, QUANTITY='TURBULENCE RESOLUTION'/
&SLCF PBY=0.0, QUANTITY='VOLUME FRACTION', SPEC_ID='OXYGEN'/
&SLCF PBX=0.6, QUANTITY='TEMPERATURE'/
&SLCF PBX=0.6, QUANTITY='PRESSURE'/
&SLCF PBX=0.6, QUANTITY='TURBULENCE RESOLUTION'/
&SLCF PBX=0.6, QUANTITY='VOLUME FRACTION', SPEC_ID='OXYGEN'/
&BNDF QUANTITY='RADIOMETER'/


&TAIL/
```